



Institute of Translational Medicine

Department of Molecular and Clinical Cancer Medicine

**Defining the model for Human papillomavirus driven
oropharyngeal squamous cell carcinoma and the role of
epithelial to mesenchymal transition in disease
dissemination**

Thesis submitted in accordance with the requirements of the University
of Liverpool for the degree of Doctor of Philosophy by

Frances Sarah Teresa Greaney

July 2020

Abstract

Human papillomavirus (HPV)-positive oropharyngeal squamous cell carcinoma (OPSCC) incidence is rising rapidly in the western world. Understanding of this disease, and modelling the therapeutic response requires a suitable *in vitro* cell model. Groups around the world have struggled to culture OPSCC epithelial cells naturally infected with HPV and rely on a limited number of commercially available, long term cell cultures that do not match the common patient clinicopathological features of HPV-positive OPSCC. The research presented in this thesis sought to derive primary cells and low passage cell lines from HPV-positive OPSCC patients that retained HPV16 E6 and E7 oncogenes and activity. Although eight cell lines were successfully established, HPV16 viral oncogene expression (E6 and E7) were absent by real-time qPCR testing. If the available secondary cell lines are to be suitable representation of HPV-positive head and neck disease, a comprehensive understanding of these resources is of great importance. In this thesis, viral oncogene presence, expression, pathological HPV testing and migration profiling for the six HPV-positive head and neck cell lines confirmed that they remain suitable as an ongoing model for

HPV-positive head and neck cancer, yet researchers should be aware of clinical representation as all cell lines originate outside of the oropharynx and come from smokers.

Although 90% of HPV-positive OPSCC patients present with advanced lymph node involvement prognosis is considerably better than HPV-negative cancer (3-year survival 82% for HPV-positive, 57% for HPV-negative). However, currently there are no discriminating factors to stratify outcome within the HPV-positive population and it is not known how the mechanism of invasion differs between HPV-positive and -negative disease. Tissue microarrays representing 99 OPSCC tumours were analysed by immunohistochemistry for the expression of the invasive marker podoplanin and the epithelial to mesenchymal transition (EMT) markers E-cadherin and vimentin. HPV-positive tumours had significantly increased levels of the epithelial marker E-cadherin ($p < .0001$) and podoplanin ($p = .0399$) compared to HPV-negative tumours, implying that HPV-positive cells do not undergo classical EMT yet have a more invasive phenotype. Low E-cadherin expression in HPV-negative tumours correlated with poor outcome at 36 months (OS $p = .022$; DFS $P = .006$) and could indicate that cells with EMT-associated profile are less responsive

to treatment. Functional assays on eight cell lines (six HNSCC, two cervical cancers) determined that HPV infection did not appear to influence migration rates, however all the cell lines examined exhibited unique migration patterns and EMT related protein profiles.

To conclude, whilst caution should be exercised in translating future *in vitro* findings to the clinical environment, given irregularities in tumour provenance (origin site and clinicopathological features), the current model for HPV-positive OPSCC is representative. Future efforts in primary cell culture will necessarily focus on developing three-dimensional environments or the utilisation of feeder layers. The absence of an EMT-associated phenotype may have relevance to increased sensitivities to therapy in HPV-positive patients but the evidence presented here is not sufficient to support specific therapeutic de-escalation in a subset of HPV-positive patients and further analysis is required seeking reliable, predictable biomarkers.

Table of Contents

Abstract.....	ii
List of Tables.....	x
List of Figures.....	xiii
List of Appendices.....	xvii
List of Common Abbreviations.....	xviii
Acknowledgements.....	xx
Declaration.....	xxii
Chapter 1: Introduction.....	1
1.1 Head and Neck Squamous Cell Carcinoma.....	1
1.1.1 Anatomy.....	1
1.1.2 Risk Factors.....	2
1.1.3 Epidemiology.....	4
1.1.4 Diagnosis, Treatment and Prognosis of HPV-positive OPSCC.....	9
1.2 Human papillomavirus.....	18
1.2.1 HPV Types.....	18
1.2.2 Virus structure.....	20
1.2.3 Virus life cycle.....	21
1.2.4 How HPV causes cancer.....	25
1.3 Current Models of HPV disease and methods for <i>in vitro</i> research.....	26
1.3.1 Cell lines.....	26
1.3.2 Formalin fixed paraffin embedded (FFPE) tissue and Tissue Microarrays (TMAs).....	31

1.4 Epithelial-mesenchymal Transition and invasion markers..	33
1.4.1 Definition and proposed mechanism	33
1.4.2 Role in Cancer	35
Chapter 2: Thesis Aims	38
Chapter 3: Materials and Methods.....	43
3.1 List of reagents	43
3.2 Sample procurement	43
3.3 Cell Culture preparation.....	44
3.3.1 Terminology	44
3.3.2 Culturing conditions	46
3.3.3 Media preparation	46
3.4 Primary cell culture	49
3.4.1 Tissue disaggregation and explant initiation.....	49
3.4.2 Establishing a monolayer	52
3.4.3 Passaging cells from flasks.....	53
3.4.4 Cell preservation and resurrection	55
3.4.5 Counting cells	56
3.4.6 Feeder layers.....	57
3.5 Secondary Cell Culture.....	58
3.5.1 Cell line procurement	58
3.6 Nucleic Acid Extraction	59
3.6.1 Extraction from cultured cells	59
3.6.2 Extraction from blood and tissue	63
3.7 Cell line validation.....	65
3.7.1 Mycoplasma testing	65
3.7.2 Short Tandem Repeat (STR) analysis.....	66
3.8 HPV Testing	69
3.8.1 cDNA synthesis.....	69
3.8.2 Real-Time Quantitative Polymerase Chain Reaction (rt-qPCR).....	70

3.8.3 Fixing Cell Pellets and sectioning.....	74
3.8.4 p16 Immunohistochemistry (IHC).....	75
3.8.5 High-Risk HPV DNA in situ hybridisation (ISH)	75
3.8.6 High-risk HPV 16 E6/E7 mRNA detection (RNAscope®)	77
3.9 Migration - wound closing	78
3.10 Tissue Micro Arrays (TMAs)	82
3.10.1 Case identification.....	82
3.10.2 TMA construction	84
3.10.3 Calculating overall and disease-free survival	86
3.11 Staining Procedures	86
3.11.1 Haematoxylin & Eosin (H&E) staining	86
3.11.2 Immunohistochemistry (IHC).....	88
3.10.3 Slide digitalising and analysing	89
Chapter 4: Establishing primary cell cultures from patients with HPV-positive Oropharyngeal Squamous Cell Carcinoma	92
4.1 Introduction.....	92
4.2 Results	93
4.2.1 Patient demographics	93
4.2.2 Primary cell culture	93
4.2.3 Primary cell culture with feeders	104
4.2.4 Cell line validation	107
4.2.5 HPV testing.....	108
4.3 Discussion	110
Chapter 5: Characterisation of the available secondary cell lines used for <i>in vitro</i> HPV-driven OPSCC studies.....	117
5.1 Introduction.....	117
5.2 Results	119
5.2.1 Cell line clinic-pathology and demographics	119

5.2.2 Cellular growth characteristics and cell line validation	119
5.2.3 Migration	123
5.2.4 Defective division	123
5.2.4 HPV testing – HPV16 gene and transcript presence and fixed cell pellet HPV diagnostics	127
5.2.5 HPV testing – Fixed cell pellet HPV diagnostics.....	128
5.2.6 IHC on fixed cell pellets for invasion proteins and epithelial-mesenchymal transition markers	131
5.3 Discussion	134
Chapter 6: Epithelial to Mesenchymal Transition (EMT) and expression of the invasive marker Podoplanin (PDPN) in Oropharyngeal Squamous Cell Carcinoma (OPSCC).....	141
6.1 Introduction.....	141
6.2 Results	144
6.2.1 Patient Demographics.....	144
6.2.2 Antibody Optimisation	144
6.2.3 Primary Tumour	149
6.2.4 Nodal Tissue.....	150
6.2.5 Vimentin staining.....	151
6.2.6 Podoplanin.....	156
6.2.7 E-cadherin	160
6.2.8 Epithelial-Mesenchymal Transition (EMT)-Associated Phenotypes and Invasiveness	165
6.2.9 Impact on Nodal status	166
6.2.10 Overall survival and Disease-free survival	170
Discussion	180
Chapter 7: Discussion, Limitations and Future Works	183
The Model of HPV OPSCC: Primary and Secondary Cell Lines	186

EMT and Podoplanin: potential biomarkers for invasion in HPV-positive OPSCC.....	197
Chapter 8: Publications supporting this thesis	205
Chapter 9: References	206
Chapter 10: Appendices	245
10.1 List of Reagents.....	245
10.2 Primary cell culture patient demographics	247
10.3 real-time-qPCR (Primary cell lines).....	248
10.4 real-time qPCR CT results (Secondary cell lines)	248
10.5 Organotypics	260
10.5.1 Materials and Methods.....	260
10.5.2 Results.....	263
10.6 Migration videos	264
10.7 TMA Overall scoring sheets.....	264

List of Tables

Table Number and Title	Page number
Table 1.1 Tumour categories for HPV-positive and -negative oropharyngeal tumours. TNM8	15
Table 1.2 Clinical node definitions with TNM8 between HPV-positive and negative OPSCC	15
Table 1.3 Pathological node definitions for HPV-positive OPSCC	16
Table 1.4 HPV-positive OPSCC cancer staging using clinical and pathological TNM scores	16
Table 1.5 HPV-negative OPSCC cancer staging dependent on TNM scores	17
Table 3.1 Primary culture and low passage cell line media supplementation	47
Table 3.2 Continuous cell line media supplementation	48
Table 3.3 Media for primary cultures on 3T3 feeder layers	49
Table 3.4 Contents of e-Myco™ Mycoplasma PCR Detection Kit	66
Table 3.5 PCR Conditions for mycoplasma testing	66
Table 3.6 PCR Amplification mix for amplification of extracted DNA for STR Typing	67
Table 3.7 Thermal cycling protocol for STR Typing	68

Table 3.8 Reverse-transcription reaction components	70
Table 3.9 Primer and probe sequences for HPV16 E2, E6, E7 and HPV18 E6 rt-qPCR	72
Table 3.10 Thermal cycling conditions for rt-qPCR	73
Table 3.11 Haematoxylin & Eosin protocol	90
Table 3.12 Protocol for IHC on bench top	91
Table 4.1 Demographics of donors for primary cell culture	97
Table 4.2 Demonstration of STR typing for HPV-positive OPSCC cell lines matched with controls	108
Table 5.1 Demographics of cell lines	120
Table 5.2 STR results for secondary cell lines compared to published figures	122
Table 5.3 Presence of HPV16 viral genes	129
Table 5.4 Description of each cell line and IHC expression	133
Table 6.1 Patient cohort and clinicopathological features in relation to HPV status	145
Table 6.2 Relationship of scores for vimentin, podoplanin and E-cadherin between primary and nodal tissue	151
Table 6.3 Vimentin scores for primary and nodal tissue	156
Table 6.4 Podoplanin scores for primary and nodal tissue	160
Table 6.5 E-cadherin scores for primary tumour and nodal tissue.	164

Table 6.6 Combination of EMT and invasion markers in primary and nodal tissue	168
Table 6.7 Effect of protein expression on nodal status	169

List of Figures

Figure number and Title	Page Number
Figure 1.1 Sites of HNSCC.	1
Figure 1.2 Global estimated figures of new cancer incidences in 2018	5
Figure 1.3 Global incidences of OSCC (A) and OPSCC (B)	6
Figure 1.4 The universal HPV vaccination programme poster	8
Figure 1.5 Phylogenetic tree of HPV types	20
Figure 1.6 Diagram of HPV genome	22
Figure 1.7 Illustration of the mechanism of HPV replication	23
Figure 1.8 Schematic showing the degradation of p53 by HPV E6 and binding of Rb by HPV E7	26
Figure 1.9 Hypothesised method of EMT	34
Figure 3.1 Flowchart for cell passaging from explant initiation to nucleic acid extraction	54
Figure 3.2 Example of cell counting results screen	56
Figure 3.3 Reaction process for DNA ISH.	76
Figure 3.4 Process for RNAscope [®] .	78
Figure 3.5 Process of seeding cells within chambers (Ibidi [®])	79

Figure 3.6. Correct directory and subdirectory set up for TScratch analysis	80
Figure 3.7 Workflow for TScratch analysis	82
Figure 3.8 Example of H&E slide mark up for tumour	84
Figure 3.9 Constructed TMA with matching H&E section	85
Figure 4.1 Schematic of final stage of each attempted OPSCC primary cell culture.	98
Figure 4.2 Fibroblast explant (A); Keratinocyte explant (B)	100
Figure 4.3 Fibroblast explants encased in ECM	101
Figure 4.4 Comparison of cell morphology as explants and after trypsinisation into monolayers.	102
Figure 4.5 Normal keratinocytes and HPV-negative keratinocytes	103
Figure 4.6 Representation of successful cell lines derived from HPV-positive OPSCC	104
Figure 4.7 The debris caused by feeder cells required additional washes which increased the risk of precious tissue detachment.	106
Figure 4.8 Comparison of 3T3 (A-B) and Liv86Normal fibroblasts (C-D) as feeder layers.	106
Figure 4.9 Example of a negative mycoplasma test	107
Figure 4.10 Amplification plots for Liv91tumour keratinocytes and Liv111 tumour keratinocytes grown without feeders.	109
Figure 5.1 Brightfield images of characterised HNSCC cell lines	121

Figure 5.2 Series of time points capturing tripolar mitosis in SiHa cell culture.	124
Figure 5.3 Representative images from differing time points	125
Figure 5.4 Graphs of time to gap closure.	126
Figure 5.5 HPV diagnostic testing on fixed cell pellets.	130
Figure 5.6. Examples for each cell line on expression of E-cadherin, podoplanin and vimentin.	132
Figure 6.1 Representative of H&E and IHC staining on repeat cores	147
Figure 6.2 Staining patterns of normal tissue with H&E and IHC	148
Figure 6.3 Representation of each vimentin scoring category for primary tissue	154
Figure 6.4 Representation of vimentin-positive staining for (A) partial (B) entire and (C) negative advancing fronts.	155
Figure 6.5 Examples of podoplanin cores with each scoring criteria	158
Figure 6.6 Nodal tissue with positive (score 2) podoplanin staining (A) and negative (score 0) staining (B)	159
Figure 6.7 Representative cores for each scoring criteria for E-cadherin both cytoplasmic (A-C) and membranous staining (D-F).	162
Figure 6.8 Example of loss of membrane staining at advancing front in tumour	163

Figure 6.9 Overall and Disease-free survival for HPV-positive and HPV-negative patients.	170
Figure 6.10 Nodal status as a prognostic indicator in HPV-negative and HPV-positive overall and disease-free survival	171
Figure 6.11 Vimentin expression on overall and disease-free survival.	173
Figure 6.12 Effect of E-cadherin on overall and disease-free survival.	174
Figure 6.13 Effect of podoplanin on overall and disease-free survival	175
Figure 6.14 Effect of 'Classical EMT' on overall survival and disease-free survival	176
Figure 6.15 Defining invasiveness by high podoplanin and low E-cadherin and its effect on overall survival and disease-free survival.	178
Figure 6.16 An alternative criterion for invasiveness: High podoplanin with high vimentin and its effect on overall survival and disease-free survival.	179

List of Appendices

10.1 Material and methods reagent and supplier list

10.2 Patient demographics for primary cell culture

10.3 real-time qPCR results for primary cell culture and snap
frozen tissue

10.4 real-time qPCR results for secondary cell lines

10.5 Organotypics

10.5.1 Materials and Methods

10.5.2 Results

10.6 Migration videos (USB attached to back cover)

10.7 Combined IHC scoring for E-cadherin, vimentin and
podoplanin

List of Common Abbreviations

AJCC	American Joint Committee on Cancer
ASR	Age-standardised rate
BOT	Base of tongue
BPE	Bovine pituitary extract
CAF	Cancer-associated fibroblasts
cDNA	Complementary DNA
DAB	3,3'-diaminobenzidine
DFS	Disease-free survival
DMEM	Dulbecco's modified Eagles' medium
DMSO	Dimethyl sulphoxide
DNA	Deoxyribonucleic acid
DNase	Deoxyribonuclease
ECS	Extracapsular spread
EGF	Epidermal growth factor
EMT	Epithelial-mesenchymal transition
FA	Fanconi Anaemia
FBS	Foetal bovine serum
FFPE	Formalin-fixed paraffin embedded
GMEM	Glasgow's modified Eagles; medium
Gy	Gray
H&E	Haematoxylin & eosin
HNSCC	Head and neck squamous cell carcinoma
HPV	Human papillomavirus
HR	High-risk
IHC	Immunohistochemistry
ISH	In situ hybridisation

kb	Kilobase
MEM	Minimum Essential Medium
NEAA	Non-essential amino acids
NICE	National Institute Care of Excellence
OPSCC	Oropharyngeal squamous cell carcinoma
ORF	Open reading frame
OS	Overall survival
OSCC	Oral squamous cell carcinoma
PDPN	Podoplanin
Pen/strep	Penicillin/Streptomycin
qPCR	Quantitative polymerase chain reaction
Rb	Retinoblastoma protein
RNA	Ribonucleic acid
RNase	ribonuclease
rt-	Real time
SFKM	Serum-free keratinocyte medium
STR	Short tandem repeat
TILS	Tumour-infiltrating lymphocytes
TMA	Tissue microarray
UICC	Union for International Cancer Control

Acknowledgements

I am grateful for the support from the Johnson Foundation who funded my position as a technician and PhD student and gave me the desire to pursue head and neck research.

The 3rd floor gang at Aintree hospital: Andy, Jenny, Jane, Helen, Ayren and the head and neck research team Shirley, Zoe, Vicky and in particular 'The Paul Banks from downstairs' – the research would not have been able to progress without their support and drive. I would also like to add a special mention to all the patients and their families who donated samples to aid this research.

I valued immensely the academic support from Lakis Liloglou, Asterios Triantafyllou, Max Robinson, Ned Powell and Carlos Rubbi who taught me invaluable techniques and furthered my knowledge for many aspects of this research.

I cannot begin to express my gratitude to my supervisory team who have been my anchor and inspiration. Richard Shaw who helped me see the importance cancer research holds, Andrew Schache for his constant encouragement and especially Janet Risk who has made me the scientist I am today.

My ever-patient parents; Frank and Geraldine – I dedicate this thesis to you. My brother Michael who instilled a love of science from when I was little, my sister and best friend Anne who I call every day on my way home. Philip, Juanfer, Tilly and all the kids (and Ollie the cat needs a mention too!) you have kept me happy and loved.

Finally, my husband Deiniol. You have kept me grounded, calm yet insanely happy since the day I met you three years ago – this thesis is as part your life as it is mine and you have given me perspective and kept me focused. Diolch.

'We must have perseverance and above all confidence in ourselves'

- *Marie Curie*

Declaration

I declare the work presented in this thesis is my own work except where referenced and under the guidance of my supervisor's Dr Janet Risk, Mr Andrew Schache and Prof Richard Shaw.

Pathological testing (p16 immunohistochemistry, HR-HPV DNA ISH and RNAscope®) of secondary cell lines UMSCC-4, 47, 74A, 104, UPCI:SCC090, 152, 154 and 93-VU-147T were performed by Dr Max Robinson, Department of Cellular Pathology, Newcastle-upon-Tyne Hospitals NHS Foundation Trust, Newcastle-upon-Tyne, NE7 7DN, UK.

FFPE tissue blocks not consented with University of Liverpool ethics (Ethical approval numbers: EC47.01; 10/H1002/53 & 09/H1010/54) were obtained from Liverpool BioInnovation Hub (LBIH) Biobank.

Chapter 1: Introduction

1.1 Head and Neck Squamous Cell Carcinoma

1.1.1 Anatomy

Head and neck cancer is a broad definition for cancers that arise from the mucosal lining of the upper aerodigestive tract encompassing the oral cavity, pharynx and larynx and is distinct from cancers originating from the brain, skull base or oesophagus (Figure 1.1). It is commonly referred to as head and neck squamous cell carcinoma (HNSCC) as over 90% originate from the squamous cells of the epithelium¹.

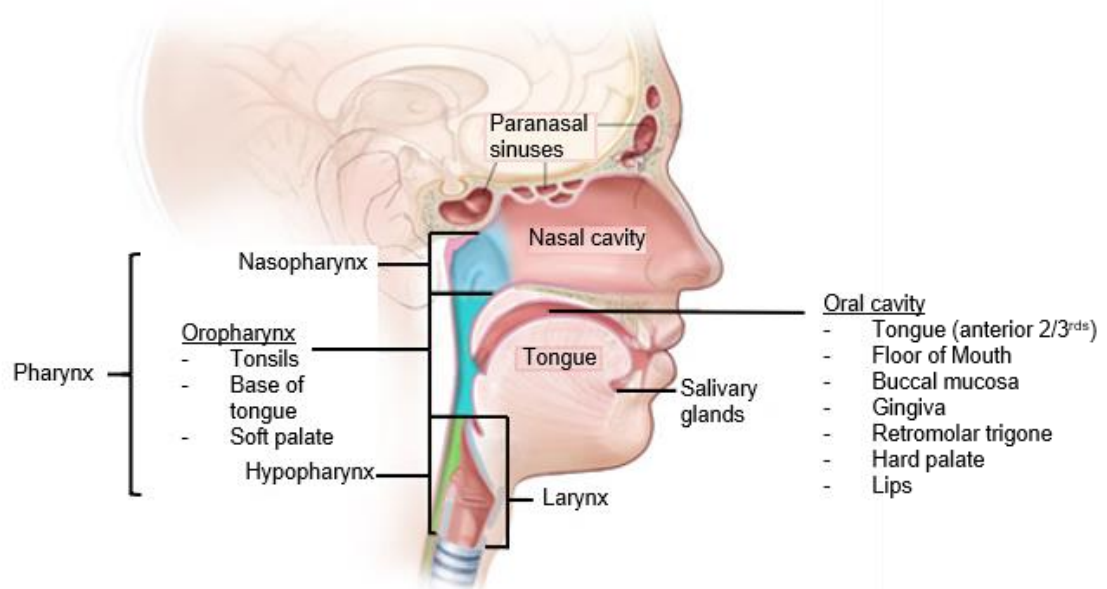


Figure 1.1 Sites of HNSCC. Adapted from the Web site of the National Cancer Institute with permission from illustrator²

1.1.2 Risk Factors

Tobacco smoking is a major risk factor for HNSCC and risk rises substantially with frequency and duration, however decreases with cessation, and returns to that of a person who has never smoked after 20 years^{3,4}. Quitting smoking whilst on treatment also decreases risk of osteoradionecrosis; a condition resulting from radiotherapy and is characterised by a loss of bone viability and ineffective tissue healing⁵. Other forms of tobacco use are linked to increased risk of HNSCC including tobacco chewing, involuntary smoking exposure and smokeless tobacco e.g. snuff⁶.

Alcohol consumption is a second major risk factor with heavy drinkers (more than 30 drinks a week) increasing their risk of HNSCC by up to 6.3 times compared to people who have never drunk alcohol⁷. Similar to smoking, it takes 20 years for the increased risk to reduce to that of a never-drinker⁴.

However, not everyone who smokes or drinks develops HNSCC and research from the INHANCE (International Head and Neck Cancer Epidemiology) consortium in 2004 determined immediate family history of head and neck cancer increases the risk by 1.7, implying there could be underlying genetic predispositions^{8,9}. The

rare recessive autosomal disease Fanconi Anaemia (FA) affects just 1 in 160,000 individuals worldwide and the chance of being a carrier is 1 in 300 yet this subset of patients has a very high incidence of head and neck cancer (3%) with poor prognosis^{10,11}. This discovery has highlighted the FA pathway as a potential source of genomic instability in patients with head and neck cancer, in particular the protein FANCD2 which has recently been implied as a prognostic marker in HNSCC¹²

Although smoking and drinking have been proven to cause squamous cell carcinoma (SCC) in all anatomic sites, an additional risk factor that almost exclusively affects the oropharynx, in particular the tonsils and base of tongue (BOT), is Human papillomavirus (HPV). Between 40-70% of all oropharyngeal squamous cell carcinomas (OPSCC) are caused by the subtype HPV16 and it is rare sites outside the oropharynx are infected¹³⁻¹⁵. Therefore, HPV-positive HNSCC is considered as a separate disease to HPV-negative HNSCC due the differences in aetiologies and prognosis and recent guidelines on disease staging is dependent on infection of HPV^{16,17}.

1.1.3 Epidemiology

HNSCC is the eighth most common cancer worldwide with an estimated 834,860 cases in 2018 affecting the oral cavity, pharynx and larynx (5% of all cancers) with males making up 75% of all cases (Table 1.1; Figure 1.2), making it the fifth most common cancer site in males and 13th in females worldwide¹⁸. Similar statistics are represented by the UK with nearly 12,000 new head and neck cases diagnosed between 2012 and 2016 (3% of all new cases)¹⁹.

Distributions of oral cavity SCC (OSCC) and oropharyngeal SCC (OPSCC) vary geographically, and are predominantly dependent on smoking and drinking habits. In high-risk countries, including India, Pakistan and Sri Lanka OSCC is the most common cancer in men, whereas OPSCC is mostly seen in developed countries and make up to 15-30% of all HNSCCs (Figure 1.3)²⁰.

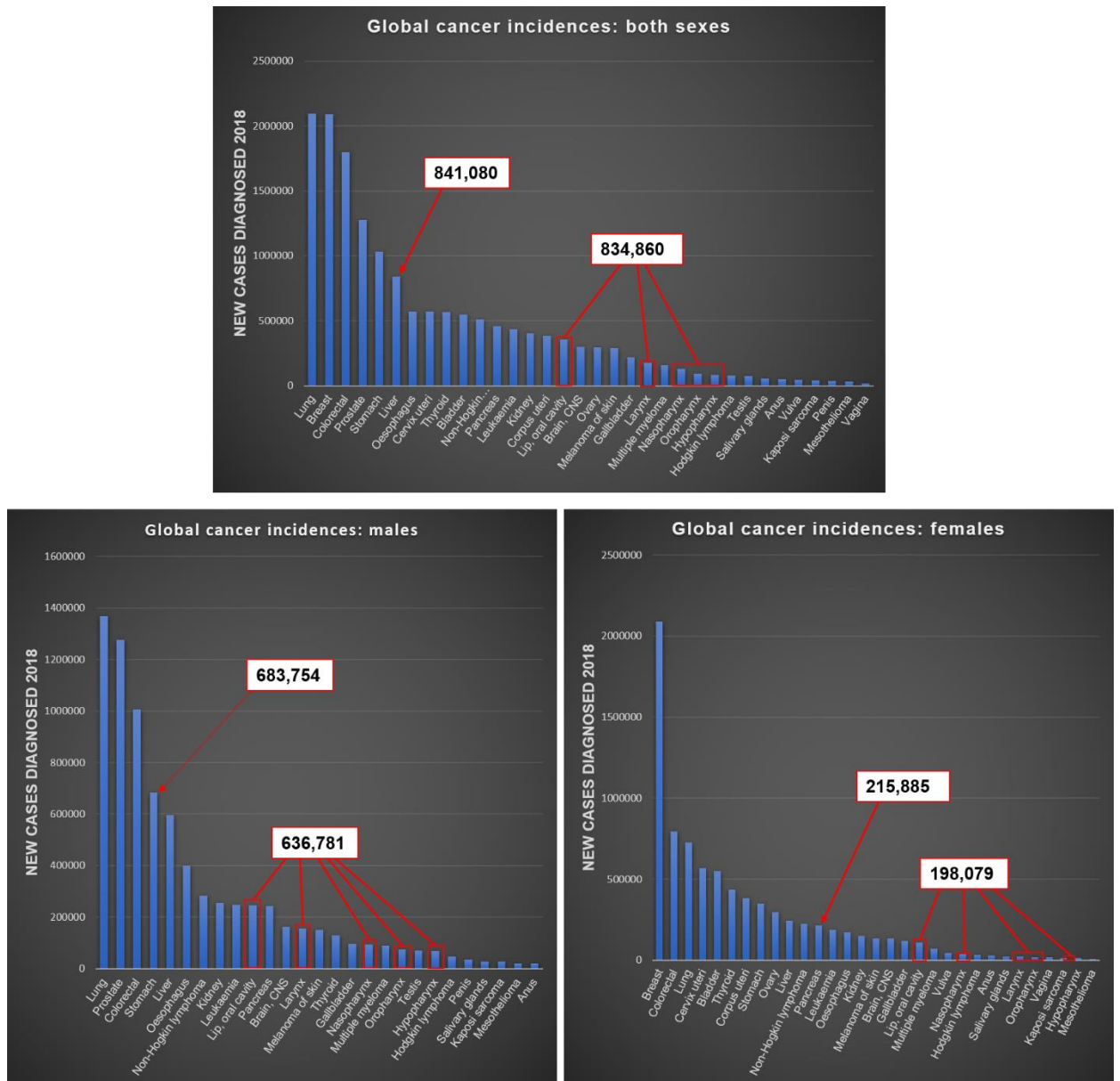


Figure 1.2 Global estimated figures of new cancer incidences in 2018. Reproduced from the GLOBOCAN study¹⁸.

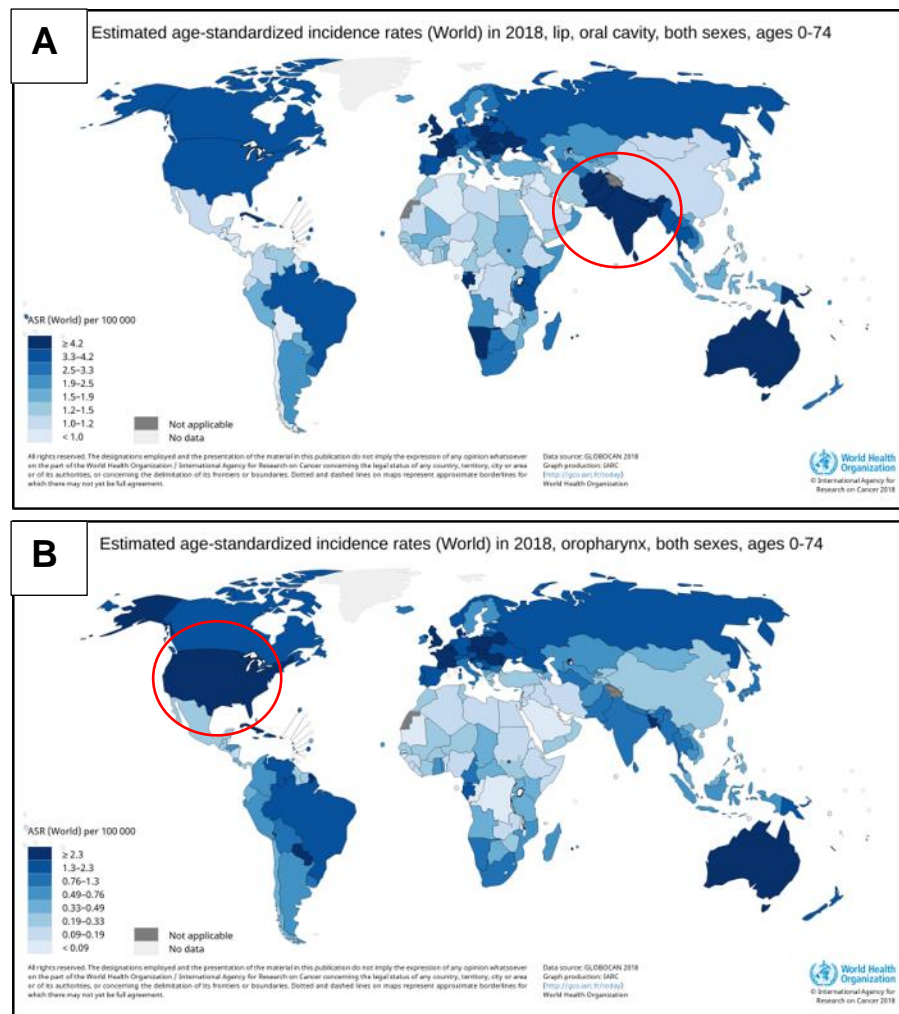


Figure 1.3 Global incidences of OSCC (A) and OPSCC (B) for both sexes by age-standardised rate (ASR). Red circles represent countries with high incident numbers. Produced using the IARC: Cancer today²¹.

Trends in HNSCC incidences are also dependant on anatomical site and in developed countries the campaigns for smoking cessation is leading to a decrease in tobacco-related OSCC, whilst there has been a significant increase in OPSCC incidences

since 1983 as described by the comprehensive worldwide analysis carried out by Chaturvedi et al²².

This increase in OPSCC has been attributed to HPV-infection and affects younger men compared to HPV-negative OPSCC and OSCC (median age 52 vs 60 vs 63) and White, non-Hispanic populations have higher incidences than HPV-negative OPSCC (93% vs 82%)^{23,24}. The exposure to HPV is primarily transmitted through sexual contact and lifetime exposure is estimated to be over 80% for women and over 90% for men, however it is important to clarify not all HPV infections develop into carcinoma, and the mechanisms of HPV oncogenesis will be covered later in this chapter^{13,25}. The rapid rise of HPV-positive OPSCC cases has led to estimates that by the end of 2020 oropharyngeal tumours infected by HPV will overtake cervical infection rates and by 2030 nearly half of all head and neck cancers will be from the oropharynx²⁶.

An intervention into avoiding this projected statistic was the introduction of the HPV prophylactic vaccine Gardasil™ (Merck) which protects against the high-risk HPV types HPV16 and

HPV18 and the lower risk HPV6 and HPV11. The vaccine is prophylactic as it prevents the virus from binding to the basal layer of the epithelium by triggering an immune response rather than as a therapeutic vaccine to clear current infection. For this reason, teenage girls who have not had sexual contact exposure have been offered the vaccine from 2006 and from 1 September 2019 all boys and girls in years 8 (aged 12-13) are currently offered the vaccine (Figure 1.4)²⁷.

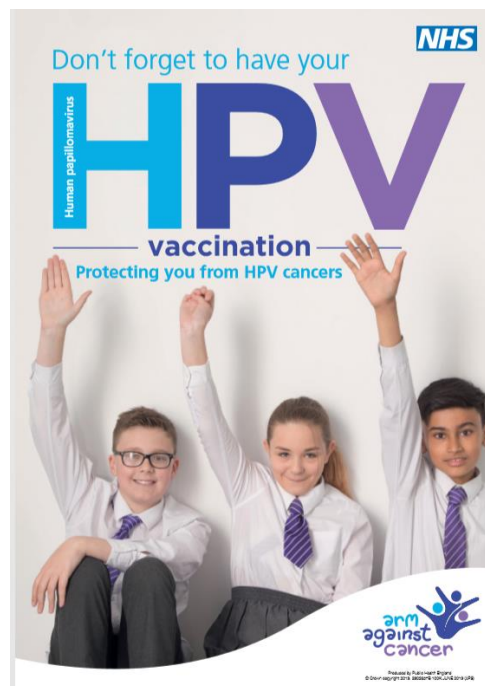


Figure 1.4 The universal HPV vaccination programme poster. Vaccination is available to all school children from year 8 to year 13. Taken from Public Health England²⁷.

1.1.4 Diagnosis, Treatment and Prognosis of HPV-positive OPSCC

As previously discussed, HPV-positive tumours arise predominantly in young men who have minimal to no smoking history²⁴. This epidemiological factor could account for the majority of HPV-positive patients presenting with clinicopathologically advanced disease as symptoms are overlooked by patients and potentially clinicians. The main symptoms of oropharyngeal cancers are: persistent sore throat, difficulty in swallowing and/or a visible lump in the neck. The majority of HPV-positive patients present with cancer metastases to the lymph nodes in the neck and occasionally the cancer is initially discovered in the nodes before a primary site is located²⁸.

Diagnostically, suspicious lesions are confirmed as cancer via histopathology of a biopsy samples usually taken under general anaesthetic or by fine needle aspiration of neck lumps guided by ultrasound²⁹. National Institute for Health and Care Excellence (NICE) guidelines (2018) state that all SCC tumours arising from the oropharynx should undergo HPV testing on either biopsy or resection tissue³⁰. Clinical HPV testing initially tests for

overexpression of the protein p16INK4A (p16) by immunohistochemistry (IHC) from formalin fixed paraffin embedded (FFPE) tissue and a p16 positive result is confirmed when >70% cells are strongly stained in the cytoplasm or nucleus³¹. However, the sensitivity and specificity of the single p16 IHC test are 0.94 and 0.82 respectively^{32,33} and a HPV-positive test is only clinically confirmed when subsequent high-risk (HR) HPV-DNA in situ hybridisation (ISH) or RNA-ISH testing also yields a positive result.

Confirmation of nodal metastasis is via Magnetic Resonance Imaging (MRI) or Computed Tomography (CT) imaging followed by histopathology confirmation via Ultrasound-guided fine needle aspiration. The results dictate whether the patient is to undergo a neck dissection, a surgically aggressive treatment where the lymph nodes are surgically removed and recent developments to identify the sentinel node (the hypothetical first node tumour cells migrate to from the primary tumour) could allow for specific nodal removal and surveillance³⁴.

The classification of cancer stage depends primarily on the size of the tumour and if nodal or distant metastases have occurred and the international accepted method is the TNM system defined by the Union for International Cancer Control (UICC) and the American Joint Committee on Cancer (AJCC)³⁵. The recent eighth edition now recognises HPV-positive OPSCC as a distinct disease to HPV-negative OPSCC and other HNSCC sites³⁶. The criteria for tumour staging are highlighted in Table 1.1 with the main differences showing there is no carcinoma in situ for HPV-positive cancer and HPV-negative T4 tumours can be categorised based on severity of invasion. Nodal stage also differs depending on HPV status as outlined in Table 1.2. After resection, pathological staging (pTNM) is applied to only HPV-positive tumours to account for number of involved lymph nodes (Table 1.3), therefore HPV-positive OPSCC is defined by a clinical TNM stage and pathological TNM stage.

M stage documents distant metastasis, and although rare in head and neck cancer can involve lung, bones, liver or lymph nodes outside of the neck and is believed to be transported via the blood stream³⁷. Any M1 staging gives dismal survival chances with a

mean survival at just 7.5 months³⁸. This type of metastasis is categorically different to nodal metastasis, where tumour cells migrate to the lymph nodes in the neck via the lymphatic system and possibly via lymphangiogenesis; where new lymphatic vessels are formed within the tumour to allow for direct access to the lymphatic system.

Overall cancer staging is determined by the TNM score and Tables 1.4 and 1.5 demonstrates the differences between HPV-positive and HPV-negative OPSCC using the classifications from Tables 1.1-1.3.

A crucial area of head and neck research is why and how the disease progresses, and what impact it has on the patient. It is well documented presence of lymph node metastasis in oral cavity cancer³⁹ and oropharyngeal cancer⁴⁰ is a predictor of poor survival, however recent studies by El Asmar et al⁴¹ and Meyers et al⁴² imply nodal status is not a negative prognostic factor in HPV-positive oropharyngeal cancer. However, regardless of outcome, 90% HPV-positive patients present with advanced nodal disease requiring extensive neck surgery for clearance⁴³.

Treatment of HNSCC can be complex and personalised based on the clinical staging, co-morbidities and also patient preference.

Patients with early disease are often treated primarily with surgical clearance and radiotherapy, however if radiotherapy can be avoided this reduces the amount of unnecessary late toxic effects and provides radiotherapy as an alternative treatment in the future⁴⁴. Advanced disease requires combination of either surgery, chemotherapy or radiotherapy (chemoradiotherapy) to improve survival chances⁴⁵.

Prognosis in HNSCC varies dramatically, particularly between HPV-positive and -negative disease; between 19-59% HNSCC patients survive 10 years after diagnosis and between 2015 and 2017 there was 3,989 deaths in the UK⁴⁶. A pivotal study by Ang et al determined HPV-positive OPSCC patients have significantly better prognosis and lower chance of recurrence than HPV-negative OPSCC patients regardless of treatment given (% overall survival at 3 years 82.4 vs 57.1 and percentage of local-regional relapse 13.6 vs 35.1)⁴⁷. Researchers have queried if this is due to the healthier, younger populations developing this

disease, if the tumours are intrinsically easier to resect or more sensitive to treatment^{13,48}. Regardless of HPV status, treatment regime between the cohorts remain the same as per NICE guidelines²⁹, however the TNM8 changes ultimately downstage HPV-positive patients, subjecting them to less aggressive treatments compared to their HPV-negative counterparts. This has huge implications as the younger demographic presenting with this disease ultimately have longer to live with the devastating side effects⁴⁹. It is important to clarify however, although a reported 82.4% HPV-positive OPSCC patients are cured of the disease there are still HPV-positive patients who do not survive and as yet, there are no differentiating factors separating outcome groups within the HPV-positive population. Other clinical parameters exist that categorise patients into good and poor outcome, but are not investigated in this thesis including; extracapsular spread in lymph nodes where tumour extends outside the lymph node capsule and is one of the most significant adverse prognostic indicator in head and neck cancer⁵⁰; 'close' (<5mm) and involved surgical margins increases risk of recurrence, impacting survival and occurs when <100% of tumour cells are removed in the resection⁵¹.

	HPV-Positive OPSCC	HPV-Negative OPSCC
Tx		Primary tumour cannot be assessed
Tis		Carcinoma in situ
T0	No primary identified	
T1	Tumour <2cm in dimension	
T2	Tumour >2cm <4cm	
T3	Tumour >4cm or extension to lingual surface	
T4	Moderately advanced local disease; tumour invades larynx, extrinsic muscles of tongue, hard palate, or mandible or beyond	Moderately advanced or very advanced local disease
T4a		Moderately advanced local disease; tumour invades larynx, extrinsic muscles of tongue, hard palate, or mandible or beyond
T4b		Very advanced local disease; tumour invades larynx or skull base

Table 1.1 Tumour categories for HPV-positive and -negative oropharyngeal tumours. TNM8, adapted from Lydiatt et al³⁵

	HPV-Positive OPSCC	HPV-Negative OPSCC
NX	Regional lymph nodes cannot be assessed	
N0	No regional lymph nodes with metastasis	
N1	>1 ipsilateral lymph node, >6cm	Metastasis in a single ipsilateral node <3cm; ECS negative
N2	Contralateral or bilateral nodes >6cm	Single or multiple nodes >3cm, <6cm, ECS negative
N2a		Single >3cm, ECS negative
N2b		Multiple ipsilateral nodes <6cm, ECS negative
N2c		Multiple bilateral/contralateral nodes <6cm, ECS negative
N3		Either lymph node >6cm and ECS negative; Any nodes ECS positive
N3a		Lymph node >6cm, ECS negative

N3b		Any lymph node metastasis, ECS positive
-----	--	---

Table 1.2 Clinical node definitions with TNM8 between HPV-

positive and negative OPSCC. Abbreviations ECS: Extracapsular spread

N Category	Pathological criteria for HPV-positive OPSCC
NX	Lymph nodes cannot be assessed
pN0	No regional lymph nodes with metastasis
pN1	≤4 involved lymph nodes
pN2	>4 involved lymph nodes

Table 1.3 Pathological node definitions for HPV-positive OPSCC.

HPV-positive OPSCC		Clinical N stage / pathological N stage			
		N0	N1	N2	N3
Clinical T stage	T0	n.a	I	II	III
	T1	I	I	II	III
	T2	I	I	II	III
	T3	II	II	II / III	III
	T4	III	III / II	III	III
Any M1 is IV					

Table 1.4 HPV-positive OPSCC cancer staging using clinical and pathological (black border) TNM scores. Only T3pN2 and T4pN1 have differing cancer staging after pathological analysis

HPV-negative OPSCC		Clinical N stage			
		N0	N1	N2a,b,c	N3a,b
Clinical T stage	T1	I	III	IVA	IVB
	T2	II	III	IVA	IVB
	T3	III	III	IVA	IVB
	T4a	IVA	IVA	IVA	IVB
	T4b	IVB	IVB	IVB	IVB
Any M1 is IVC					

Table 1.5 HPV-negative OPSCC cancer staging dependent on TNM scores

An increasing area of interest for predicting prognostic outcome for many types of cancer is the role of the body's immune system to target and kill cancer cells, with particular focus on levels of tumour-infiltrating lymphocytes (TILS)⁵². In a number of studies, increased TILS represented a better prognosis and they could have a direct effect on viral-associated tumours by initiating a specific adaptive immune response^{53,54}. Ward et al demonstrated high TIL levels in HPV-positive OPSCC were correlated with improved survival, and HPV-positive tumours with a low TIL profile mimicked HPV-negative disease (3-year survival, 56%)⁵⁵.

1.2 Human papillomavirus

1.2.1 HPV Types

Papillomaviruses (PV) are an ancient, highly diverse group of viruses belonging to the *Papillomaviridae* family that have evolved over millions of years to infect mammals, birds and reptiles, however they have been predominantly studied in humans⁵⁶. Genomic isolates of PVs are classed as PV 'types' and there are over 150 different types of Human papillomaviruses (HPV), with new types being identified yearly and inputted to the major papillomavirus sequence database The Papillomavirus Episteme⁵⁷. Novel HPV types are defined by a 10% difference in the conserved late (L)1 open-reading frame (ORF) from other known types, whereas differences of 2-10% results in a new variant of that type^{58,59}. Figure 1.5 demonstrates the phylogenetic tree of the known papillomavirus types from 2015 and the major groups or supergroups can be categorised in multiple 'genera' (Alpha, Beta, Gamma, Mu and Nu) and share less than 60% similar nucleotide sequence in their L1 ORF. Within each genus, further subgroups form based on overall shared genomic similarities and clinically, the Alpha genus contains the types most commonly implicated in human pathological disease and will be the only genus this thesis focuses on⁶⁰. Within the Alpha genus,

there are two types of papillomavirus; cutaneous and mucosal i.e. those that infect the skin (e.g. HPV 2 causing common warts) and those that infect the mucosal lining of the body (e.g. HPV6 and 11 that cause genital warts). The defining factor between 'high risk' and 'low risk' HPV is the ability to immortalise keratinocytes and they are highlighted in pink and yellow respectively in Figure 1.5 with 'high-risk' subtypes categorised exclusively within the Alpha-papillomavirus mucosal genera. This thesis focuses on the high-risk type HPV16 as this accounts for approximately 90% of HPV-positive HNSCC; other alpha-mucosal types e.g. HPV18, HPV31 and HPV33 are found at much lower frequencies in HNSCC¹⁶. This is not mimicked in cervical tissue, where HPV16 and HPV18 account for 70% of carcinomas with the subtypes 31, 33, 35, 39, 45, 51, 52, 56, 58, 59, 68, 73 and 82 making up the remainder; a different landscape to OPSCC⁶¹.

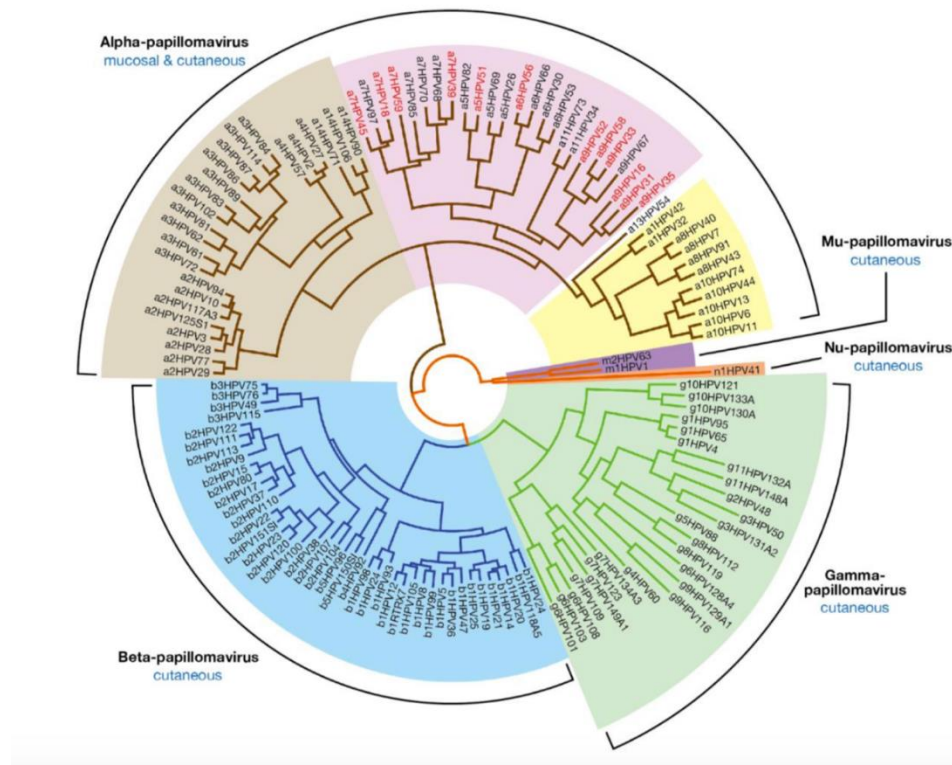


Figure 1.5 Phylogenetic tree of HPV types categorised into Alpha, Beta, Gamma, Mu and Nu genera. Alpha genus grouped by cutaneous (light brown); high-risk mucosal (pink) and low-risk mucosal (yellow). Subtypes highlighted in red text are confirmed as human carcinogenic, whereas the other types within this category are possible carcinogens. Reproduced from Doorbar et al⁵⁶

1.2.2 Virus structure

All PVs are small, non-enveloped structures made up by 72 capsomeres that contain the viral genome as a double-stranded episome around 8000 base-pairs. Two structural proteins make up 80% of the total viral protein; late (L1) and L2. HPV vaccines

have been developed by mimicking the viral capsid by single expression of L1 to create Virus-like particles (VLP)^{62,63}.

1.2.3 Virus life cycle

The virus life cycle depends upon host machinery and is linked to epithelial differentiation. The HPV genome consists of normally 8 ORFs on a single DNA strand and are categorised into early (E), late (L) and long control region (LCR) regions (Figure 1.6). The early region encodes the genes E1, E2, E4, E5, E6 and E7. E1 and E2 are responsible for DNA replication and expression; E4 and E5 proteins contribute indirectly to genomic amplification by virus release from the epithelium and enhancing epidermal growth factor signaling respectively; and E6 and E7 drive normal epithelial cells to divide, which is oncogenic in the high-risk types^{56,64}.

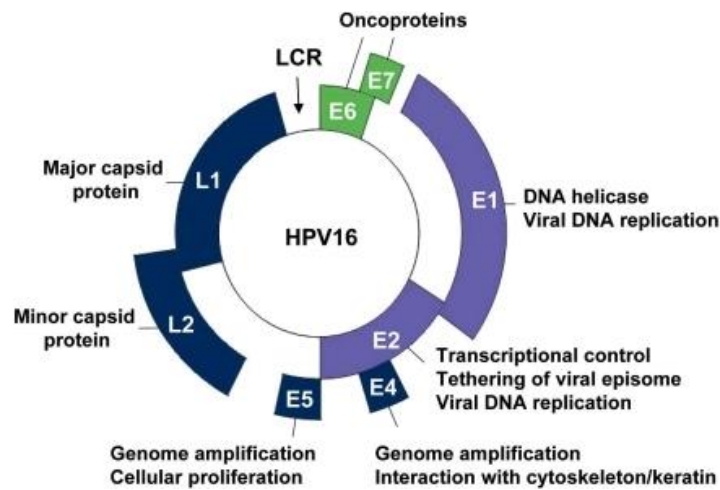


Figure 1.6 Diagram of HPV genome. Early (E) and Late (L) genes and the long control region (LCR). Reproduced from D'Abramo et al⁶⁵

HPVs have a high affinity for epithelial cells, and gain entry to basal cells of the epithelium through injury or trauma, after which they maintain genome replication in low numbers via E1 and E2, and it is thought a virus can maintain in this state for decades before transforming and is termed a latent infection^{60,66} (Figure 1.7). As stated, HPV uses the host keratinocyte differentiation pathway to increase infection and carcinogenesis occurs primarily after inactivation of the cell's natural tumour suppressor proteins by HPV E6 and E7.

Micro-abrasions allow entry of virus

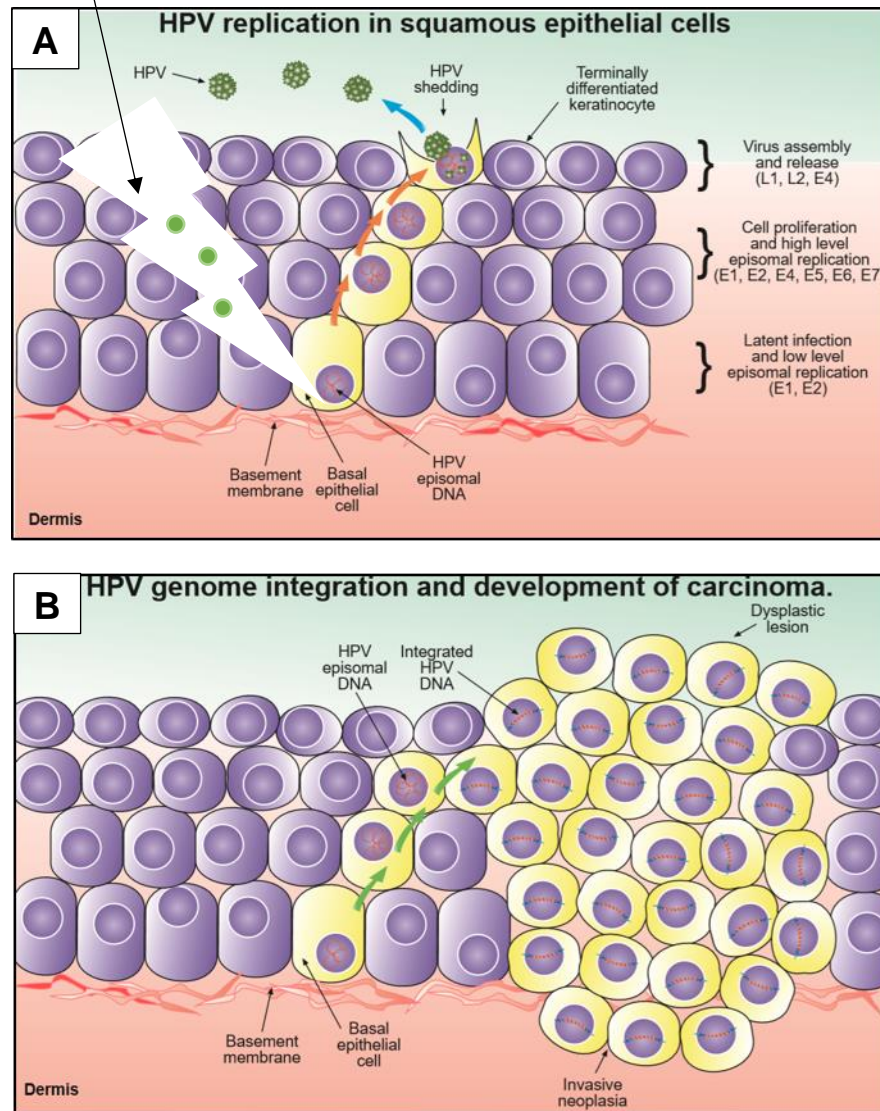


Figure 1.7 Illustration of the mechanism of HPV replication through the epithelium (A) How increased cell division leads to carcinoma (B). Reproduced from immunopedia⁶⁷

HPV DNA Integration

Early after infection, when the virus is modulating early gene expression via E2, it is thought the HPV genome remains in an extrachromosomal circular form (episomal) in the basal epithelial cells⁶⁸. In some premalignant cells this DNA is integrated into the host DNA, consequently splitting its genome within the E1 and E2 regions. The method of integration is not part of the virus' life cycle but usually results in dysregulation of E6 and E7 due to this loss of E2 function; leading to uncontrolled proliferation and the percentage of cells with integrated HPV DNA increases as the cancer progresses⁶⁹. Many studies have alluded to this integration step being crucial for carcinogenesis, and research by The Cancer Genome Atlas Research Network demonstrated >80% cervical cancers had integrated HPV DNA. Of these cancers; 100% of those that were HPV18-positive were fully integrated vs 76% in HPV16-positive cancers⁷⁰. Although widely studied in cervical cancer and integration events marked from early dysplasia (abnormal) to transformation, the same level of experimentation has not been performed on HPV-positive OPSCC and some studies have demonstrated the incidence of integrated viral DNA is lower than that seen in cervical carcinoma

and more lesions appear as episomal, or a mixture of both integrated and episomal^{71,72}. An experiment using the cervical dysplasia cell line W12 demonstrated cells harbouring more integrated HPV DNA did not have a growth advantage to those retaining episomal DNA⁷³.

1.2.4 How HPV causes cancer

Cells usually have mechanisms in place if abnormalities arise in genetic replication, usually resulting in programmed cell arrest or apoptosis. p53 is a vital protein that binds to specific areas of DNA and is upregulated in response to unscheduled DNA replication and is termed a tumour suppressor protein. Oncogenic HPV types such as HPV16 disrupts this mechanism via the oncoproteins E6 and E7. The binding of E6 to p53 promotes degradation of p53 via the ubiquitin pathway and is dependent on the E6-associated protein (E6-AP)⁷⁴. Another tumour suppressor protein is retinoblastoma protein (Rb) and its role is to inhibit the cell cycle entering S Phase and dividing⁷⁵. In normal cells, Rb binds and represses the E2F transcription factor that promotes the transition of G1 to S phase⁷⁶. E7 has a high affinity for Rb and

upon binding, this allows E2F to progress with the cell cycle⁶⁴
(Figure 1.8).

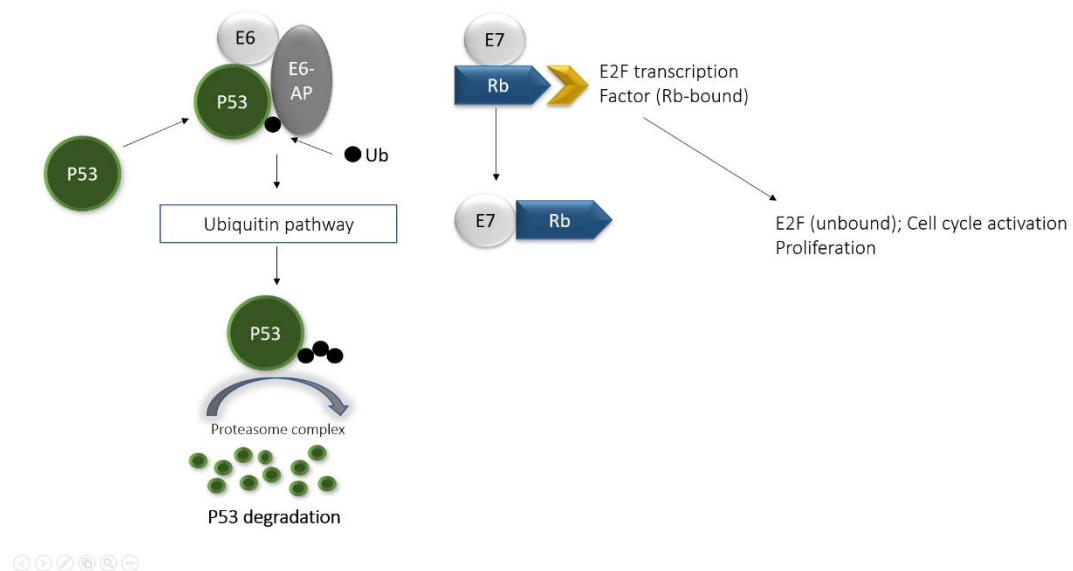


Figure 1.8 Schematic showing the degradation of p53 by HPV E6 and binding of Rb by HPV E7 promotes E2F to bind to DNA and induce cell cycle activation. Adapted from Ruttkay-Nedecký et al⁷⁷

1.3 Current Models of HPV disease and methods for *in vitro* research

1.3.1 Cell lines

Translational research, or bench-bedside has been the focus of cancer medicine research for nearly 50 years; since the signing of the National Act on Cancer in the USA in 1971⁷⁸. To introduce

new therapies, successful translational studies require a robust *in vitro* model, usually starting in commercially available cell lines before advancing to *in vivo* animal models. The field of *in vitro* cancer models is vast and detailed, with many researchers moving away from homogenous two-dimensional monolayers of cell populations on plastic and opting instead for intricate three-dimensional cell cultures, termed the holy grail of cancer research⁷⁹. These models allow the introduction of an *in vitro* tumour microenvironment with cancer associated stroma and even infiltrating immune cells⁸⁰ and includes systems with complex scaffolds that allow for realistic oxygen and nutrient gradients⁸¹, spheroids of cells which mimic tumour shape and drug effects⁸² and permits more sophisticated invasion assays⁸³. Regardless of the exciting applications achievable with 3D cultures, even the most complex cell models require initial individual cell procurement and expansion and, especially for viral-driven cancers, evidence that original drivers of tumorigenesis e.g. HPV16/18 oncogenes are still present when cells are cultured *in vitro*.

An immortal cancer cell line, one that can be subcultured indefinitely, not only would be hugely beneficial for -omics research in HPV-related head and neck cancer but also in phenotypical studies involving cell migration, proliferation and further understanding into the improved patient survival outcome seen in this cohort of patients⁴⁷. Currently it is speculated the lack of co-morbidities and potential low mutation rates in HPV-positive patients account for the high cure rate^{84,85}, and evidence has been shown for differences in chemoradiotherapy sensitivities in cell line experiments^{86,87}. Cell lines derived from cervical premalignant lesions have also offered insight into the role of HPV DNA integration. W12, a cell line derived from a CIN-I (cervical dysplasia) lesion shows the HPV16 genome remains stable at high passage numbers yet is predominantly episomal⁸⁸. Although a similar premalignant model is not available for HNSCC progression, this cell line provided understanding of the HPV life cycle and method of carcinogenesis in simple *in vitro* experimentation, including mapping integration sites⁸⁹, neoplastic progression⁹⁰ and the correlation between integration events and cellular growth⁷³. However, issues lie within secondary cell lines as a model for HPV-positive head and neck cancers, and will be discussed fully in the Chapter 5 although briefly, all secondary cell

lines generally suffer from the years of growing on plastic and usually present with genetic drift away from the original tissue genotype⁹¹. Primary cells do not show genetic drift and are therefore a good representation of the patient and tissue they have been established from.

Currently there isn't a universal method for successfully establishing primary HPV-positive keratinocytes, even though the oldest and probably most famous cell line established in 1952, HeLa (named after the patient Henrietta Lacks from which it was derived) is HPV18-positive. Multiple labs around the world have attempted to produce HPV-positive primary cell culture and at the time of this research, only cervical explants had been successful^{92,93}. One of these cell lines originated from a CIN-I (dysplasia) cervical sample; W12 and retains the HPV16 genome predominantly as episomal DNA, providing insight into the HPV DNA organisation in premalignant disease⁹⁴. The process appeared to be full of technical difficulties, primarily in the adherence of tissue to allow for explants to grow onto the plastic directly from the carcinoma sample and groups attempting to overcome this by increasing serum levels, using specialised

media or utilising the supplementation of growth hormones. Perhaps the most persuasive method in HPV-positive *in vitro* models was the introduction of 'feeder cells' that acts as 1) a structural component (or scaffold) to allow adherence for epithelial cells, and 2) a source of growth factors and cytokines found *in vivo*. The most common feeder cell type is fibroblasts, particularly Swiss mouse 3T3 fibroblast cells that are first pre-treated, commonly by irradiation, to arrest cellular divisions so not to overgrow the epithelial cells yet still providing cytokines and structural integrity⁹⁵. Feeder layers were initially characterised for cervical keratinocyte growth by Stanley et al in 1979 and most recently, Powell's group in Cardiff have successfully established two novel immortal HPV-positive oropharyngeal cell lines using Stanley's technique^{96,97}, for it to take 40 years to successfully transfer over to oropharyngeal explants highlights the obstacles groups focusing on HPV-positive head and neck cancer face for developing an *in vitro* cell model. The use of feeder cells in this research was introduced for the later attempts at primary cell culture

1.3.2 Formalin fixed paraffin embedded (FFPE) tissue and Tissue Microarrays (TMAs)

Oncology diagnosis is routinely via FFPE tissue with surgical resected tissue being 'fixed' at the point of removal and stored within paraffin. Once embedded, thin slices (4-5 μ M) can be mounted onto slides for staining assays to allow for microscopic examination by researchers and pathologists. Various fixation methods exist with different mechanisms of action; coagulating fixatives are primarily alcohol-based and dehydrate cells, causing the denaturation of proteins, altering their usually tertiary structure and therefore their solubility in water producing a permeable meshwork of protein strands, however this method leads to poor preservation of mitochondria and secretory granules as well as significant cytoplasm shrinkage⁹⁸. Alternatively, the most common fixative used in diagnostic pathology, and thus the majority of tissue available for research, is formaldehyde, a non-coagulant fixative which creates covalent cross-links between molecules, creating a much stronger permeable meshwork of cell integrity and commonly 10% buffered formalin (w/v 4% formaldehyde) is used^{99,100}. This permeable tissue is amenable for immunohistochemistry (IHC) for protein expression studies and haematoxylin and eosin (H&E) staining to visualise cell

morphology on a light microscope. Whole slides can be prepared for IHC to observe the protein expression across an entire section of tissue, but a much more efficient method is the construction of tissue microarrays (TMAs), in which multiple biopsies of FFPE tissue are deposited into a single recipient paraffin block, first developed by Kononen et al in 1998 and detailed technical notes on their construction published by Parsons 10 years later^{101,102}. TMAs can hold 100s of cores from a range of anatomical and cellular sites from different patients and tissue microarrayers can be semi-automated or manual, both with capabilities of depositing cores ranging in diameters from 0.6mm to 2mm. The 'tissue amplification' achieved by only depositing areas of interest preserves precious, finite tissue as well as permitting simultaneous analysis of protein expression by IHC, creating a truly high-throughput system, with identical experimental conditions not achievable by whole mount staining¹⁰³. Many validation studies have shown protein expression concordance of targeted and random sampling to whole tissue mounts¹⁰⁴⁻¹⁰⁶ and that tumour heterogeneity, particularly seen in HNSCC^{107,108}, is fully represented in TMA constructs of 0.6mm cores¹⁰⁹. However, an obstacle during TMA construction are the small sizes of TMA cores make them prone to loss/damage and unless all cores are

the same depth, usually rectified with depth stop kits, sectioning can lead to incomplete arrays. Overall, the benefits of using FFPE tissue rather than live cells combined with the high-throughput capabilities and preservation of precious sample material allows TMAs to be suitable models for studying biomarkers in a medium-large cohort.

1.4 Epithelial-mesenchymal Transition and invasion markers

1.4.1 Definition and proposed mechanism

A process widely discussed and hypothesised as a method of cancer cell migration is epithelial-mesenchymal transition (EMT) (Figure 1.9). The method of cell migration is described as epithelial cells losing their structural integrity and gaining the spindle-shaped morphology of mesenchymal cells, allow them to move through the basal membrane. Epithelial cells retain tissue integrity due to their basal-apical polarity, and are held together by junction complexes, which are formed by tight-, adherens- and gap-junctions and desmosomes^{110,111}. A major adheren studied in cancer is E-cadherin as these forms one of the vital components of the epithelial junction complex. It is hypothesised this breakdown of connections during EMT causes epithelial cells to

change to front-back polarity, allowing for dissemination through the basal membrane and behave like mobile mesenchymal cells leading to cancer cells transporting to secondary sites via the lymphatic and blood systems¹¹². Many studies have defined EMT effectors as proteins that upregulate mesenchymal markers or downregulate the epithelial proteins and include TFG- β , EGF, Wnt and PI3-K. These have only been confirmed *in vitro* and it is unknown whether the same effectors are present in sufficient concentrations *in vivo*^{113,114}. Furthermore, little functional evidence of cells physically transitioning *in vivo* have been published.

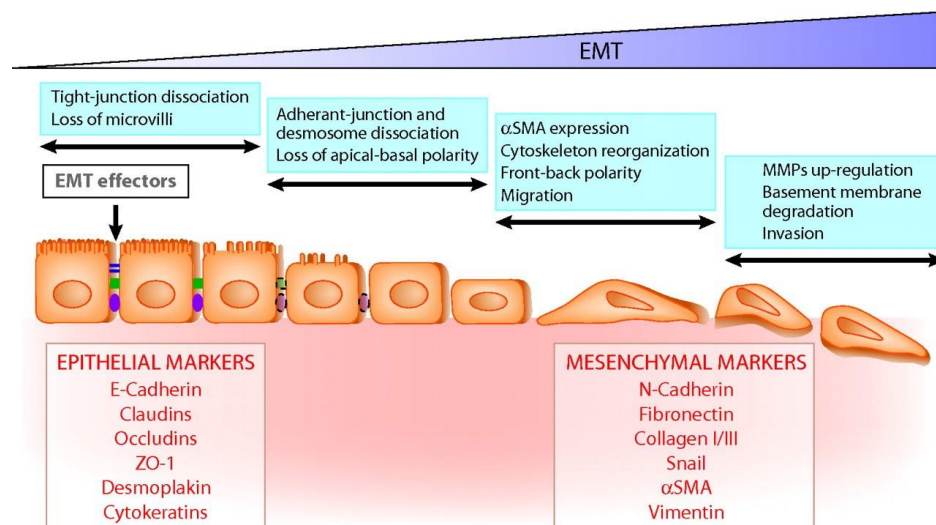


Figure 1.9 Hypothesised method of EMT. EMT effectors include TFG- β , EGF, Wnt, PI3-K. Reproduced from [96].

An emerging protein that has been implicated in the invasion pathway of cancers is podoplanin, a small transmembrane protein

present primarily on endothelial cells¹¹⁵. Although its role in normal cell development is not fully understood, mice knock out models are not viable due to poor lung, heart and lymphatic function¹¹⁶. *In vitro* manipulation of cell lines with upregulation of podoplanin results in greater migratory characteristics and therefore is included in this analysis¹¹⁷.

1.4.2 Role in Cancer

E-cadherin, a transmembrane protein responsible for cell-cell adhesion has been a protein of focus for many years and mixed results have been published on its expression and correlation to nodal metastasis¹¹⁸⁻¹²¹. A meta-analysis on the expression of E-cadherin and nodal metastasis concluded decreased expression of E-cadherin resulted in poor prognosis in patients with HNSCC¹²². However, their analysis only included one study that included a low subset of oropharynx samples. A study that limited their sample selection to 154 HPV-negative oropharyngeal tumour samples concluded that E-cadherin was reduced in primary tissue but this did not significantly affect overall survival or disease-free survival¹²¹. The possibility of E-cadherin as a biomarker for nodal metastasis is particularly important in patients who present as node negative or are planning to undergo sentinel lymph node

biopsies, a procedure that samples part of the lymph nodes before opting for a full neck dissection. It is also important for HPV-positive patients as it could give evidence for the first time the cause of such high incidences of nodal metastasis. Two independent studies conducted by Huber et al on 120 HNSCC patients undergoing the sentinel lymph node procedure (91.7% oral cavity; 8.3% oropharynx) confirmed down regulation of E-cadherin in the primary tumour significantly correlated to lymph node metastasis, and upregulation of podoplanin is also significantly associated to nodal status, however the two markers were not tested in parallel^{123,124}.

The role of EMT and podoplanin in HPV-positive disease is just beginning and Hu et al¹²⁵ demonstrated the necessity of HPV16 E6 and E7 to promote EMT via the downregulation of the epithelial marker E-cadherin and the upregulation of the mesenchymal marker N-cadherin in cervical cell lines. However, results in the literature are mixed when observing the relationship of podoplanin and prognosis in oral and oropharyngeal cancers. Wakisaka et al¹²⁶ had a small sample size (n=22) and determined EMT was upregulated in HPV-positive OPSCC samples, yet podoplanin was conversely downregulated which led to lymph

node metastasis which does not appear to fit with *in vitro* functional analysis of this protein. Lefevre et al¹²⁷ utilised a much larger cohort of HPV-positive patients from the papillophar study and determined there was “no significant association of EMT to HPV status”. Preuss et al¹²⁸ concluded there was not a prognostic role of podoplanin expression in oropharyngeal SCC, regardless of HPV status.

There are various flaws in the design of these studies, primarily the numbers of HPV-positive cases are small and numbers of patients with poor outcome are even fewer making statistical significance difficult to achieve. The varied results from different groups implies there is still no universal understanding on the role of podoplanin in OPSCC and whether it is linked to nodal progression or overall survival.

Chapter 2: Thesis Aims

Approximately 5% of all human cancers worldwide are caused by HPV¹²⁹, and within the head and neck region the incidence of oropharynx cancer caused by the virus is rising rapidly each year. It was estimated in 2011 that if the incidence trend continued there would be more HPV-positive oropharyngeal cancers by the end of this year (2020) than cervical cases²⁶. The introduction of cervical cancer screening in women can detect precancerous lesions, increasing early detection, preventing invasive cancer incidence, however this approach is not applicable for head and neck disease as it is unknown whether precancerous HPV-positive oropharyngeal lesions exist¹³⁰. There are differences in epidemiological factors driving OPSCC depending on HPV status with HPV-positive patients being younger (median age is five years less than HPV-negative HNSCC at 54)²⁰, more likely to be White and from minimal to no smoking or alcohol consumption backgrounds^{48,84}. This represent a significant shift from HPV-negative oropharyngeal and oral cavity cancers where tobacco and alcohol misuse are major risk factors¹³¹. The majority of oropharyngeal cancers presenting with late stage disease and advanced nodal involvement^{20,132}. Regardless of this apparently

advanced stage of disease, HPV-positive patients respond well to treatment and a major study by Ang et al showed 3-year survival was 82.4% for HPV-positive OPSCC patients compared to 57.1% in HPV-negative OPSCC patients, irrespective of stage, cohort or treatment method⁴⁷.

Many questions remain unanswered, primarily why do more HPV-positive cancer patients experience such a high nodal burden of disease compared with HPV-negative tumours; what underlies the increased sensitivity of these tumours to treatment; and is there a biomarker which can predict outcome in the HPV-positive cohort? The latter is of great importance as more trials are opening to study the effect of de-escalation of treatment based on HPV testing¹³³, improving quality of life by reducing unnecessary side effects from aggressive treatment. However, a reliable prognostic marker could allow clinicians to confidently assign patients to a more suitable, personalised treatment regime because, by inference, 17.6% of HPV-positive tumours do poorly and should not have de-escalated plans.

Currently the study of HPV-positive disease is restricted to animal models or a limited number of commercially available cell lines, as many labs have tried and failed to establish HPV-positive primary cell lines from the oropharynx with little evidence in the literature of successful methods. The limited HPV-positive cell lines available originate from anatomical sites outside of the oropharynx which are rarely HPV-driven e.g. ventral tongue and floor of mouth¹⁵. Furthermore, the cell lines are derived from smokers and heavy alcohol drinkers who do not accurately represent the disease in the population.

The initial aims for the research presented in this thesis are to:

- i) Develop a fully characterised and better representative *in vitro* cell model for HPV-derived OPSCC by successfully culturing primary cells from HPV-positive OPSCC patients.
- ii) Fully characterise the limited number of commercially available cell lines (n=6) to verify their continued use as a research tool in HPV-positive OPSCC *in vitro* studies.

The hypothesis is:

Additional primary cell culture models can be created from a cohort of tissue donated from patients having primary surgical resections for HPV-positive OPSCC and the commercially available HPV-positive HNSCC cell lines accurately reflect the molecular biology of HPV-derived cancer.

If a successful model is validated, this could be used to investigate the mechanism of the aggressive disease dissemination seen in HPV-positive patients.

Studies have reported that the protein podoplanin is an indicator of cancer invasion in breast, lung and pancreatic cancer^{117,134,135} however there is conflicting evidence on its role in oral and oropharynx SCC^{124,126,128}. Epithelial to mesenchymal transition (EMT) remains a widely discussed concept in cancer implying that cells exhibiting an EMT-associated phenotype have the potential to migrate to distant sites.

Further aims of this thesis are:

- iii) Perform cell migration and invasion assays on HPV-positive and HPV-negative OPSCC cells to understand *in vitro* cell movement.
- iv) Determine the EMT signature and the expression pattern of podoplanin for HPV-positive and -negative OPSCC cells by immunohistochemistry and immunofluorescence.

The hypothesis is:

The clinical observation of an increased rate of lymph node invasion indicates that HPV-positive OPSCC cells will exhibit an EMT-associated phenotype and upregulated podoplanin expression, resulting in faster cell migration and invasion in functional assays.

Chapter 3: Materials and Methods

3.1 List of reagents

See Appendix 10.1

3.2 Sample procurement

All patients undergoing surgical resection or pathological biopsy for OPSCC at Aintree University Hospital, Liverpool, UK between November 2013 and October 2016 were approached for informed consent (REC No 10/H1002/53) for an additional sample from tumour, adjacent normal and nodal tissue, if applicable. Patient inclusion criteria was any WHO performance, any tumour staging, over age 18 and any gender. Exclusion criteria was only if they were not fit for surgery. Tumour tissue was identified and removed by the surgeon from planned resected areas and where research sampling would not interfere with diagnosis and pathological margin analysis. Sizes of samples varied from small ($\sim 1\text{mm}^3$) to large ($\sim 3\text{mm}^3$) and were procured from trans-oral laser resection or open surgery. Under the same ethical coverage, 5ml blood was collected and frozen for Standard Tandem Repeat (STR) analysis.

As per NICE guidelines from February 2016 all squamous cell carcinomas of the oropharynx are HPV tested using p16 immunohistochemistry and regarded as a positive result only if there is “strong nuclear and cytoplasmic staining in more than 70% of tumour cells”. However, the detection of p16 alone does not always constitute HPV infection, and thus additional “high-risk HPV DNA or RNA in-situ hybridisation (ISH) in all p16-positive cancers” should also be considered to confirm HPV status³⁰. The protocol routinely carried out for Aintree University Hospital oropharyngeal patients was the combination of p16/DNA ISH and was performed at the Royal Liverpool hospital pathology department on either the biopsy tissue or the resection.

3.3 Cell Culture preparation

3.3.1 Terminology

Definitions derived from ATCC glossary for animal cell culture guide¹³⁶.

- *Cell culture*. Cells are cultivated and maintained *in vitro* and are no longer organised in tissue formation.

- *Cell line*. Once a primary cell successfully subcultures it becomes a cell line. Implies lineage of cells originally present in the primary culture.
 - *Continuous cell culture*. Also referred to as immortal cell culture, cells have the capacity for unlimited proliferation if provided sufficient media and space.
 - *Finite cell culture*. A cell culture with a limited number of population doublings (20-80 passages).
- *Feeder layer*. Cells which are nondividing but metabolically active due to irradiation and can be used as a feeder surface for cell culture.
- *Immortalization*. Cell cultures gaining the attributes of a continuous cell line, whether by perturbation or intrinsically.
- *Passage*. Synonymous with subculture. The transfer or transplantation of cells from one culture vessel to another, with or without dilution.
- *Passage number*. The number of times passaging has occurred since colony initiation. Allows relative cultural 'age' to be calculated.
- *Population density*. Also referred to as confluence. The percentage of cells per unit area of a culture vessel.

- *Primary culture.* A culture initiated from organs, tissues or cells taken directly from an organism. Can be referred to as primary cell lines after initial subculture.
- *Secondary cell lines.* This thesis defines secondary cell lines as those procured from outside the University of Liverpool and have continuous cell proliferation

3.3.2 Culturing conditions

All procedures unless otherwise stated were carried out with aseptic technique in a class II biological safety cabinet with all waste decontaminated with 2% virkon before incineration. Cells and tissue explants were maintained at 37°C in a 5% CO₂ humidified incubator. A 6.27Mm solution of Copper(II) sulphate (CuSO₄) was made by adding 10g CuSO₄ to 10L pure water with 0.2g EDTA to sterilise water baths and humidify the incubator.

3.3.3 Media preparation

Tables 3.1 and 3.2 describes media supplementation for primary cell culture and culturing for continuous cell lines.

Primary culture and low passage cell lines		Media				Supplementation					
		DMEM High Glucose	SFKM	F12	RPMI 1640	FBS (10%)	L- Glutamine (1%/2mM)	Penicillin-streptomycin (2%/200U/mL)	Amphotericin B, Penicillin, streptomycin (2%/5µg/mL, 200U/mL)	BPE 25mg	EGF 2.5µg
Name	Use										
Transport media Nov 2013 – Feb 2016	Washing primary tissue	✓				✓	✓	✓			
Transport media Feb 2016 – Oct 2016	Washing primary tissue	✓				✓	✓		✓		
RPMI	Culturing fibroblasts				✓	✓	✓				
DMEM:F12	Culturing fibroblasts	✓ (50%)		✓ (50%)		✓	✓				
SFKM	Culturing epithelial cells		✓							✓	✓

Table 3.1 Primary culture and low passage cell line media supplementation. Abbreviations DMEM: Dulbecco's Modified Eagles Medium with 4500mg/L; SFKM: Serum-free keratinocyte medium; F12: Nutrient mixture F-12 HAM; FBS: Foetal Bovine Serum; BPE: Bovine Pituitary Extract; EGF: Epidermal Growth Factor, Human Recombinant

Continuous cell lines		Media		Supplementation			
		DMEM High Glucose	MEM	FBS	L-Glutamine (1%/2Mm)	Penicillin- streptomycin (1%/100U/mL)	NEAA (1%)
Name	Use						
DMEM	UMSCC, 93-VU- 147T, SiHa, CaSki, 3T3s culturing	✓		✓ (10%)	✓	✓	
MEM	UPCI:SCC culturing		✓	✓ (15%)	✓	✓	✓

Table 3.2 Continuous cell line media supplementation. Abbreviations DMEM: Dulbecco's Modified Eagles Medium with 4500mg/L; MEM: Minimum Essential Media; FBS: Foetal Bovine Serum; NEAA: Non-Essential Amino Acid

Media for feeder layer primary cultures		
Component	Initial supplements	Additional supplements (48hours after cell seeding)
Glasgow Modified Eagles Medium (GMEM)	10% FBS 500ng/mL hydrocortisone 0.1nM Cholera toxin 100U/mL penicillin-streptomycin	10ng/mL Epidermal Growth Factor (EGF)

Table 3.3 Media for primary cultures on 3T3 feeder layers.

3.4 Primary cell culture

3.4.1 Tissue disaggregation and explant initiation

Tissue destined for primary cell culture was collected directly from the surgical site by the performing surgeon as described in section 3.2. Tissue was placed immediately in separate universals containing 10ml sterile transport medium (Table 3.1). Tissue collected from Feb 2016 onwards was supplemented with additional 2.5µg/ml Amphotericin B due to increased incidences of fungal contamination (Table 3.1). Tissue was immediately transported at ambient temperature to the laboratory based at

Aintree University Hospital where it was processed within an hour of excision.

Oral cavity primary cells were isolated previously following the explant method which is described in detail by Kedjarune et al and Jagtar Dhanda^{137,138} and the same technique applied for these oropharyngeal tumours, normal tissue and nodal tissue. Briefly, tissue was washed in sterile transport media three times for 30mins before being transferred to a CellBind™ 6-well plate for dissection of any visible blood vessels and fat cells. Tissue was suitably minced by two no.11 Swann scalpels until a homogenous consistency was achieved. Cell populations were dispersed by a Pasteur pipette into the remaining 5 wells with repeat mincing of large fragments if required. Sterile transport medium was added dropwise until a 'film' covered the surface of each well. Plates were incubated at 37°C/5% CO₂ for 2hours to maximise tissue adherence.

To encourage distinct cell populations to grow, specific media was used in duplicate wells. Table 3.1 describes the supplementation for RPMI 1640, High Glucose DMEM (4500mg/L):Nutrient Mixture

F-12 HAM (1:1) (DMEM:F12) and serum-free keratinocyte media (SFKM). Due to the fast degradation of SFKM supplementation, small quantities (50ml) were prepared for each time point. Fresh media was prepared every 4 weeks.

After incubation, 1ml of appropriate media was added dropwise down the side of each well to avoid tissue dislodging. The plate was returned to the incubator and left undisturbed for 48hours before an additional 1ml media was added with the same method. Media was changed twice weekly, and to encourage further colony production from small floating pieces of tissue of cells, the first wash after tissue adherence was transferred to T25 flasks (combining duplicate wells).

Each well and culture flask had a unique nomenclature to allow for distinct colony identification and to allow later passages of a cell line to be traced back to their starting well conditions. The nomenclature was derived from:

1. Liv(patient#)
2. Tumour(T)/Normal(N)/Node

3. Fibroblasts(F)/Keratinocytes(K)/mixed(M)
4. RPMI(R)/SFKM(S)/DMEM:F12(D)
5. Well#(1-6)/Blank(combined medium in flasks)

For example, Liv64TFR4 refers to tumour fibroblasts from patient number 64 which originated from well 4 originally containing RPMI medium.

3.4.2 Establishing a monolayer

Once colonies were established from adhered tissue or single cells they were monitored visually with an upright EVOS XL Core Microscope. Colonies were ready for transfer to flasks when they reached 2-3mm in diameter, when cells started growing on top of each other or when cells began lifting off encased in extracellular matrix (ECM). To remove cells, media was removed and wells washed gently with 2ml sterile Phosphate Buffered Saline (PBS) and incubated at 37°C in 1ml Trypsin-EDTA for 3mins. After incubation, cells were mechanically removed with a 1.8cm cell scraper and neutralised with 20ml DMEM:10% FBS. Cell suspensions were spun down in an Eppendorf centrifuge at 1200rpm with added brake for 5mins and the cell pellet resuspended in 2ml media. Depending on size and rate of colony growth cells were dispersed into T12.5 or T25 flasks and topped

up to 4ml or 8ml respectively. Keratinocytes and fibroblasts then grew in colonies until monolayers formed and passaged 1:2 as described in Figure 3.1 at 60-70% confluence using Trypsin-EDTA.

3.4.3 Passaging cells from flasks

Cells were subcultured (passaged) around 70-80% confluence. Flasks were washed with PBS and incubated with Trypsin-EDTA for 3mins at 37°C. Flasks were agitated to dislodge cells and neutralised with 20ml DMEM+10% FBS. Cell suspensions were centrifuged as previous described and resuspended in multiple vessels. If a proportion were for cryopreservation an additional centrifugation step was added after the correct number of cells were placed in fresh flasks.

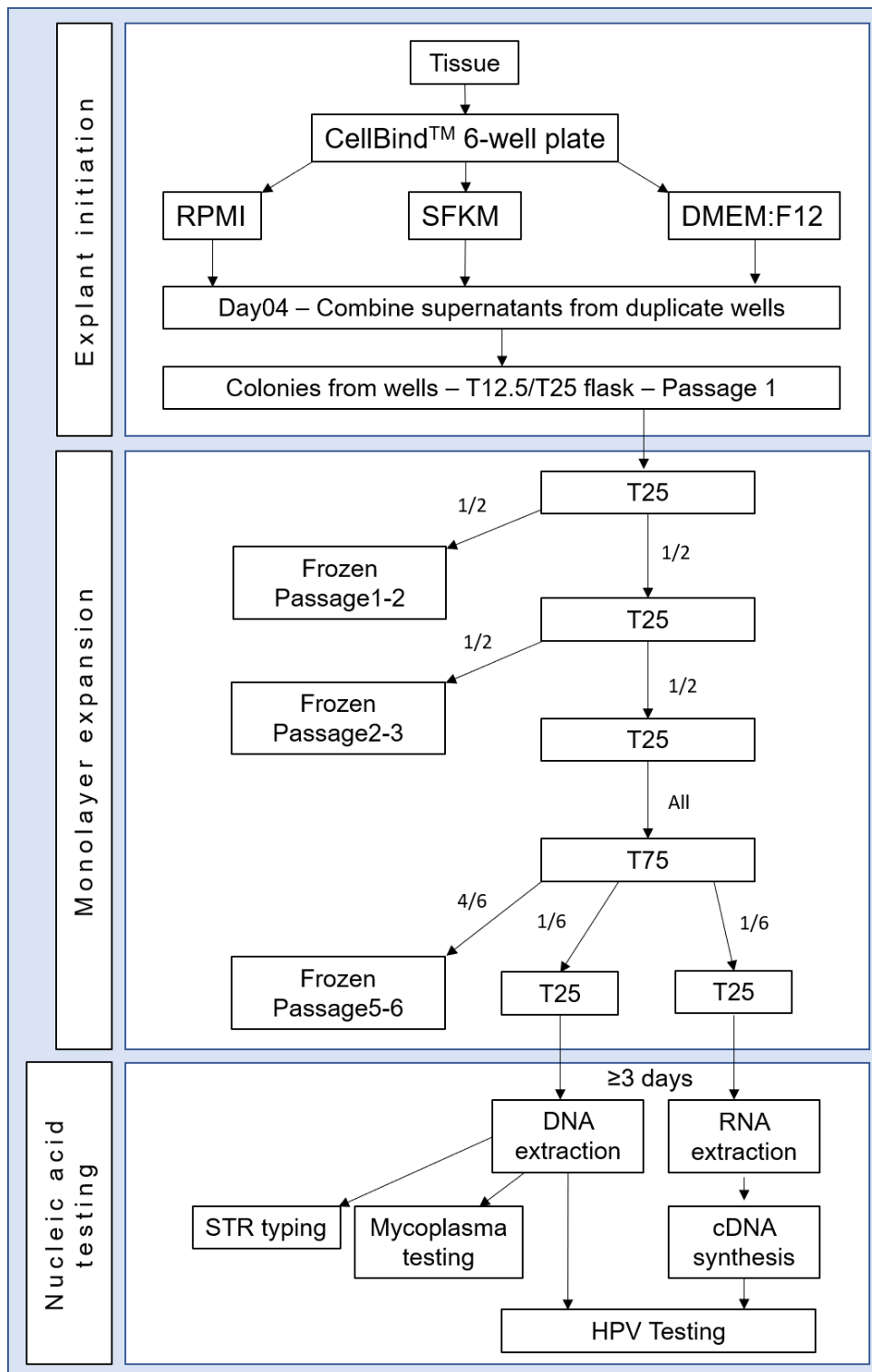


Figure 3.1 Flowchart for cell passaging from explant initiation to nucleic acid extraction

3.4.4 Cell preservation and resurrection

At each passaging step demonstrated in Figure 3.1, at least half of the flask contents was cryogenically frozen for storage. Cells were washed in PBS, pelleted and resuspended in 1ml cold cell-freezing medium, containing the cryopreserving solvent dimethyl sulfoxide (DMSO) which protects against crystal formation during freezing and must be added dropwise to reduce cell injury due to sudden exposure to DMSO content¹³⁹. Cell suspensions were transferred to 1.8ml external thread cryovials and stored for 24hours in Mr Frosty with isopropanol in -80°C freezer with a cooling rate -1°C min⁻¹. The slow freezing protocol reduces the formation of intracellular freezing which is lethal to cells^{140,141}. Once frozen, cryovials were transferred to vapour phase liquid nitrogen (LN2) storage and documented. For continuous cell lines cultured at higher cell densities, 1x10⁶ cells/cryovial were counted using the method described below (3.4.5)

Resurrection of cells required fast thawing at 37°C to limit ice recrystallisation and reduced cell viability^{142,143}. DMSO was diluted by warmed PBS and cells pelleted and resuspended in suitable a

suitable vessel. Media was changed the following day to dilute any remaining DMSO in solution.

3.4.5 Counting cells

A Beckman Coulter Z series cell counter was used to count cells. Cells were initially trypsinised and resuspended in 20ml media and 10 μ L of cell suspension added to 10ml Isoton II Diluent in an accuvette cup with cap. Cap was replaced and solution mixed by inverting. A profile was set up on the Z series to input the dilution factor as 1E +02 and minimum cell size (6 μ M) and maximum cell size (18 μ M). Machine was initially blanked with Isoton II Diluent before sample processed to give a in cells/ml. Example in Figure 3.2. Total cell number = concentration x initial volume (20ml).

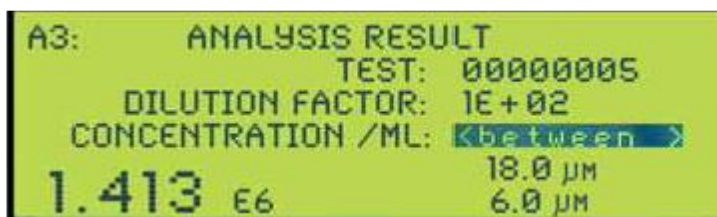


Figure 3.2 Example of cell counting results screen. Final concentration is given /1ml e.g. 1.416E6

3.4.6 Feeder layers

Samples collected from August 2015 (Liv94 – Liv111) were seeded on additional plates with a 'feeder' layer of irradiated fibroblasts. The protocol has been previously used for cervical keratinocytes⁹⁶ and recently proved successful in Dr N Powell's lab for culturing HPV-positive oropharyngeal cell lines⁹⁷. Initially, low passage (<20) mouse 3T3 fibroblasts, gifted from Dr Powell, were cultured in T75 flasks with DMEM+supplements (Table 3.2) until 80% confluent. The entire flask was then irradiated in the benchtop irradiator CellRad[®] by Faxitron at a rate of 2Gy/min for a total of 60Gy irradiation.

Irradiated fibroblasts were trypsinised as described in 3.4.3 and pelleted at the same time as tissue disaggregation. A T75 flask was sufficient to coat 3x6-wells in a NUNC coated plate. The protocol from 3.4.1 was followed however tissue was dispersed across 2x6-well plates (CellBind[™] and NUNC). After tissue adherence, explants with feeders were supplemented with GMEM media (Table 3.3) and $\sim 1 \times 10^6$ 3T3 fibroblasts/well. After the 48hour incubation period, GMEM media was replaced with EGF-positive media (Table 3.3). Cells were under daily observation

and for any spaces that developed in the feeder layer, additional fibroblasts were added during the later media changes.

For initiation of Liv110 and Liv111, 3T3s were replaced with irradiated normal Liv86 fibroblasts which had been established during cell line development. GMEM and SFKM was used in separate wells with feeders.

3.5 Secondary Cell Culture

3.5.1 Cell line procurement

10 head and neck cell lines were procured on the basis of their previously reported HPV status. UMSCC-4, UMSCC-6, UMSCC-19, UMSCC-74A (HPV-negative) and UMSCC-47 and UMSCC-104 (HPV-positive) were a kind gift from Dr Thomas Carey, University of Michigan, Michigan, USA. UPCI:SCC090, UPCI:SCC152 and UPCI:SCC154 (HPV-positive) were gifted by Dr Susanne Gollin, University of Pittsburgh, Pittsburgh, USA and finally 93-VU-147T (HPV-positive) was a kind gift from Dr Josephine Dorsman, VU University Medical Centre, Amsterdam, The Netherlands. Two HPV-positive cervical cell lines; SiHa

(ATCC-LGC-HTB-35) and CaSki (UK Health protection Agency Culture Collection – 87020501) were used as controls.

Media preferences for each cell line are documented in Table 3.2.

3.6 Nucleic Acid Extraction

3.6.1 Extraction from cultured cells

3.6.1.1 DNA extraction

DNA extraction from cultured cells utilised direct lysis of 80% confluent T25 flasks (max 5×10^6 cells) >3 days after trypsinisation, due to the possible interference of trypsin on mycoplasma detection¹⁴⁴.

The spin column protocol from DNeasy Blood and tissue kit was followed and buffers AW1 and AW2 were diluted with the given volume of 100% ethanol on first use. Briefly, flasks were washed with PBS, allowing for 200 μ L to remain in the flask. 20 μ L proteinase K was added directly to the flask and to ensure total surface coverage, flask was gently rocked side to side. 200 μ L Buffer AL was added directly to flask and mixed by tilting flask to

ensure lysis of the whole area. Flasks were stood upright and 200 μ L ethanol (100%) added to lysed cell solution and mixed by pipetting. Total volume (420 μ L) was transferred to a 1.5ml tube and vortexed for 10seconds. The mixture was pipetting directly into the DNeasy Mini spin column and centrifuged for 1min at $\geq 6000 \times g$. Flow-through was discarded and 500 μ L buffer AW1 pipetted into column before an additional centrifuge for 1min at $\geq 6000 \times g$. This process was repeated with buffer AW2 twice, with the second centrifuge for 3mins at 20,000 $\times g$ to ensure the membrane was fully dry and all ethanol removed. DNA was eluted using 200 μ L warmed (56 $^{\circ}$ C) Buffer AE. Total DNA quantity and quality were assessed by NanoDropTM One/One^C Microvolume UV-Vis Spectrophotometer. DNA absorbs at 260nm, proteins absorb at 280nm, other contaminants e.g. EDTA absorb at 230nm so ratios of these values can provide details on the purity of sample. DNA passed quality control if $A_{260}/A_{280} > 1.8$ and A_{260} reading was between 0.1 and 1.0. If A_{260} was higher, the elution was diluted as necessary. Lysates were stored at -20 $^{\circ}$ C.

3.6.1.2 RNA extraction

miRNA and total RNA were extracted simultaneously using miRNeasy kit for tissue and cells. Initially, Buffer RWT and Buffer RPE were diluted with 30ml 100% ethanol. If expected RNA yield is $<1 \mu\text{g}$ ethanol was substituted with 45ml isopropanol. Work was performed quickly at room temperature and all surfaces, pipettes and tubes sprayed with RNaseZapTM before commencing. Briefly, $<3 \times 10^6$ cultured cells (80% confluence T25 flask) were trypsinised (3.4.3), pelleted and disrupted with 700 μl QIAzol Lysis Reagent and homogenised by vortexing for 1min before incubating at room temperature for 5mins. 140 μL chloroform was added, tube secured before shaking vigorously for 15sec in a fume cupboard and incubating at room temperature for 2-3mins. Mixture was centrifuged at 4^o C for 15mins at 12,000 x *g*. After centrifugation there were three distinct phases in which only the top, colourless aqueous phase contains RNA. This upper phase (estimated 350 μL) was transferred to a new collection tube and 1.5 volume (525 μL) 100% ethanol added and mixed thoroughly by pipetting. Immediately 700 μL of the sample was transferred into a RNeasy Mini spin column and centrifuged for 15sec (room temperature) at $>8000 \times g$. This was repeated for the remainder of the sample and the flow-through discarded. As downstream

analysis e.g. real-time quantitative-Polymerase Chain Reaction (rt-qPCR) is very sensitive to small amounts of contaminated DNA it is important to include an on-column DNase digest step at this point (preparation described below).

On-Column DNase Digest Preparation

The initial preparation of DNase I stock solution required dissolving the lyophilized DNase I (1500 Kunitz units) in 550 μ L RNase-free water. To avoid loss of powder, water was injected using an RNase-free needle and syringe and mixed. As DNase I is sensitive to physical denaturation, mixing was done by gently inverting rather than vortexing and 10 μ L aliquots prepared and frozen at -20 $^{\circ}$ C until use.

After the remaining sample has passed through the membrane, flow-through was discarded and 350 μ L Buffer RWT was pipetted onto the column and centrifuged at room temperature at >8000 x *g* for 15seconds. 10 μ L reconstituted DNase I stock was diluted in 70 μ L Buffer RDD and mixed gently by inverting the tube and pipetted directly onto the column membrane to be incubated at room temperature for 15mins. An additional 350 μ L Buffer RWT

was added and column centrifuged at $>8000 \times g$ for 15secs before adding 500 μ L Buffer RPE and repeating the 15sec spin. To ensure no ethanol was carried over to the RNA elution, an additional Buffer RPE wash was performed with longer 2min spin. To elute RNA from the membrane 30-50 μ L RNase-free was pipetted directly onto the column membrane in a new 1.5ml collection tube and centrifuged for 1min at $>8000 \times g$. If expected yield is high ($>30\mu$ g), this step was repeated. However, if RNA yield was expected to be low, concentration could be increased by reusing the first eluate. RNA quality and quantity were measured using NanoDropTM and total amount noted. RNA passed quality control when $A260/A280 > 2$ and $A230/A280$ between 2.0 and 2.2¹⁴⁵. Lysates were stored at -80°C .

3.6.2 Extraction from blood and tissue

The only difference with DNA and RNA extraction protocols for tissue and blood were lysis and homogenisation/disruption steps respectively.

Patient matched DNA was extracted from blood or snap frozen tissue (normal for STR typing, tumour for HPV testing) that was

taken during surgery. <25mg tissue was cut up into small pieces with two scalpels and added to 180µL Buffer ATL with 20µL proteinase K, vortexed and incubated overnight at 56°C until completely lysed. 10µL blood sample was added to 20µL proteinase K and total volume adjusted to 220µL with PBS before adding 200µL Buffer AL, vortexed and incubated for 10mins at 56°C. DNA extraction continued as per instructions for cultured cells and lysates transferred to a DNasy Mini spin column.

Tissue for HPV testing and RNA extraction was homogenised using stainless steel beads (5mm) and a TissueLyser II. Tubes were kept on dry ice and tissue and 700µL QIAzol Lysis Reagent added together and secured. Tubes were placed in the TissueLyser Adapter and ran for 2mins at 20-30 Hz and repeated until on tissue debris was visible. Protocol continued as per instructions for cultured cells and chloroform added and shaken.

3.7 Cell line validation

3.7.1 Mycoplasma testing

Mycoplasma testing was done using e-MycTM Mycoplasma PCR detection Kit with the required PCR reaction components premixed in reaction tubes (Table 3.4). 20 μ L volume of 50-100ng template DNA and DNase/RNase-free water was added to each tube. Negative controls had no template DNA and positive control was provided control recombinant DNA that contained partial 16S sequence of *M. hyorhina* and diluted by addition of 1 μ L in 19 μ L DNase/RNase-free water. PCR reaction was carried out in standard PCR machine with the protocol detailed in Table 3.5.

5 μ L PCR products were loaded on a 2% agarose gel made with 1X TBE buffer (1L) with 10 μ L SYBR Safe DNA gel stain. 5 μ L 1Kb ladder was added on either side of samples wells. A 6cm gel ran for 40mins at 100V before being imaged under UV light.

Contents	Composition
DNA Polymerase	2.5U
Chemical Stabilizer	1x
Loading Buffer	1x
dNTPs	250mM each
Tris-HCl (pH 8.3)	10mM
KCl	50mM
MgCl ₂	1.5mM
Mycoplasma Primers Set	
Internal Control	
8-MOP (dissolved in DMSO)	

Table 3.4 Contents of e-Myco™ Mycoplasma PCR Detection Kit

PCR condition		Temperature	Time
	Initial denaturation	94°C	1 min
35 cycles	Denaturation	94°C	30 sec
	Annealing	60°C	20 sec
	Extension	72°C	1 min
	Final Extension	72°C	5 min

Table 3.5 PCR Conditions for mycoplasma testing

All primary cell lines were negative for mycoplasma. All secondary cell lines except UMSCC-19, UMSCC-47 and UMSCC-6.

UMSCC-6 and UMSCC-19 were removed from characterisation profiling and UMSCC-47 was not used for migration assays.

3.7.2 Short Tandem Repeat (STR) analysis

To ensure that the novel cell lines produced originated from the original patients, STR analysis of various passages were compared to blood/fresh tissue DNA using GenePrint® 10 System.

DNA Amplification

DNA was normalised to 2.5ng/ μ L for the addition of 5ng total DNA to the PCR Amplification mix detailed in Table 3.6 for a final volume of 10 μ L. Initially water, mastermix and primer vortexed to mix and added to the PCR plate (volume 8 μ L) or PCR strip. 2 μ l template DNA/negative control (amplification grade water) was added to each well and mixed by pipetting. The plate was then placed on a thermal cycler with protocol detailed in Table 3.7.

If fragment analysis was not immediate, amplified products were stored at -20°C in light-protected box.

Component	Volume per reaction	
Water, Amplification Grade	4 μ L	Mix together and plate 8 μ L/reaction well
<i>GenePrint</i> ® 10 5X Master Mix	2 μ L	
<i>GenePrint</i> ® 10 5X Primer Pair Mix	2 μ L	
Template DNA (2.5ng/ μ L)	2 μ L	
Total reaction volume	10 μ L	

Table 3.6 PCR Amplification mix for amplification of extracted DNA for STR Typing

Temperature	Time	Cycles
96°C	1min	
94°C	10sec	30 cycles
59°C	1min	
72°C	30sec	
60°C	10min	
6 °C	Hold	

Table 3.7 Thermal cycling protocol for STR Typing

Fragment Analysis

A loading cocktail was initially made from the Internal Lane Standard (ILS) 600 and Hi-Di™ formamide as follows:

$$[(0.5\mu\text{L ILS 600}) \times (\# \text{ samples})] + [(9.5\mu\text{L Hi-Di}^{\text{TM}} \text{ formamide}) \times (\# \text{ samples})]$$

This total volume was vortexed and 10 μL pipetted into each well of a 96-well plate with 1 μL amplified DNA from 3.8.1. In addition to the positive DNA control, a reaction for 1 μL *GenePrint*® 10 Allelic Ladder (AL) mix was required. After mixing, the plate was centrifuged to remove air bubbles and denatured at 95°C for 3 minutes before immediately getting chilled on crushed ice for 3 minutes. This step had to be done immediately prior to loading to

the Applied Biosystems 3130 Genetic Analyser for processing.

Results were analysed using GeneMapper® software.

The STR Loci tested were Amelogenin, CSF1P0, D13S317, D16S539, D5S818, D7S820, THO1, TPOX and vWA.

3.8 HPV Testing

3.8.1 cDNA synthesis

To test for HPV oncogene expression, RNA was converted to cDNA via reverse transcription (RT). To further eliminate any genomic DNA, 200ng-1µg Total RNA was incubated with 2µL gDNA Wipeout Buffer 7x for 2mins at 42°C and then immediately transferred to ice (Final volume 14µL). The RT Mastermix was prepared as described in Table 3.8 and added to the 14µL Template RNA before incubation at 42°C for 15mins followed by 95°C for 3mins to inactivate the reverse transcriptase enzyme. If reaction was not proceeding immediately to rt-qPCR, reactions were stored at -20°C.

Component	Volume per reaction	
Quantiscript Reverse Transcriptase (contains RNase inhibitor)	1 μ L	
Quantiscript RT Buffer 5X (contains Mg ²⁺ and dNTPs)	4 μ L	If doing routine reverse transcription, can premix, aliquot (5 μ L) and store at -20°C
RT Primer Mix	1 μ L	
Template RNA	14 μ L	
Total reaction volume	20 μ L	

Table 3.8 Reverse-transcription reaction components

3.8.2 Real-Time Quantitative Polymerase Chain Reaction (rt-qPCR)

Primers and Probes

To detect HPV oncogenes and semi-quantify their expression, real-time quantitative PCR (RT qPCR) was used for HPV16 E6, HPV16 E7, HPV16 E2 and HPV18 E6 using TaqMan® technology (Applied biosystems) with custom primer and probe sequences designed previously within our lab group and published by Schache et al¹⁴⁶. Briefly, primers and probes were designed using the Primer Express v2.0 Software and validated with Basic Local Alignment Search Tool (BLAST) and detailed in Table 3.9. The single-copy gene RNase P and β -Actin acted as internal control

and primers and probes were commercially available with TAMRA and VIC reporters respectively. Primer/Probe mixtures were prepared as 500nmol/L (5 μ L) forward/reverse : 250nmol/L (2.5 μ L) probe with 87.5 μ L amplification grade water before adding to PCR reactions and could be stored at -20°C for long-term storage.

Reaction preparation

DNA and cDNA samples were normalised to 50ng/ μ L. Samples were run in duplicate in FAST Optical 96-well plates. β -Actin and RNase P were endogenous controls for cDNA and DNA respectively and CaSki and SiHa acted as positive controls for HPV16 and HeLa for HPV18. Each reaction had a final volume of 20 μ L consisting of 10 μ L TaqMan[®] Universal PCR Mastermix; 0.2 μ L Uracil-DNA glycosylase (UNG); 1.8 μ L Target Primer/Probe mix; 1 μ L endogenous control Primer/Probe mix; 5 μ L ddH₂O and 2 μ L (1000ng) template DNA/cDNA. Reactions were mixed in duplicate volumes and split into 2 x 20 μ L reactions.

Target	Forward sequence	Reverse sequence	Probe (FAM-Labelled MGB Taqman)
HPV16 E6	CTGCGACGTGAGGTATATGACTT T	ACATACAGCATATGGATTCCCATC T	CTTTTCGGGATTTATGC
HPV16 E7	TTCGGTTGTGCGTACAAAGC	AGTGTGCCCATTAACAGGTCTTC	CACGTAGACATTCGTACT T
HPV16 E2	GATGGAGACATATGCAATACAAT GC	CACAGTTACTGATGCTTCTTCACA AA	TACAAACTGGACACATAT AT
HPV18 E6	AAACCGTTGAATCCAGCAGAA	GTCGTTCTGTCGTGCTCG	TTGCAGCACGAATGG

Table 3.9 Primer and probe sequences for HPV16 E2, E6, E7 and HPV18 E6 rt-qPCR

Plates were processed on Applied Biosystems 7500 FAST system with the thermal cycle described in Table 3.10.

Stage	Temperature	Time	Cycles
UDG Incubation	50°C	20sec	
Activation	95°C	10mins	
Denaturation	95°C	15sec	45 cycles
Annealing/Extension	60°C	1min	

Table 3.10 Thermal cycling conditions for rt-qPCR

DNA threshold detection

The detection threshold for HPV-positive status was set to a gene copy number/diploid cell of >1 after normalising to the internal single gene RNase P control. The threshold had to be met in both duplicate samples and an average of the CT values were taken to calculate each ΔCT . Negative ΔCT = Positive integration.

$$\Delta CT = CT_{Target} - CT_{Housekeeper}$$

cDNA / Relative gene expression

Relative gene expression was calculated by the $RQ=2^{-\Delta\Delta CT}$ method by comparison to CaSki for each run for HPV16 expression and to HeLa for HPV18 expression.

$$RQ = 2^{-\Delta\Delta CT}$$

$$\Delta\Delta CT = \Delta CT_{testing\ sample} - \Delta CT_{calibrating\ control}$$

ΔCT was calculated as an average of duplicate runs.

3.8.3 Fixing Cell Pellets and sectioning

To observe morphology, protein expression and presence of HPV DNA/RNA of cell lines, 2×10^6 cells were trypsinised (3.3.4) and pelleted at high speed (700 x g) in 15ml falcons and carefully fixed with 4% paraformaldehyde (PFA) before getting shipped to Prof Max Robinson at Newcastle pathology department for sectioning and staining (p16 IHC, DNA ISH and RNAscope).

To mount cell pellets, PFA was carefully removed and the bottom of the tube clipped to expose the cell pellet which was then gently removed using a mounting needle into biowrap tissue. The wrapped sample was placed in labelled cassettes for embedding

using a short (2h 20min) biopsy programme with all pump/vacuum, and agitation steps turned off to maintain integrity of the pellet. The paraffin-embedded cell pellet blocks were sectioned (4 μ M) and mounted on frosted slides.

3.8.4 p16 Immunohistochemistry (IHC)

p16 IHC was carried out by Prof Max Robinson at Newcastle pathology facility. Briefly, sections were stained with proprietary kits and the manufacturer instructions followed (CINtec Histology, mtm laboratories AG, Heidelberg, Germany) using a Ventana Benchmark Autostainer. Samples were deemed positive if the p16 stain occupied >70% cells³¹.

3.8.5 High-Risk HPV DNA in situ hybridisation (ISH)

Similar to p16 staining, sections underwent ISH staining at Newcastle pathology facility. The Inform HPV III Family 16 Probe B kit from Ventana Medical Systems Inc. was utilised and manufacturer's instructions followed using a Ventana Benchmark Autostainer. The kit contains a cocktail of labelled probes from different high-risk HPV genotypes including HPV 16 and 18 and is formulated to work with the ISH iVIEW_{BLUE} Plus Detection Kit. The

reaction is illustrated in Figure 3.3 when the probe is initially located by an anti-DNP antibody a series of secondary antibodies bind and are conjugated with Streptavidin-AP (alkaline phosphatase).

The complex is visualised on a light microscope by a blue precipitate formed by 5-Bromo-4-chloro-3-indolyl phosphate (BCIP) and nitro blue tetrazolium (NBT) chromogen. Samples were classed positive if any cells showed nuclear blue staining for any High-Risk HPV oncogene.

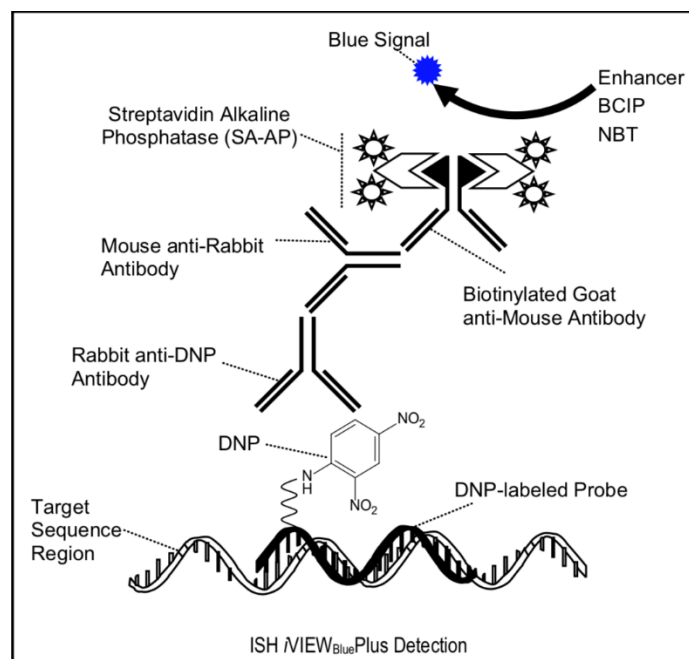


Figure 3.3 Reaction process for DNA ISH. Taken from INFORM HPV III Family 16 Probe User Manual (Ventana; Roche).

3.8.6 High-risk HPV 16 E6/E7 mRNA detection (RNAscope®)

Cell pellet sections underwent RNAscope, a highly sensitive test for HPV E6/E7 mRNA detection at Newcastle pathology facility within a week of sectioning. The RNAscope® 2.5 VS Assay with target-specific probes for E6 and E7 genes of seven high-risk HPV genotypes (HPV16, 18, 31, 33, 35, 52, 58) (Advanced cell diagnostics) were used following the manufacturer's instructions and as previously described^{146,147}. Briefly, sections were pre-treated with heat and protease before the process ran up to 16hours on the Benchmark DISCOVERY® XT System. Initially, the target-specific probes were hybridised to target mRNA, followed by a cascade of hybridisation to horseradish peroxidase (HRP)- and alkaline phosphatase (AP)-labelled probes (Figure 3.4). Detection was via DAB (3,3'-diaminobenzidine) on a light microscope and each distinct dot represented a single RNA transcript. Control probes for Ubiquitin C (*UBC*) (positive control) and the bacterial gene *dapB* (negative control) were processed in parallel¹⁴⁶. A positive result had to have any brown staining (that was higher in intensity than *dapB*) in cytoplasm and/or nucleus.

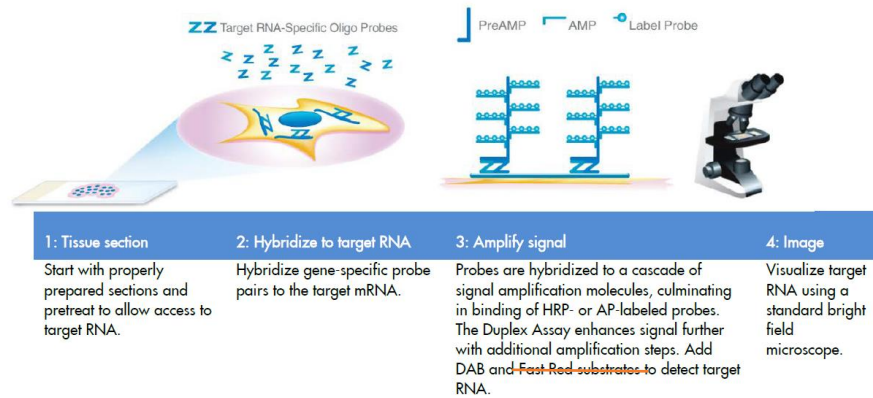


Figure 3.4 Process for RNAscope[®]. Only DAB was used to detect RNA. Taken from RNAscope[®] VS Duplex Assay use manual.

3.9 Migration - wound closing

UMSCC-4, UMSCC-74A, UMSCC-104, UPCI:SCC154, 93-VU-147T, SiHa and CaSki produced suitable monolayers for migration analysis. To observe cell movement in real time, cells were initially seeded in 2-well chambers set 700 microns (μm) apart (Ibidi[®]) Figure 3.5. Initially a single chamber was transferred aseptically to each well in a TC-treated 12-well plate and secured by the adherence bottom of the insert. Each chamber was seeded with $\sim 350,000$ cells/ $70\mu\text{L}$ suitable media in triplicate experiments and incubated overnight. Due to its faster doubling time UMSCC-74A was seeded at a lower density (175,000 cells). The following day the inserts were removed with disposable forceps and the plate washed carefully with PBS and replaced with 3ml media.

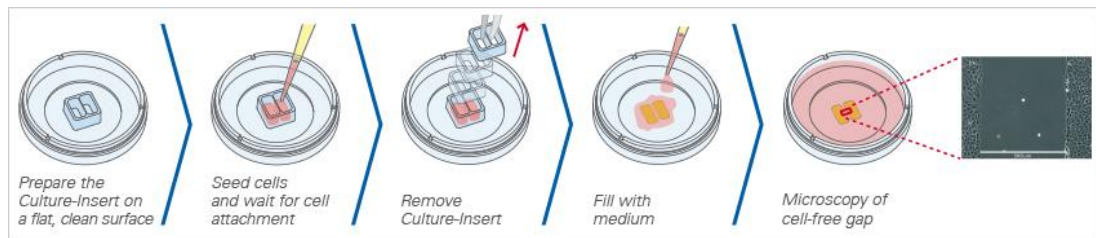


Figure 3.5 Process of seeding cells within chambers (Ibidi®)

Imaging

The plate was placed in a 37°C humidified chamber supplied with 5% CO₂ attached to a Nikon Eclipse T2300 inverted microscope.

Live filming was programmed using Micro-manager 4 through phase/contrast exposure. Two distinct positions across the gap were saved at x10 magnification, away from the top/bottom and in areas clear of floating cells/adhered cells in the gap. Images were saved at 10min intervals for 48hours to capture full wound/gap closing. Only UPCI:SCC154 required an additional 48hours to capture full closure.

Analysis

Video files (.tif files) were imported to ImageJ¹⁴⁸ and macros designed by Dr Carlos Rubbi to adjust phase/contrast intensities and alignment ran on all files. This prevents images shifting from the starting position and normalises the effect of environment light

on the images. An additional stop clock macro was added and video adjusted to frame size 480 x 360 pixels and frame rate 15 frames per second (Appendix10.6). Freeze-point images were acquired per hour and saved as .jpg files.

Rate of wound closure was measured using the software TScratch¹⁴⁹ that allows for automated area calculations. Acquired image were saved under different subdirectories under one top directory, using the same file names for images taken from the same well in the form “cell_line_position number” Figure 3.6 to allow for correct grouping in TScratch analysis.

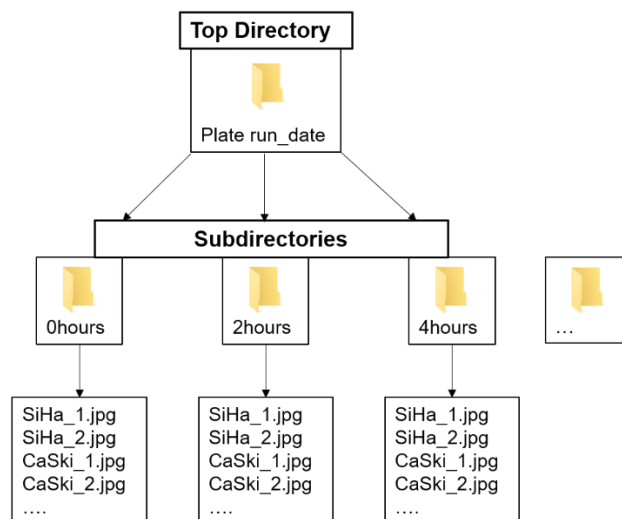


Figure 3.6. Correct directory and subdirectory set up for TScratch analysis

Within the programme, the desired plate run was selected with the option to analyse as a time series, this prompts the user to select the first time point directory. Threshold levels can be altered per image if gap edge is not covered and the output file generated as a text file which can be imported to excel (Figure 3.7). The raw data gives total area of 'free space' i.e. the gap remaining from the total image and so the beginning value is <100% due to the small areas of cells included in the image.

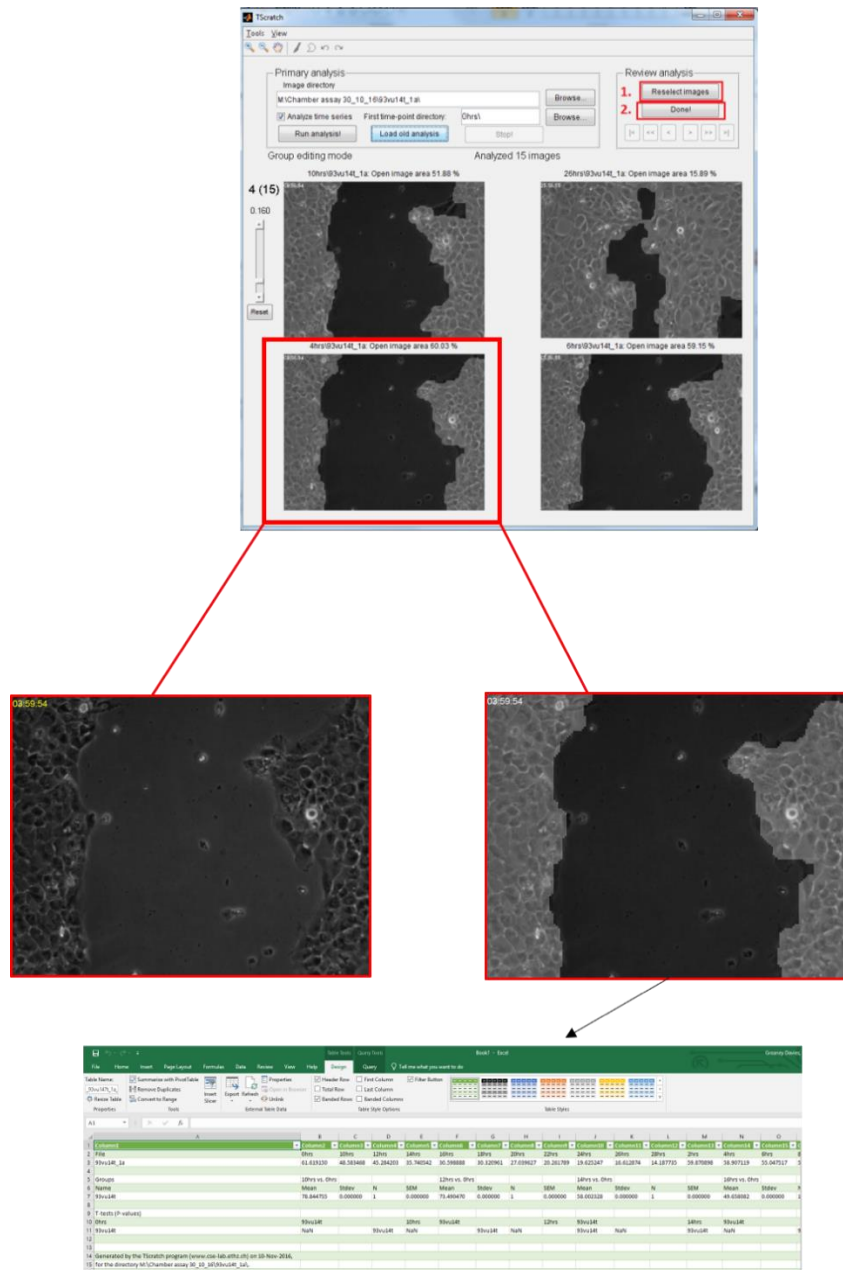


Figure 3.7 Workflow for TScratch analysis

3.10 Tissue Micro Arrays (TMAs)

3.10.1 Case identification

Patients who had surgery for OPSCC between 1988 and 2014 and who had consented to research (Ethical approval numbers: EC47.01; 10/H1002/53 & 09/H1010/54) were identified and

pathology slides and FFPE blocks from their resection sourced. Clinic-pathological details were collected and tumour staging was classified by the reporting pathologist during diagnosis following TNM7 guidelines¹⁷. HPV status was confirmed by p16/ISH positivity in previous publications^{33,146}.

Blocks containing tumour tissue were sectioned (4 μ M) and dried overnight at 37°C before being stained with H&E protocol (section 3.10.1) for visualisation of tumour and normal tissue. Areas of interest (tumour core, advancing front, normal epithelium) were marked by Dr Asterios Triantafyllou on each case H&E slide which could be aligned to the original FFPE block, which is labelled as the donor block (Figure3.8). The planning of each TMA was carefully managed and implemented as described by Parsons et al¹⁰¹ to ensure each block had a unique identifier, the sample cores were arranged asymmetrically, triplicates were deposited away from each other and patients were not replicated along an edge.

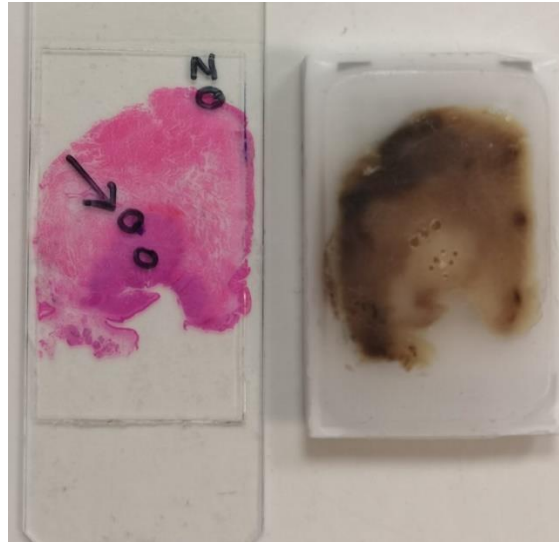


Figure 3.8 Example of H&E slide mark up for tumour (black circle), arrow depicting advancing front and (N)ormal epithelium.

3.10.2 TMA construction

Blank paraffin blocks (recipient blocks) were moulded and x-rayed to ensure they contained no air bubbles. 1mm core punches were attached to the manual tissue microarrayer (Mitogen) with the depth stop kit (3mm). The depth stop kit ensured the same volume of sample is deposited at exactly the same level across cores and therefore sectioning of the TMA included all samples. Initially, recipient blocks were secured to the arrayer and the vertical/horizontal microtomes reset to 0 in the starting position (Core A1). The height of the punches was adjusted to allow for only 3mm cores to be taken (using the depth stop kits) and the recipient

core taken and discarded. Switching punches, 3mm was taken from the donor FFPE block from designated areas and deposited in the hole just created in the recipient block. This process was repeated at 2mm intervals working horizontally before moving down to the next row. Internal controls of liver, kidney, breast and spleen were added to each block and identifiers were either blank spaces or dark-stained waste tissue.

When all cores had been deposited, blocks were incubated at 37°C for 1hour to adhere the donor cores and the top flattened with a microscope slide before being sectioned to 5µM thickness by the Liverpool BioInnovation Hub (LBIH). A total of 11 tumour tissue TMAs, a single TMA with normal tissue cores (reduced core diameter 0.6mm) and a single TMA with 1mm cores from the pelleted cell lines (section 3.8.3) constructed (Figure 3.9)

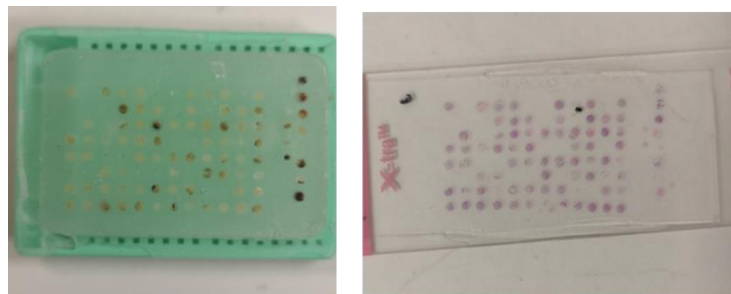


Figure 3.9 Constructed TMA with matching H&E section.

3.10.3 Calculating overall and disease-free survival

Follow up was shortened to 30 months and overall survival calculated as the date of OPSCC diagnosis to date of death if applicable. Patients who had died were censored (defined by “1”) and survival curves generated using Kaplan-Meier method in SPSS 25. Disease-free survival was defined as the date of diagnosis to either date of death or date of recurrence, whichever came first.

3.11 Staining Procedures

3.11.1 Haematoxylin & Eosin (H&E) staining

H&E staining is used routinely by researchers and histology groups to visualise cellular structures due to the differing reactions between tissue and dye. Haematoxylin, a blue-purple basic dye stains basophilic structures e.g. chromatin, ribosomes containing nucleic acids. In contrast, eosin is an acidic dye which counterstains basic elements such as cytoplasm, muscle, red blood cells (RBCs) and collagen with various intensities of pink dye.

Freshly sectioned tissue resulted in stains with the most intensity and uniformity and the full protocol is described in Table 3.11 and follows the basic protocol of dewaxing, dehydration,

Haematoxylin, differentiation, Eosin, dehydration, clearing and finally cover-slipping.

All staining was carried out in a fume extraction cabinet.

Reagent preparation

95%, 80% and 70% ethanol were prepared by diluting 100% ethanol in deionised water. 1% acid alcohol was prepared by diluting Hydrochloric acid in 70% ethanol 1:100. Scott's tap water was provided at x10 concentration and was diluted 1:10 with deionised water. Haematoxylin required filtering before use due to the accumulation of oxidation products after opening. Eosin was an aqueous solution ready made by Thermo Fisher.

Coverslips were applied by placing on blue roll and pipetting a small amount of DPX mountant onto each coverslip with a Pasteur pipette. Stained slides were gently tilted over the coverslips and dropped so mountant spread completely between slide and coverslip. Slides were left to dry overnight at room temperature in fume extraction cabinet.

3.11.2 Immunohistochemistry (IHC)

IHC was performed manually on the benchtop using Dako reagents and equipment. Initially sections of whole tonsil tissue were used to optimise the antibodies N-cadherin, E-cadherin, vimentin and podoplanin with concentrations 1:50, 1:100 and 1:200 diluted with Envision-flex diluent to a total volume [(number of slides x 100 μ L) x 1.10]. Negative controls were made using equal IgG₁ concentrations diluted with Envision-Flex diluent as stated in the data sheets. Staining of TMAs followed the same protocol yet volumes were doubled to ensure full slide coverage.

Dewaxing, rehydration and antigen retrieval

All slides used the Envision-flex (E-F) High pH target retrieval solution within the Dako PT-Link machine. When PT-Link reached

65°C, samples were placed in staining rack and processed. The PT-Link heated to 96°C for 20mins before returning to 65°C (total time 1hour 10mins) and slides placed immediately in E-F wash buffer (diluted with deionised water 1:20) for 5-15mins. Slides were removed from wash and samples destined for staining

circled widely with a hydrophobic pen. At no point were slides left to dry-out and E-F wash was applied routinely.

Staining

All staining was carried out at room temperature on a staining tray following the protocol in Table 3.12.

After slides were dipped in distilled water they were haematoxylin stained as per protocol from step 10 on Table 3.11 but with no eosin counterstain.

3.10.3 Slide digitalising and analysing

All stained TMAs (H&E and IHC) were digitally scanned at x40 magnification by the LBIH using Leica Aperio CS2 slide scanner.

The uploaded files were visualised using the Leica software Aperio ImageScope [v12.4.0.5043].

Step	Component	Process	Time
1	Xylene 1	Dewaxing	5 mins
2	Xylene 2		5 mins
3	Xylene 3		5 mins
4	100% EtOH 1	Dehydrating	20 sec
5	100% EtOH 2		20 sec
6	100% EtOH 3		20 sec
7	95% EtOH		20 sec
8	80% EtOH		20 sec
9	70% EtOH		20 sec
10	Running tap water		2 mins
11	Haematoxylin	Nucleic acid staining	5 mins
12	Running tap water		20 sec
13	1% Acid Alcohol	Differentiation	Dip <5 sec
14	Scott's tap water	Bluing	2 mins
15	Eosin	Cytoplasm staining (counterstain)	2 mins
16	Running tap water		20 sec
17	70% EtOH	Dehydrating	20 sec
18	80% EtOH		20 sec
19	95% EtOH		20 sec
20	100% EtOH 1		20 sec
21	100% EtOH 2		20 sec
22	100% EtOH 3		20 sec
23	Xylene 1	Clearing	5 mins
24	Xylene 2		5 mins
25	Xylene 3		5 mins
26	Coverslip		

Table 3.11 Haematoxylin & Eosin protocol

Step	Component	Volume	Time
1	Envision-flex block	100µL	5mins
2	Diluted primary antibody/negative control	100µL	30mins
3	Appropriate Linker (mouse)	100µL	15mins
4	Horseradish peroxidase (HRP)	100µL	20mins
5	DAB (3,3'-diaminobenzidine)*	100µL	20mins
6	Distilled water	Dip whole slide in	

Table 3.12 Protocol for IHC on bench top. Between each step there was an Envision-Flex Wash repeated 2-3 times. *fresh DAB was prepared by adding 1 drop DAB/1ml DAB substrate buffer

Chapter 4: Establishing primary cell cultures from patients with HPV-positive Oropharyngeal Squamous Cell

Carcinoma

4.1 Introduction

The initial aim of this thesis was to successfully culture cells derived from HPV-positive oropharyngeal tumours that retained HPV16 E6 and E7 oncogenes and had continuous cell growth capabilities.

In addition to isolating keratinocytes that represent the cancer tissue, research around the microenvironment and influence of tumour stroma has been building in recent years^{150,151} and the opportunity to establish cancer-associated fibroblast cell lines as well as normal cell lines would provide a vital resource for future studies.

Owing to the previous success of establishing cell lines from oral cavity cancers, a similar method was initially used for isolating normal and tumour keratinocytes and fibroblasts¹³⁷. The established system for human tissue bio-banking at Aintree University hospital allowed for suitable tissue to be collected routinely and thus multiple experimental approaches to culturing techniques attempted on a large turnaround of samples.

4.2 Results

4.2.1 Patient demographics

Between November 2013 and October 2016, patients with OPSCC undergoing surgery with curative intent consented to donate biopsy-sized samples of their resected primary tumour (n=38), adjacent normal tissue (n=30) and if applicable, nodal tissue (n=6). Details of tissue procurement methods are described in Section 3.2. Under the routine clinical HPV-testing protocol, 65.7% (25/38) patients had confirmed p16/ISH positive tumours. Table 4.1 illustrates available clinicopathological data on available tissue for primary cell culture. Successful cultures could then be linked to pathological identifiers, as demonstrated by Jagtar Dhanda who successfully cultured matched aggressive oral cavity cell lines from ECS-positive patients¹³⁷.

4.2.2 Primary cell culture

Explant initiation

Out of the available 25 HPV-positive primary tumour tissue, seven were placed in duplicate on feeder layers bringing the total number of plates seeded to 32. Due to bacterial/fungal contamination at tissue disaggregation, presumably from the primary site, 22% (7/32) of the total cell cultures were discarded

at the early stages of cell culture. From the remaining 25 plates, 17 samples successfully produced explants from the primary tissue (68%) (3 from plates with a feeder layer) and from these, 12 samples (48%) could successfully be subcultured. One tissue grown on feeder cells reached the passaging stage and Liv105 nodal tissue also produced epithelial cells capable of passaging. The details of each stage per primary cell culture is illustrated in Figure 4.1. Five non-contaminated cultures yielded no viable cells after 4 weeks of culture.

Cancer-associated fibroblasts (CAFs) were more readily isolated from primary cell culture and all the epithelial cells that were subcultured had paired fibroblast cell lines established from the same tissue. Plates prepared with feeder cells were only supplemented to encourage keratinocyte growth. The method to grow distinct cell type populations in isolated wells by media selection proved very successful, and no co-cultures of keratinocytes and fibroblasts were formed.

Success of HPV-negative primary cell culture saw similar outcomes with 5/13 (38%) reaching the subculturing stage and for

two of these (Liv54 and Liv100) only epithelial cells from nodal tissue successfully grew. Normal epithelial cells had a better success rate at 63% (19/30 samples were successfully subcultured) and had similar passaging capabilities as the tumour cells (<passage 5). Overall, 16 individual keratinocyte cell lines were successfully subcultured from 38 oropharynx cases (42% success rate) regardless of HPV status.

Cell morphology

Cell growth was considered to be an explant if they originated from the adhered tissue and remained in contact, whilst cells growing separate from the tissue and, presumably, originating from a single or small number of cells were classed as colonies. Therefore, explants were defined in 6-well plates in the presence of tissue but described as colonies when in flasks. The two derived cell types were fibroblastic and epithelial in appearance and were visually differentiated based on cell morphology, with fibroblasts being elongated cells which grew in all directions, sometimes forming 'swirls' of colonies in a confluent flask whereas epithelial cells form tight, close colonies which are likened to a cobblestone street. Figure 4.2 demonstrates two explants; fibroblasts with no extracellular matrix (A) and

keratinocytes (B). As the donor tissue originated from the core of the resection tumour, any epithelial cells arising from tumour tissue were considered to most likely be tumour cells, whereas fibroblasts were considered to be cancer-associated fibroblasts (CAFs) that make up a substantial part of the tumour stroma. It was observed that most fibroblast explants and unexpectedly some keratinocytes, were initially encased in extracellular matrix (ECM) that, if left too long, led to detachment of the entire colony (Figure 4.3). ECM production seemed to be halted after the cells underwent trypsinisation and grew in a monolayer without the presence of tissue (Figure 4.4). Detachment of donor tissue was incredibly detrimental to explant growth and rarely adhered again once in suspension.

Explants and monolayers originating from HPV-negative tumours and HPV-positive normal tissue produced cells with similar morphology to cells from HPV-positive tumour tissue (Figure 4.5) and had similar proliferation rates.

Factor	Total	HPV-positive (n=25)	HPV- negative (n=13)
Gender			
Male	28	22	6
Female	10	5	5
Unknown	2	0	2
Age			
≤60	10	7	3
>60	15	11	4
unknown	13	7	4
TNM			
T stage			
T1-T2	27	17	10
T3-T4	9	7	2
Unknown	2	1	1
Nodal status			
N0	7	1	6
N+	26	20	6
Nx	5	4	1
ECS			
Positive	14	10	4
Negative	12	10	2
Smoking History			
Current smoker	8	3	5
Ex-smoker	10	8	2
Never smoked	10	8	2
Alcohol consumption			
Heavy (>28units/week)	5	4	1
Moderate (<28units/week)	14	10	4
Non-drinker	4	1	3

Table 4.1 Demographics of donors for primary cell culture

Primary cell culture

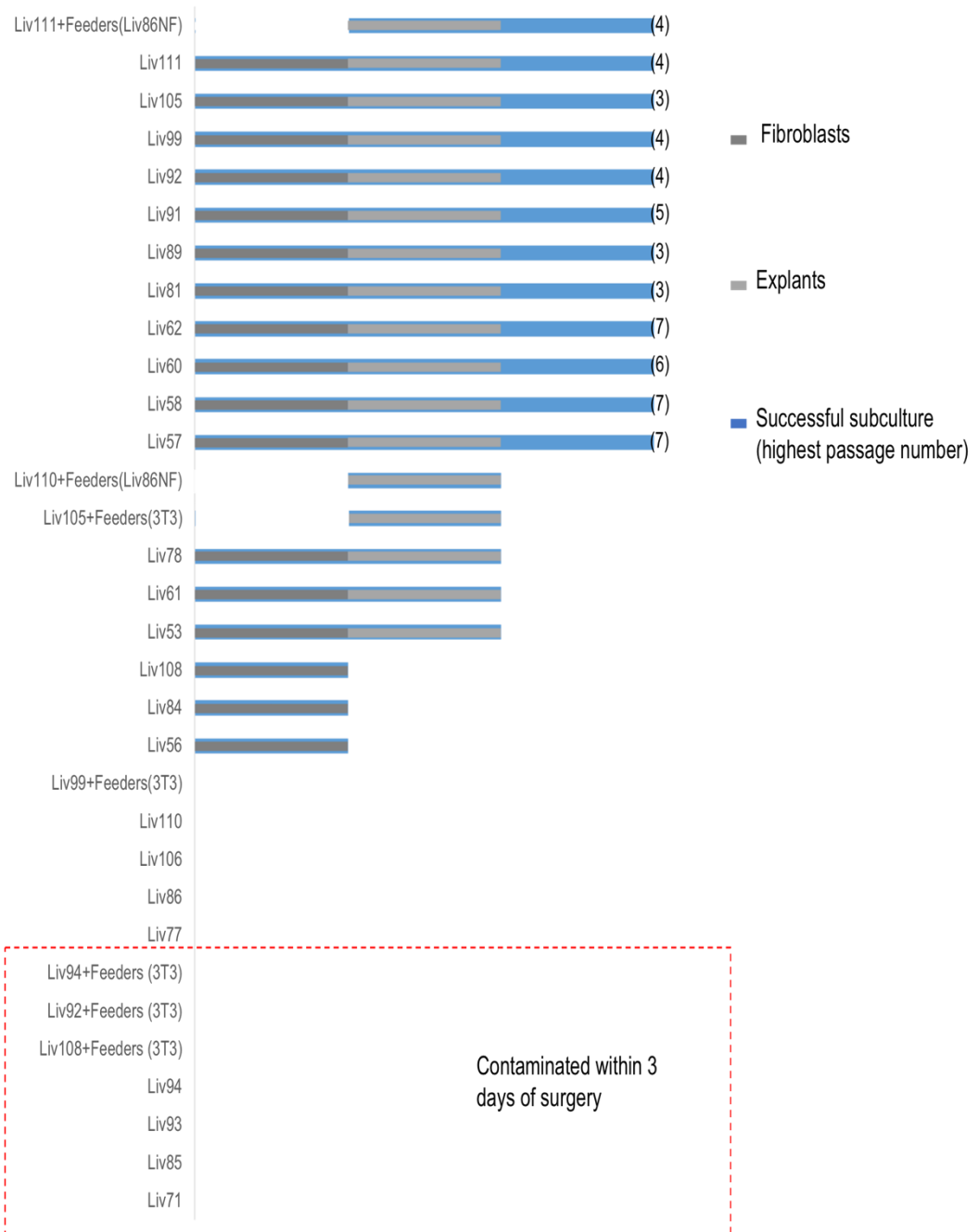


Figure 4.1 Schematic of final stage of each attempted OPSCC primary cell culture.

Cell expansion

From the 12 HPV-positive samples that were successfully subcultured, eight reached sufficient cell numbers for DNA and RNA extraction (Liv57, Liv58, Liv60, Liv62, Liv91, Liv92, Liv111 and Liv111 grown on feeders). Liv61, Liv81, Liv89 and Liv105 could only grow for 3 passages and subsequent cell growth yielding insufficient DNA and RNA for further analysis. HPV-negative keratinocytes and all fibroblasts reached DNA extraction for mycoplasma testing but did not go through HPV-testing.

For all cell types, over confluency affected cell viability and cell adhesion detrimentally and once cells were overgrown and detached they were difficult to re-establish even in fresh flasks.

Cell proliferation rates varied between tumour specimens, with the quickest cell lines reaching passage 6 in as little as 2 weeks (Liv57 and Liv91), having been subcultured every 48hours whereas the remaining successful cell lines took on average 1 month to reach a high enough cell number for DNA extraction and final cell storage. Figure 4.6 illustrates varies time points for cell expansion with Liv57 and Liv58 showing better cell viability than Liv60 at passage 6. Liv60 began to show cell senescence, demonstrated by the lack of dividing colonies and enlarged cells.

Figure 4.6DE demonstrates the change in explant growth and explants could be present after 48hours initial incubation

Frozen cells were resurrected successfully but did not grow past the finite passage number, implying those cells were destined for a limited number of divisions. The two quickest cell lines Liv57 and Liv62 began to slow down their growth past passage 5 implying they are not capable of continuous cell passaging but this was not tested.

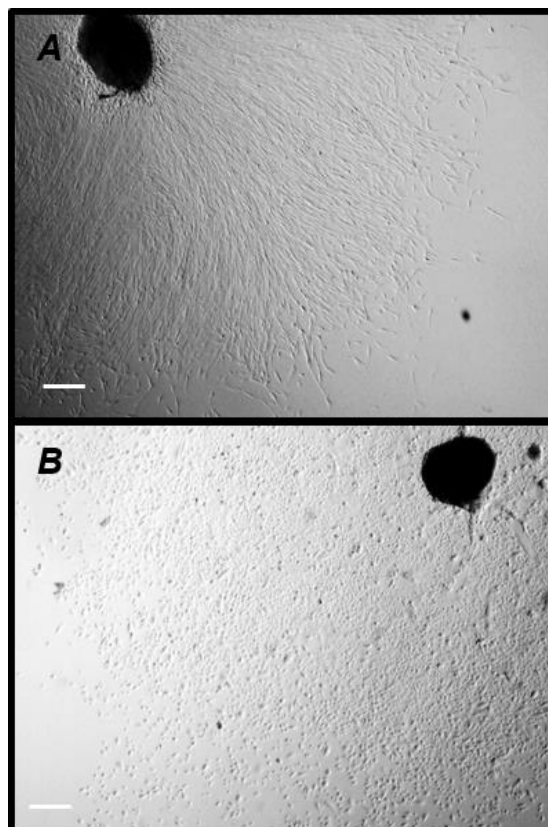


Figure 4.2 Fibroblast explant (A); Keratinocyte explant (B). Both show cells at high density around the donor tissue with

keratinocytes starting to grow on top of one another.

Magnification x10 Scale bar=60 μ M

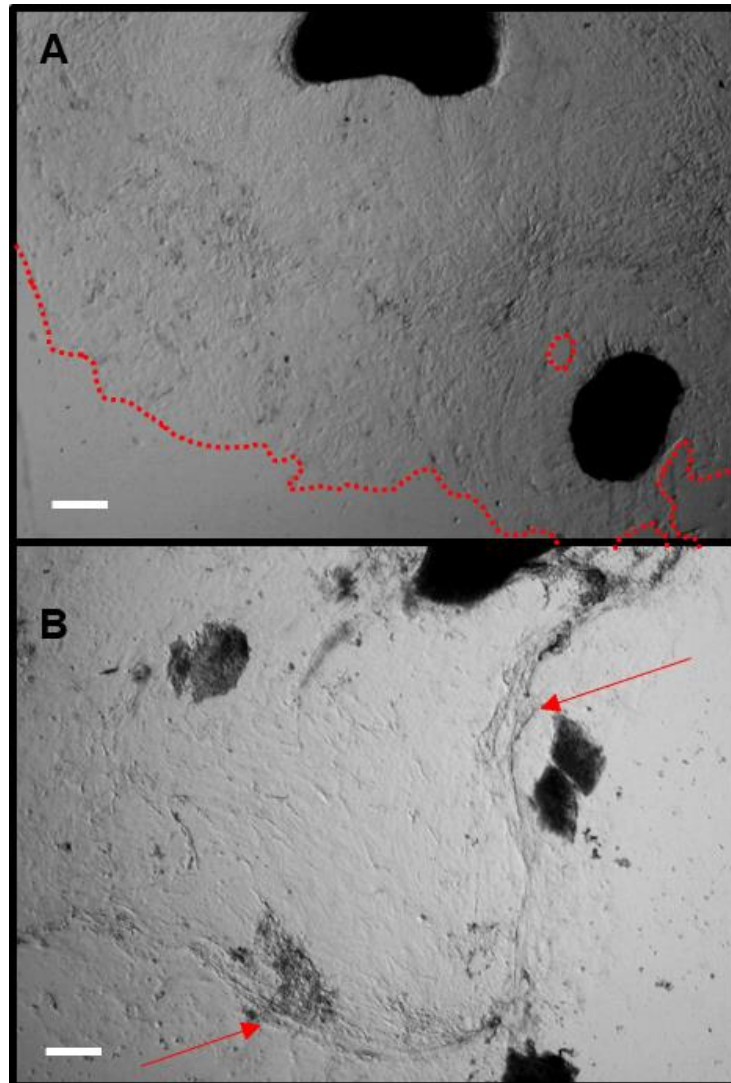


Figure 4.3 Fibroblast explants encased in ECM, outlined in red. B shows the detachment of the matrix (arrows) which, if not trypsinised could lead to detachment of the explant, Magnification x10 Scale bar=60 μ M

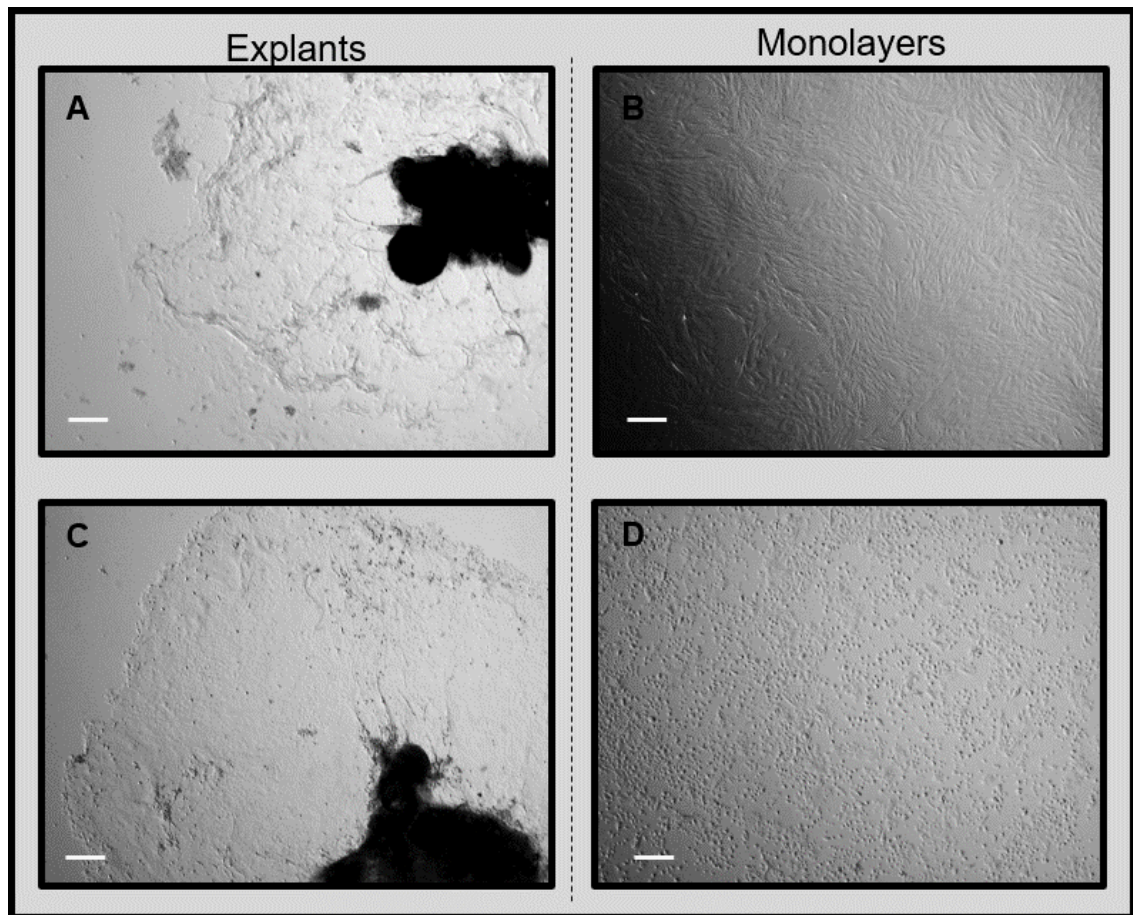


Figure 4.4 Comparison of cell morphology as explants and after trypsinisation into monolayers. A-B Fibroblast explant and colonies; C-D Keratinocyte explant and colonies. Magnification x10 Scale bar=60 μ M

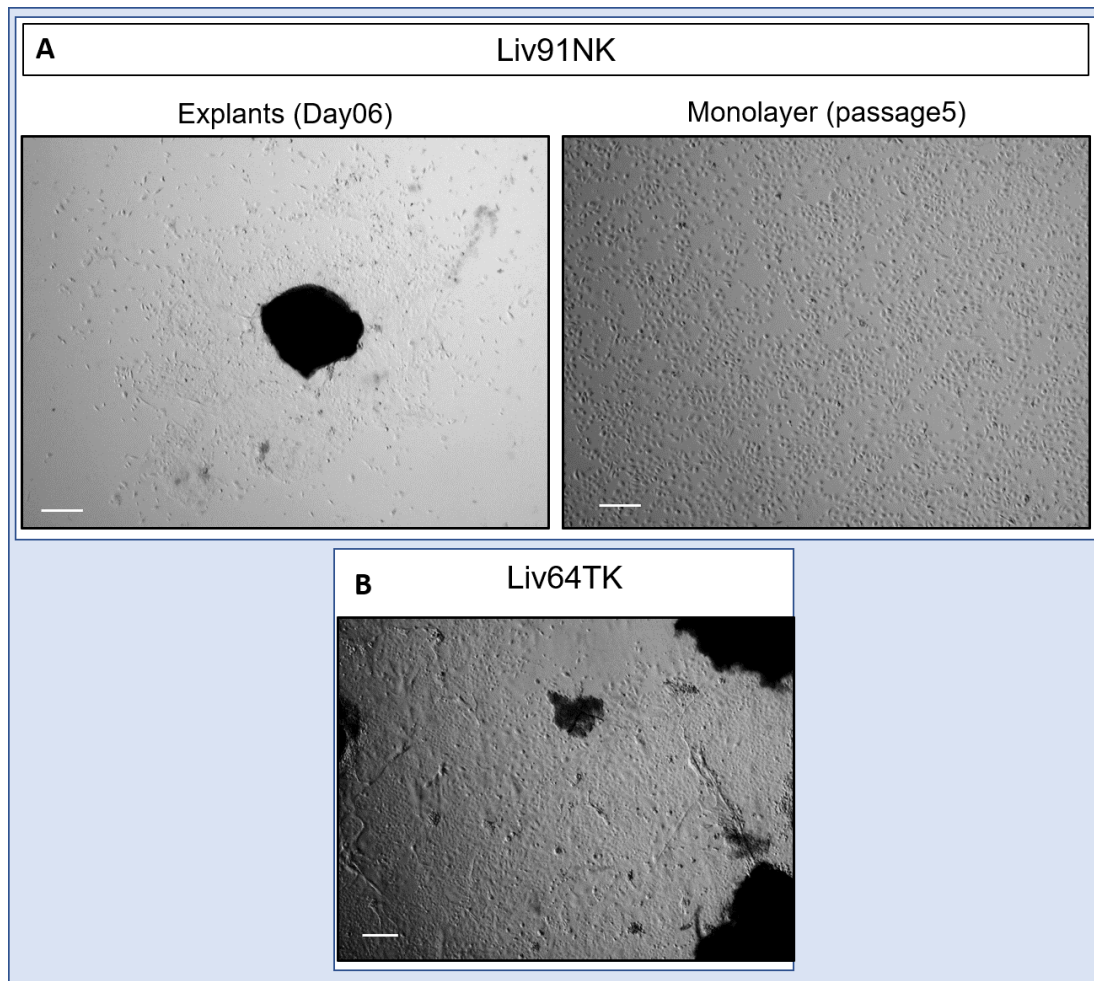


Figure 4.5 (A) Normal keratinocytes and HPV-negative keratinocytes from Liv91 successfully reaching passage 5 with similar proliferation rates to Liv91TK. (B) Large keratinocyte explants from HPV-negative tumour tissue (Liv64) Magnification x10 Scale bar = 60 μ M

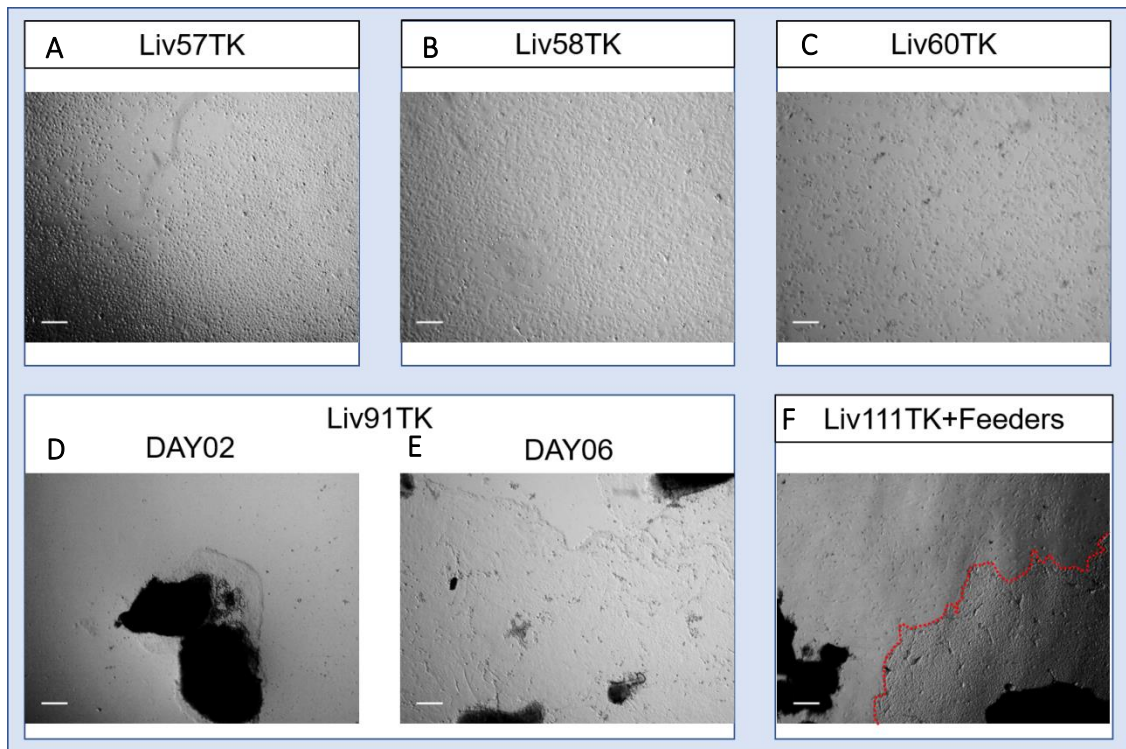


Figure 4.6 Representation of successful cell lines derived from HPV-positive OPSCC. Liv57 and Liv58 (A-B) successfully reached passage 6 with continual good confluence whereas Liv60 (C) senesced at the same time point. Liv91 (D-E) represents keratinocyte explants on plastic on day02 and day06 and Liv111 on Liv86NF feeders (F) with a large explant that is distinguishable from the feeder layer underneath. Scale = 60 μ M.

4.2.3 Primary cell culture with feeders

Chapter 3 describes the process of supplementing adhered tissue with suitable irradiated fibroblasts. Liv92-Liv108 had low passage

(<20) mouse 3T3 cells for any explants to anchor to. A major problem with this protocol was the detachment of the feeder cells, leading to high cell debris that required additional washing and risk of losing adherence of the precious primary tissue (Figure 4.7). Furthermore, the introduction of additional cell types increased the risk of contamination and 3/7 feeder plates became contaminated. Due to this occurrence, Liv110 and Liv111 were supplemented with irradiated Liv86 normal fibroblasts (Liv86NF). This particular cell type was chosen as it closely represents the environment which surrounds *in vivo* tumour cells and as they were established from an HPV-positive non-smoker/moderate drinker they should have a low mutational burden which could influence co-culture with tumour cells. Furthermore, Liv86NF were capable of high passage numbers (>20) and once irradiated they adhered to a high confluence to CellBind™ 6-well plates. Figure 4.8 demonstrates the differences between explants established on 3T3 and Liv86 feeders.

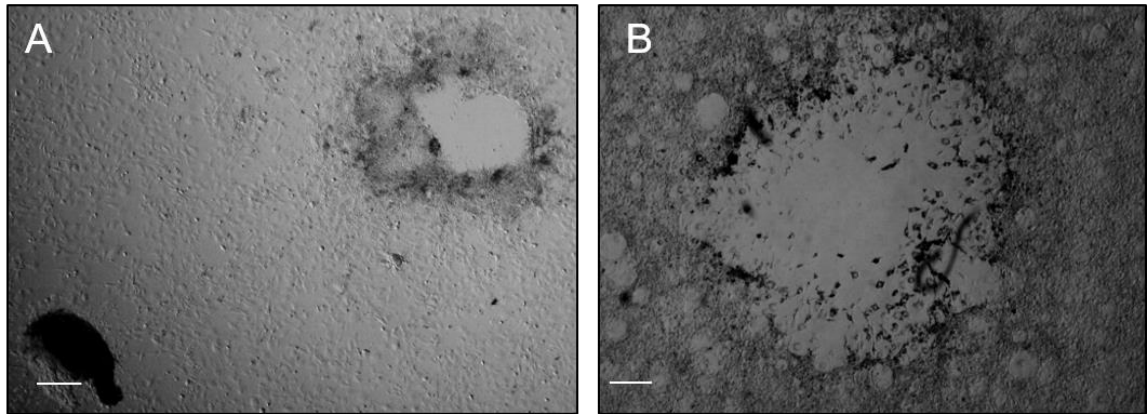


Figure 4.7 The debris caused by feeder cells required additional washes which increased the risk of precious tissue detachment.

(A) Magnification x 10 Scale bar=6 μ M (B) Magnification x20 Scale bar=30 μ M

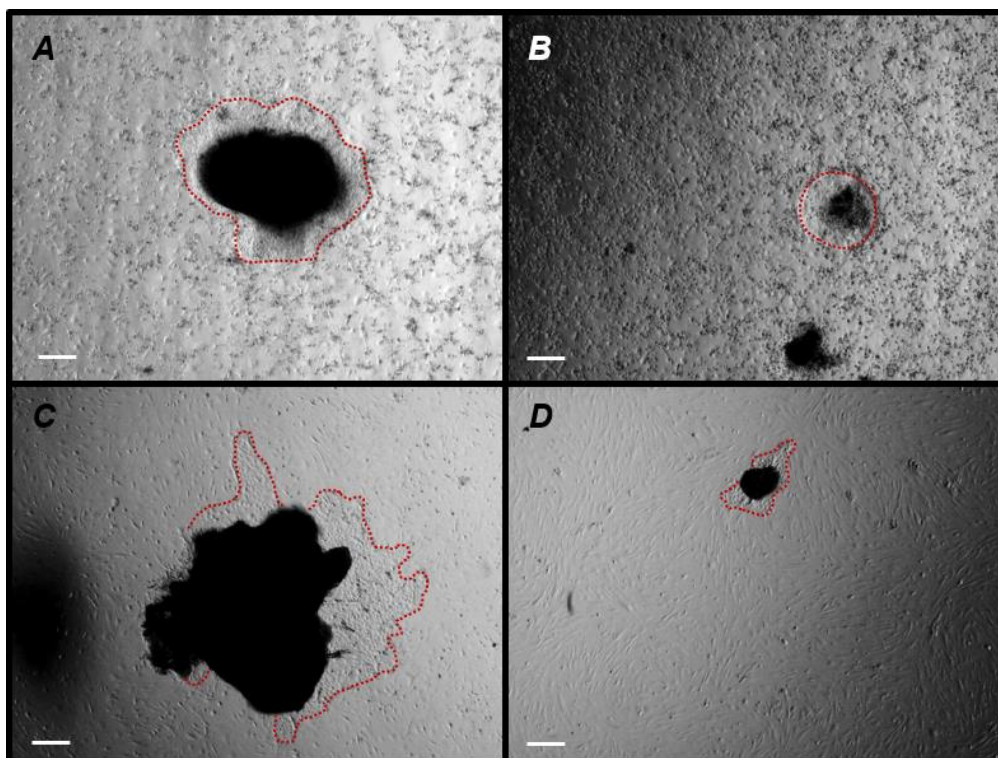


Figure 4.8 Comparison of 3T3 (A-B) and Liv86Normal fibroblasts (C-D) as feeder layers. Explants are outlined in red. Magnification x10 Scale bar=60 μ M

4.2.4 Cell line validation

Mycoplasma testing on all primary cell cultures were negative.

Example of agarose gel demonstrated in Figure 4.9.

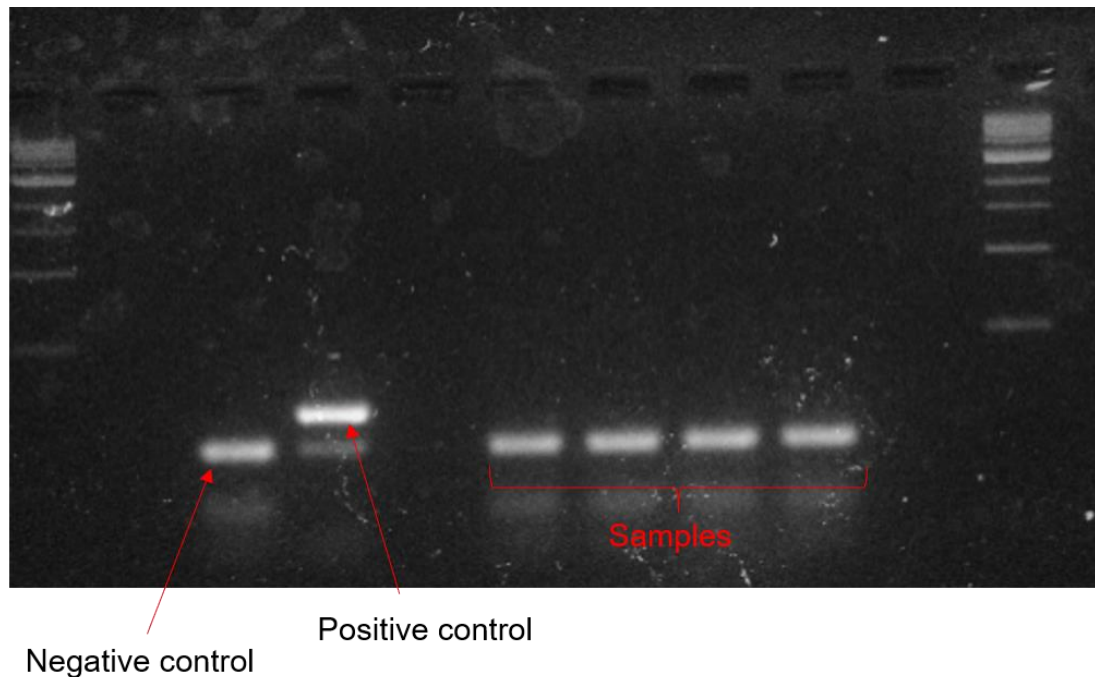


Figure 4.9 Example of a negative mycoplasma test

Short Tandem Repeat (STR) analysis was performed on the cell lines from HPV-positive OPSCC Liv57, Liv58, Liv60, Liv62 and Liv91 as well as other oral cell lines that were simultaneously growing at the same time. All show identical DNA fingerprints to their control material (blood or tissue) stored at time of surgery. Table 4.2 shows the alignment of tested extracted DNA with control tissue.

	Liv57				Liv58				Liv60			
	Control (T)	Liv57TK p3	Liv57NK p5	Liv57TK p6	Control (T)	Liv58TKP3	Liv58TKP5	Liv58TF	Control	Liv60TF p5		
TH01	8		8		TH01	6	6	6	6	TH01	8	8
TH01	9.3	9.3	9.3	9.3	TH01	9.3	9.3	9.3	9.3	TH01	9.3	9.3
D21S11	30	30	30	30	D21S11	28	28	28	28	D21S11	29	29
D21S11	32	32		32	D21S11	32.2	32.2	32.2	32.2	D21S11	31.2	31.2
D5S818	9		9		D5S818	9	9	OL	OL	D5S818	9	
D5S818	11	11	11	11	D5S818	12	12	12	12	D5S818	10	10
D13S317	11		11	11	D13S317	8	8	8	11	D13S317	10	10
D13S317	12	12	12	12	D13S317	11	11	11	8	D13S317	12	12
D7S820	8	8	8	8	D7S820	8	8	8	8	D7S820	OL	OL
D7S820	9		9		D7S820	11	11	11	11	D7S820	10	10
D16S539					D16S539	11	11	11	11	D16S539	11	11
D16S539					D16S539	12	12	12	12	D16S539	13	13
CSF1PO	10	10	OL	10	CSF1PO	10	10	10	10	CSF1PO	12	12
CSF1PO	11	11	OL	11	CSF1PO	11	11	11	11	CSF1PO	13	13
AMEL	X	X	X	X	AMEL	X	X	X	X	AMEL	X	X
AMEL	Y	Y	Y	Y	AMEL	Y		Y	Y	AMEL	Y	Y
vWA	16	16	16	16	vWA	15	15	15	15	vWA	16	16
vWA	OL		17		vWA	16	16	16	16	vWA	17	17
TPOX	9	9	9	9	TPOX	8	8	8	8	TPOX	9	9
TPOX	11	11		11	TPOX	9	9	9	9	TPOX	11	11

Table 4.2 Demonstration of STR typing for HPV-positive OPSCC cell lines matched with controls. Liv57 was compared with low and later passage and normal tissue. Abbreviations T: Tumour; N: Normal, K: keratinocytes; F: fibroblasts; OL: Off Ladder

4.2.5 HPV testing

The cell lines Liv57 (passage 3 and passage 5), Liv58 (p3, p5), Liv62, Liv91, Liv92, Liv111 and Liv111+feeders were tested for HPV presence and expression. If available, snap frozen tissue taken at time of surgery was used as controls (Liv57, Liv58 and Liv62) in addition to CaSki (a HPV16-positive cervical cell line) and HeLa (a HPV18-positive cervical cell line). All cell lines and

tissue samples were positive for the endogenous control β -Actin and RNase P in cDNA and DNA samples respectively. Results showed 4/4 primary tissue were positive for HPV16 E6 expression but this was not reciprocated in the paired cell lines, regardless of passage number. Although CT values were obtained for HPV DNA presence in all samples, using the calculation from methods section 3.8.2 to calculate ΔCT , they all showed as having a product that was less than the endogenous control (RNase P) indicating <1 single gene copy and therefore a negative DNA result (Appendix10.3). The cell lines without snap frozen tissue for comparison relied on clinicopathological data and although Liv91 and Liv111 demonstrated HPV16 E6 or HPV18 E6 respectively in a single run (Figure 4.10), resurrection of cells for cell expansion and repeats was unsuccessful.

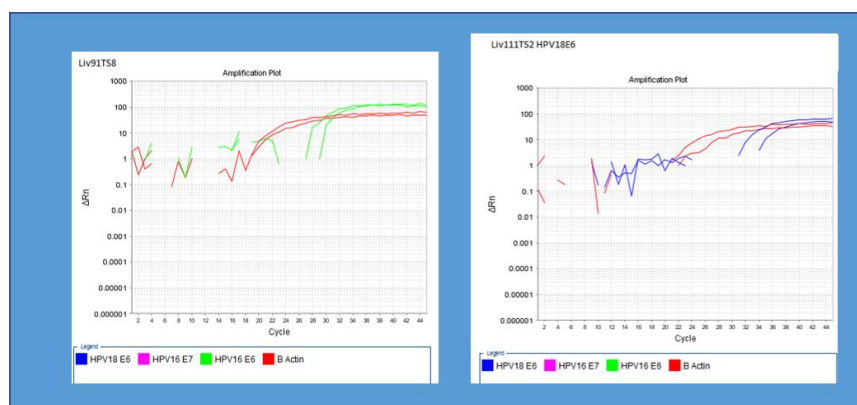


Figure 4.10 Amplification plots for Liv91 tumour keratinocytes and Liv111 tumour keratinocytes grown without feeders.

4.3 Discussion

The landscape of head and neck cancers is changing, with the incidence of OPSCC increasing each year and affecting nearly 100,000 people worldwide, this could mean potentially 70,000 cases are driven by HPV with still unanswered questions on their improved survival statistics regardless of an aggressive phenotype^{13,14}. Interventions to prevent this disease by prophylactic vaccinations is promising and could help battle the increasing incident number, however the outcome of vaccinations won't be seen for decades¹⁵². In the meantime, as the number of patients increase, so does the proportion who ultimately do not survive, or who suffer from avoidable side effects from aggressive treatment. This drives the need for a representative HPV-positive OPSCC model to characterise this cancer, to study the invasion profile of HPV-positive to gain understanding why the majority of patients present with large involved lymph nodes and discover biomarkers that could predict poor prognosis so de-escalation of treatment is more accurately prescribed.

Primary cell culture is the first step in producing a representative cell population and due to the success of growing epithelial tumour cultures from oral cavity cancer, larynx cancer and oral dysplasia cells with this method, it seemed logical to being attempts at HPV-positive and HPV-negative OPSCC culture in a similar way¹³⁷. Similarly, research carried out by Dr Cossar (unpublished) at the same research facilities establishing cervical carcinoma cell lines using the same explant model yielded two HPV-positive cell lines. The relative lack of literature on successful HPV-positive OPSCC primary cell culture highlighted difficulties that would be faced, however there was optimism when the feeder protocol was implemented and recently, Powell et al have successfully characterised two novel HPV-positive OPSCC cell lines using the 3T3 feeder method⁹⁷ first established by Margaret Stanley 40 years ago⁹⁶. The attempt at multiple types of cultures conditions during this thesis identified what challenges future researchers may care to heed and areas that are worth exploring further.

Although *in vivo* expression of the HPV oncogenes E6 and E7 contribute to the 'hallmarks' of cancer including sustained

proliferation, by-passing growth suppression to replication immortality¹⁵³, and indeed have been used as an immortalisation technique in other cancer types *in vitro*^{154,155}, there was no continuous cell growth observed in any of the primary cell cultures. Although primary explants were derived on 17 plates, only 71% could survive as a monolayer away from tissue and this number reduces further to eight that had sufficient cell viability to yield enough data for HPV testing. This could promote evidence for the requirement of co-culture to maintain viral integrity and immortalisation and it was unfortunate additional attempts using Liv86 fibroblasts as a feeder layer could not be achieved, as it was found they were much easier to maintain than the conventional mouse 3T3s due to their robust nature and prolonged adhered to plastic. However, working with feeders has its limitations and difficulties in establishing isolated cell types. Although irradiated fibroblasts should not interfere with HPV-testing it is worth noting the downstream uses of cells established on a cell population from a different patient or species (3T3s). To compare to other disease types utilising this method (OSCC and cervical carcinoma), the distinct difference in prognosis for these patient cohorts could explain the difficulty in establishing an aggressive continually growing cell line from oropharyngeal

tissue. It is plausible that just as oropharyngeal tumour cells are sensitive to cell-damaging agents such as those used in chemoradiotherapy *in vivo*, a similar effect occurs when the cells are removed from their microenvironment and plated on plastic for *in vitro* cell growth. Conversely, it is understood not all HPV-positive patients are heavy smokers or drinkers and thus their relative lack of somatic mutations could leave their apoptotic pathways intact, which under the stress of cell culture are activated. To observe for any correlation in the patient demographics and successful cell cultures it is worth noting the cell lines that could be successfully subcultured came from ex-smokers or heavy drinkers (Appendix 10.2) and therefore could have a higher mutational burden allowing for *in vitro* cell replication.

Further evidence the generation of cell lines is reliant on the prognosis of the primary tissue was highlighted by the creators of the UPCI:SCC cell lines (discussed in Chapter 5), Prof Gollin et al who successfully cultured 52 HNSCC continuous cell lines from nearly 200 patients and confirmed a bias towards tumours with poor prognosis to generate stable cell lines and the oropharynx

was the site with least success (18.8% compared to 51.1% in other sites)¹⁵⁶.

Pivotaly, the eight cell lines capable of cell numbers sufficient for DNA and RNA extraction demonstrated no presence of HPV16 E6 or E7 (Liv57, Liv58, Liv60, Liv62, Liv91, Liv99, Liv111 and Liv111 established on feeders). The sporadic positive results for Liv91 and Liv111 could not be validated due to the repeated inability to resurrect cells and replicate to a sufficient cell number, highlighting the delicate nature of primary cell lines. DNA and RNA extraction from snap frozen tissue for Liv57, Liv58 and Liv62 confirmed the starting material did have integrated HPV16 E6 and E7 and also positive expression of these oncogenes.

The possible hypotheses to explain why cell lines derived from HPV-positive tumour tissue do not contain the evidence of HPV presence and oncogene expression are:

- 1) The original subset of cells from which the cell lines were established were HPV-negative either via the isolation of non-tumour cells (normal cell populations) or the tumour cells no longer had integrated HPV

- 2) Cells were originally HPV-positive but lost their viral burden during *in vitro* replication.

It is unlikely the cells lost their viral load as Liv57 was also HPV tested at passage 3 and previous studies using this rt-qPCR technique could detect very small amounts of HPV DNA from CaSki dilutions¹⁴⁶. Evidence for the former is demonstrated via the similarities in cell morphology between normal and tumour keratinocyte populations with similar proliferation rates (Figure 4.5). Although it is unlikely normal tissue was initially obtained, due to surgeons sampling from within the core, areas of normal epithelium could have been included or transferred over. Furthermore, evidence for intra-tumour heterogeneity is poor, with little literature on the nature of HPV infection heterogeneity, although it is widely accepted that only 70% cells need to overexpress p16 to constitute a positive result, High-Risk HPV DNA ISH is either present or absent with no threshold and does not indicate the percentage of infected cells³¹.

It is apparent more intricate systems are required to maintain cell proliferation and viral integration of OPSCC cells outside the tumour environment, with the need to develop three-dimensional and feeder systems at the forefront. The preliminary results using

patient-derived irradiated fibroblasts as a feeder layer was promising and should be developed further. More advanced cell culture products are now available, including cell sorting protocols that maintain cell viability and allow for separation of tumour cells for isolated proliferation.

It is now more important than ever, with the shortage of available HPV-positive head and neck SCC cell lines and the difficulty in creating additional ones, to look at the current model for this disease; secondary cell lines that have been established from head and neck sites outside of the oropharynx yet remain the reference material for labs around the world. This is to be discussed in the next chapter with the aim to define a suitable model for HPV-positive oropharyngeal carcinoma

Chapter 5: Characterisation of the available secondary cell lines used for *in vitro* HPV-driven OPSCC studies

5.1 Introduction

As previously discussed, due to the difficulties in establishing HPV-positive primary cell culture in many labs, the majority of *in vitro* studies on HPV-positive head and neck squamous cell carcinoma (HNSCC) use established cell lines that are commercially available¹⁵⁷⁻¹⁵⁹. Results from these studies could have a drastic implication on translational studies for HPV-positive head and neck cancer and they hold limitations. Primarily, these cell lines have disparate aetiologies: they have been isolated from mainly oral SCC (OSCC), a disease not commonly driven by HPV infection¹⁵, or from recurred cancer tissue that again is uncommon in the main population of HPV-positive OPSCC. Each individual had a history of cigarette and alcohol use and poor prognosis^{156,160-163}. The method of establishing these cell lines are similar to the explant model outlined in Chapter 4 and none were supplemented with feeder layers.

The continued use of these cells as a resource requires thorough characterising to ensure they are still the best model available for study of HPV-positive head and neck cancer. Characterisation was defined by cell line validation by STR, investigation into cellular morphology and migration rates and profiles and confirmation of active HPV integration. Presence of HPV16 E2, E6 and E7 genes and its transcripts were confirmed by a range of clinical tests; p16 overexpression immunohistochemistry, High Risk HPV DNA in situ hybridisation (HR-HPV DNA ISH) and RNAScope[®], a highly sensitive RNA ISH technique. Importantly, the 'gold standard' of HPV-testing, real time quantitative PCR (rt-qPCR) was implemented to confirm presence and levels of expression of HPV16 E2, E6 and E7. Further experiments to observe invasion capabilities of these cell lines were attempted with the production of organotypics (methods section 3.9.2) and results for these attempts are documented in Appendix 10.5 The cervical carcinoma cell lines CaSki and SiHa were included as positive controls for HPV-testing.

5.2 Results

5.2.1 Cell line clinic-pathology and demographics

All cell lines were maintained as described in methods (section 3.3, Table 3.2). Each cell line is detailed in Table 5.1 including TNM staging, smoking/alcohol status, reference of establishment and site of primary tumour.

5.2.2 Cellular growth characteristics and cell line validation

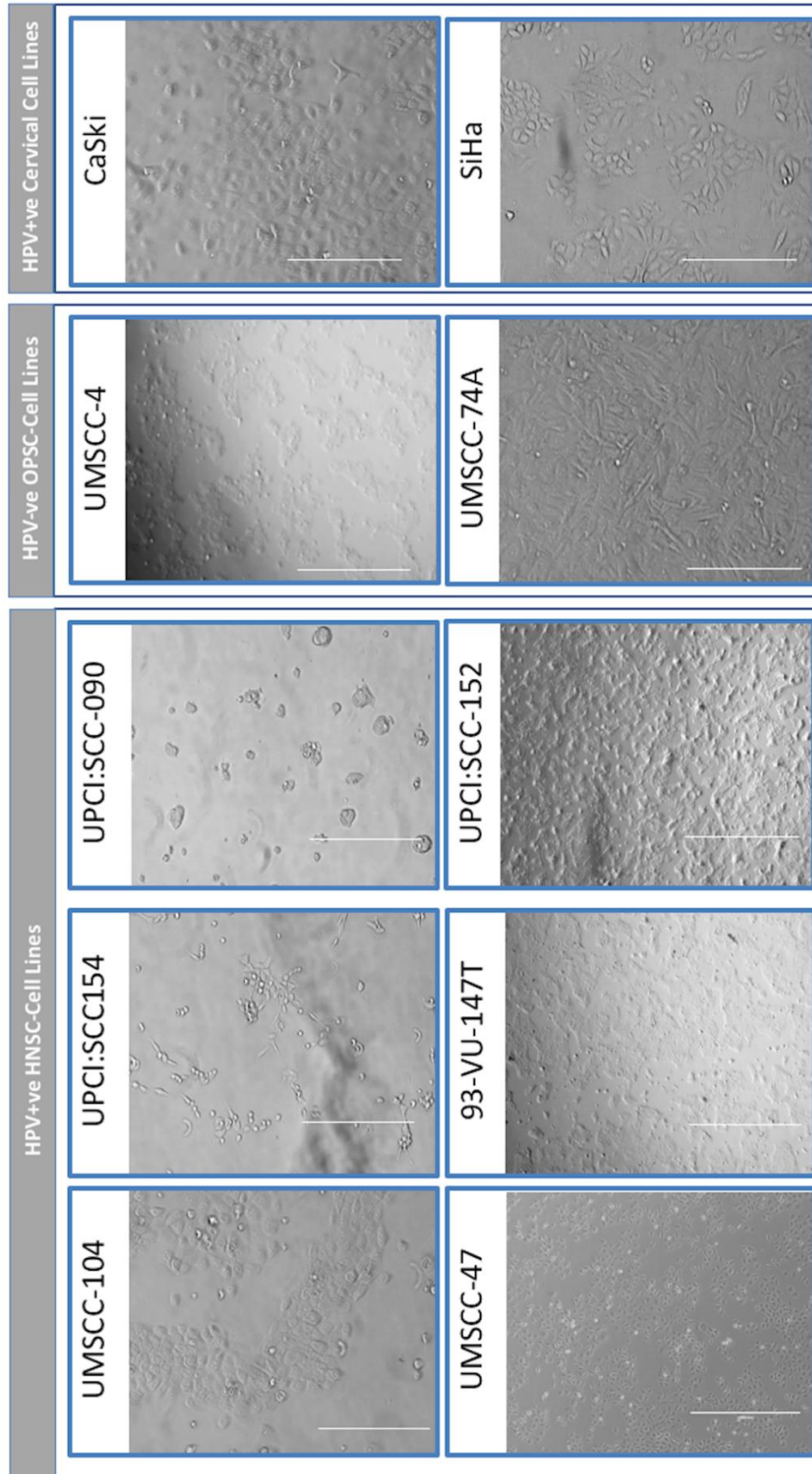
Morphology

Each cell line exhibited different phenotypes in culture (Figure 5.1). Markedly, UPCI:SCC090 and UPCI:SCC152 grew in tight individual colonies which required long incubation in trypsin for passage. UMSCC-4, UMSCC-104, 93-VU-147T grew in dense cultures with evidence of extracellular matrix (ECM).

UPCI:SCC154, UMSCC-74A, CaSki and SiHa produced cultures containing single cells

	Cell line	CaSki	SiHa	UMSCC -4	UMSCC- 74A	UMSCC -47	UMSCC -104	UPCI:SCC 090 [†]	UPCI:SCC 152 ⁺	UPCI:SCC 154	93-VU-147T
	Source	UK HPA and ATCC		University of Michigan, USA ^{143,144}				University of Pittsburgh, USA ^{139,145}			VU University, Amsterdam ¹⁴⁶
(A) Demographics	Published HPV status	Positive	Positive	Negative	Negative	Positive	Positive	Positive	Positive	Positive	Positive
	Age/gender	40/F	55/F	47/F	50/M	53/M	56/M	46/M	47/M	54/M	58/M
	Anatomical Site	Cervix*	Cervix	Tonsil	BOT	Tongue	FOM	BOT (recurrence)	Hypo-pharynx	Tongue	FOM
	TNM	n.a	n.a	T3N2aM0	T3N0M0	T3N1M0	T4N2bM0	T2N0M0	Recurrence	T4N2M0	T4N2M0
	Smoking	n.a	n.a	Y	Y	Y	Y	Y	Y	Y	Y
	Alcohol	n.a	n.a	y	y	n.a	Y	y	y	y	y

Table 5.1 Demographics of cell lines (A). Abbreviations: M: Male; F: Female; BOT: Base of Tongue; FOM: Floor of Mouth; Y: Yes; N:No; n.a: not available; +: Same patient; *: CaSki cells initially derived from cervical metastasis to small intestine



e.

Figure 5.1 Brightfield images of characterised HNSCC cell lines.

Magnification x10 on EVOS XL Core. Scale = 100µm

Cell line validation – STR Typing

Each cell line was confirmed via STR typing and compared to results in the literature for authentication (Table 5.2). As expected, UPCI:SCC090 and UPCI:SCC152 have identical STR profiles due to cell lines originating from the same patient at different time points.

	UMSCC-4		UMSCC-74A		UMSCC-47		UMSCC-104		UPCI:SCC090		UPCI:SCC152		UPCI:SCC154		93-VU-147T	
	Published	FG	Published	FG	Published	FG	Published	FG	Published	FG	Published	FG	Published	FG	Published	FG
THO1	7	6,7		6,9,3	7,9,3	7,9,3	6	6	7	7	7,9,3	7,9,3	7	7	7,9	7,9
D5S818	11	OL	12	12	11,12	11,12	12	12	11,12	11,12	11,12	11,12	11,12	11,12	11,12	11,12
D13S317	12	12	12	12	8,11	8,11	8,9	8,9	11	11	11	11	9,12	9,12	12	12
D7S820	9,10	9	11	11	11	11	10	10	9,10	9,10	9,10	9,10	9,10	9,10	10,11	10,11
D16S539	12	OL		OL	8,13	OL	9,13	OL	12,13	13	12,13	OL	13	13	9,11	9
CSF1PO	11	11		9,12	11,13	OL	10,12	10	11,12	11,12	11,12	OL	10,12	10,12	11,12	11
AMEL	X	OL	X	OL,X	X,Y	Y	X,Y	X,Y	X,Y	X	X,Y	X,Y	X,Y	X,Y	X	X
Vwa	17,18	17,18	15,16	15,16	18	18	16,17	16,17	17	17	17	17	17	17	18	17,18
TPOX	9,10	9,10		8	10,11	10,11	9,10	9,10	8	8	8	8	8,9	9	9,11	9,11

Table 5.2 STR results for secondary cell lines compared to published figures. OL; Off ladder

Cell line validation – Mycoplasma

All cell lines were Mycoplasma negative apart from UMSCC-47.

The evidence of cellular disruption by mycoplasma contamination include alterations in cellular metabolism, mobility, membrane composition and altered nucleic acid synthesis¹⁶⁴, therefore this cell line was excluded from migration analysis.

5.2.3 Migration

Due to the morphological characterisation of UPCI:SCC090 and UPCI:SCC152, they were not suitable to grow to confluence in the chambers (methods section 3.9.1) and were excluded from the analysis. Each cell line exhibited different rates and profiles of migration across a defined gap (Figure 5.3, Figure 5.4, Appendix videos 10.6). In SiHa and UMSCC-74A cultures, individual cell movement was observed, in contrast to CaSki and 93-VU-147T where cells remained in contact with one another and moved in a sheet formation. More complex patterns were observed in UMSCC-4, UMSCC-104 and UPCI:SCC154 cultures, where protrusions of faster moving 'leader' cells migrated faster than the rest of the population. The two cervical cell lines, CaSki and SiHa, were the quickest to achieve full gap closure and both of the published HPV-negative cell lines UMSCC4 and UMSCC74A demonstrated a trend towards faster gap closures compared to the HPV-positive head and neck cell lines, however this did not reach significance.

5.2.4 Defective division

A serendipitous observation whilst analysing migration videos was the capture of abnormal mitosis in SiHa cell culture (Figure 5.2;

Appendix video10.6). A leading cell prepares for cell division by increasing in size before dividing into three separate cells.

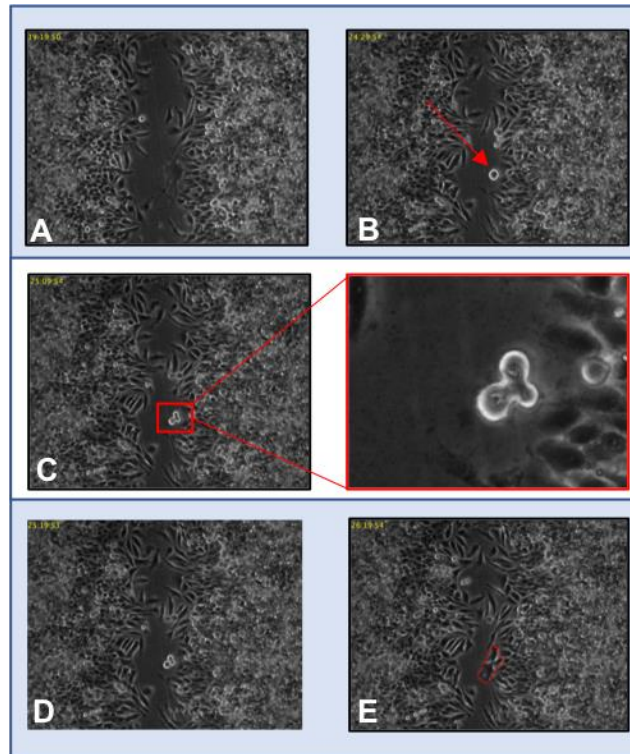


Figure 5.2 Series of time points capturing tripolar mitosis in SiHa cell culture. Leading cell increases in size (A), before dividing into 3 daughter cells (C-E).

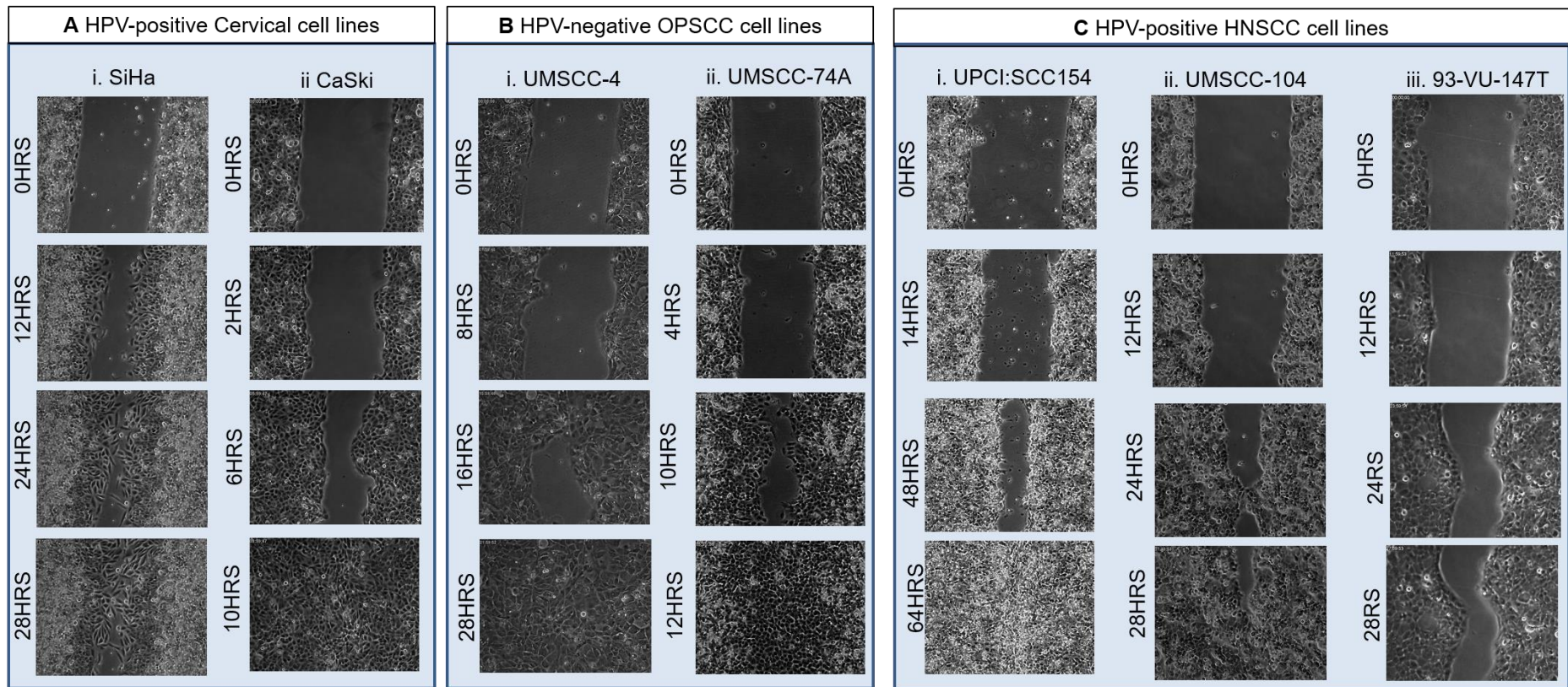


Figure 5.3 Representative images from differing time points (due to different migration speeds) demonstrating different profiles of cell migration. HPV-positive cervical cell lines (A); HPV-negative OPSCC cell lines (B); HPV-positive HNSCC cell lines (C).

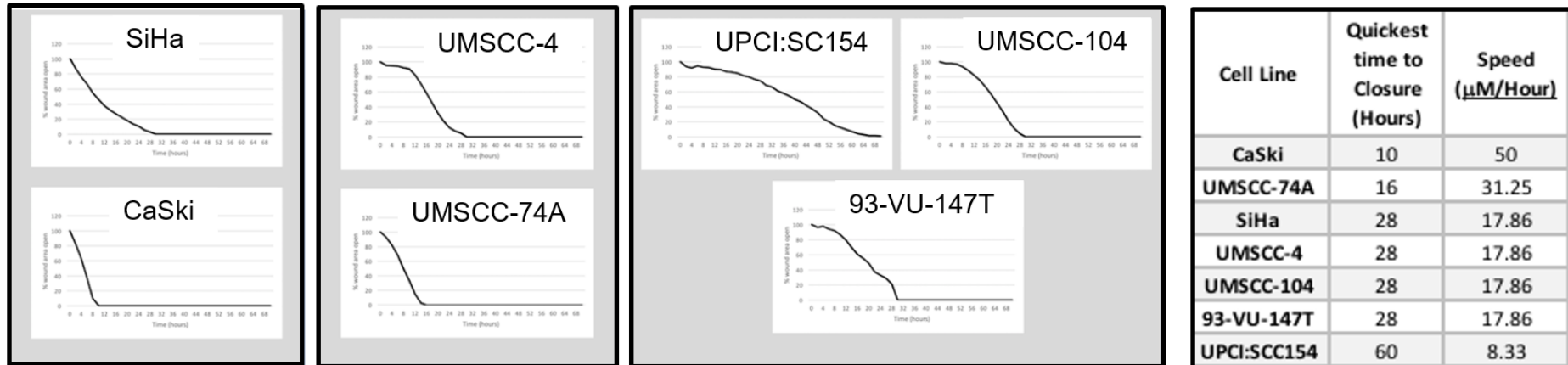


Figure 5.4 Graphs of time to gap closure. Each point on curve represents average 6 points across 3 wells per cell line (2 in each well). Time and Rate of wound closure for each cell line migration was measured. Values are of the point on the $500\mu\text{M}$ gap which showed complete closure first.

Organotypics

Multiple attempts were made at 3D cell culture utilising a collagen:Matrigel™ disc embedded with primary derived fibroblasts from Chapter 4 as a representative of tumour stroma. Various continuous cell lines were seeded on top and incubated for 14 days at the liquid:air interface (appendix 10.5). Although solidifying of the discs was a primary concern, once a suitable method was developed the keratinocytes did not remain adhered to the top of the disc. Appendix 10.5 demonstrates the method and some of the attempts that reached embedding and H&E staining stage.

5.2.4 HPV testing – HPV16 gene and transcript presence and fixed cell pellet HPV diagnostics

HPV16 genes and transcripts were absent from all previously designated HPV-negative cell lines using DNA rt-qPCR and cDNA rt-qPCR (Table 5.3A,B). All previously designated HPV-positive cell lines demonstrated the presence of the E6 and E7 genes and transcripts, except for UMSCC-47 which lacked both the E6 gene and transcripts and UPCI:SCC152 which did not express E6 even

though the gene was present (Table 5.3A,B). The E2 gene and transcripts were undetectable in SiHa, UMSCC-47 and UPCI:SCC154.

5.2.5 HPV testing – Fixed cell pellet HPV diagnostics

All previously designated HPV-negative cell lines were negative by all testing modalities (p16, HR-HPV DNA ISH and HR-HPV RNA ISH)(Figure 5.4; Table 5.3C). Previously designated HPV-positive cell lines demonstrated p16 overexpression by immunohistochemistry (IHC)³¹ and were all positive by HR-HPV RNA ISH. All except SiHa, UMSCC104 and UPCI:SCC154 were HR-HPV DNA ISH positive (Figure 5.5, Table 5.3C).

	Cell line	CaSki	SiHa	UMSCC-4	UMSCC-74A	UMSCC-47	UMSCC-104	UPCI:SCC 090 [†]	UPCI:SCC 152 ⁺	UPCI:SCC154	93-VU-147T
(A) <u>DNA</u> rt-qPCR	HPV16 E2	Y	N	N	N	N	Y	Y	Y	N	Y
	HPV16 E6	Y	Y	N	N	N	Y	Y	Y	Y	Y
	HPV16 E7	Y	Y	N	N	Y	Y	Y	Y	Y	Y
(B) <u>cDNA</u> rt-qPCR	HPV16 E2	1	0	0	0	0	>1	>1	>1	0	<1
	HPV16 E6	1	<1	0	0	0	<1	>1	0	<1	<1
	HPV16 E7	1	<1	0	0	<1	<1	<1	<1	<1	<1
(C) Fixed Cell IHC/ISH	p16 IHC	+	+	-	-	+	+	+	+	+	+
	HR-HPV DNA ISH	+	-	-	-	+	-	+	+	-	+
	HR-HPV RNA ISH	+	+	-	-	+	+	+	+	+	+

Table 5.3 Presence of HPV16 viral genes detected by DNA rt-qPCR (A) Transcript expression of viral genes detected by cDNA rt-qPCR and presented relative to expression in CaSki using $2^{-\Delta\Delta CT}$. >1: gene expression greater than CaSki; <1: gene expression less than CaSki; 0: no gene expression. (B) Clinicopathological HPV testing by p16 IHC; HR-HPV: High-Risk Human Papillomavirus; ISH: In situ hybridisation. Results were considered positive (+) if there was >70% p16 IHC staining or any staining in HR-HPV DNA/RNA ISH assays (C)

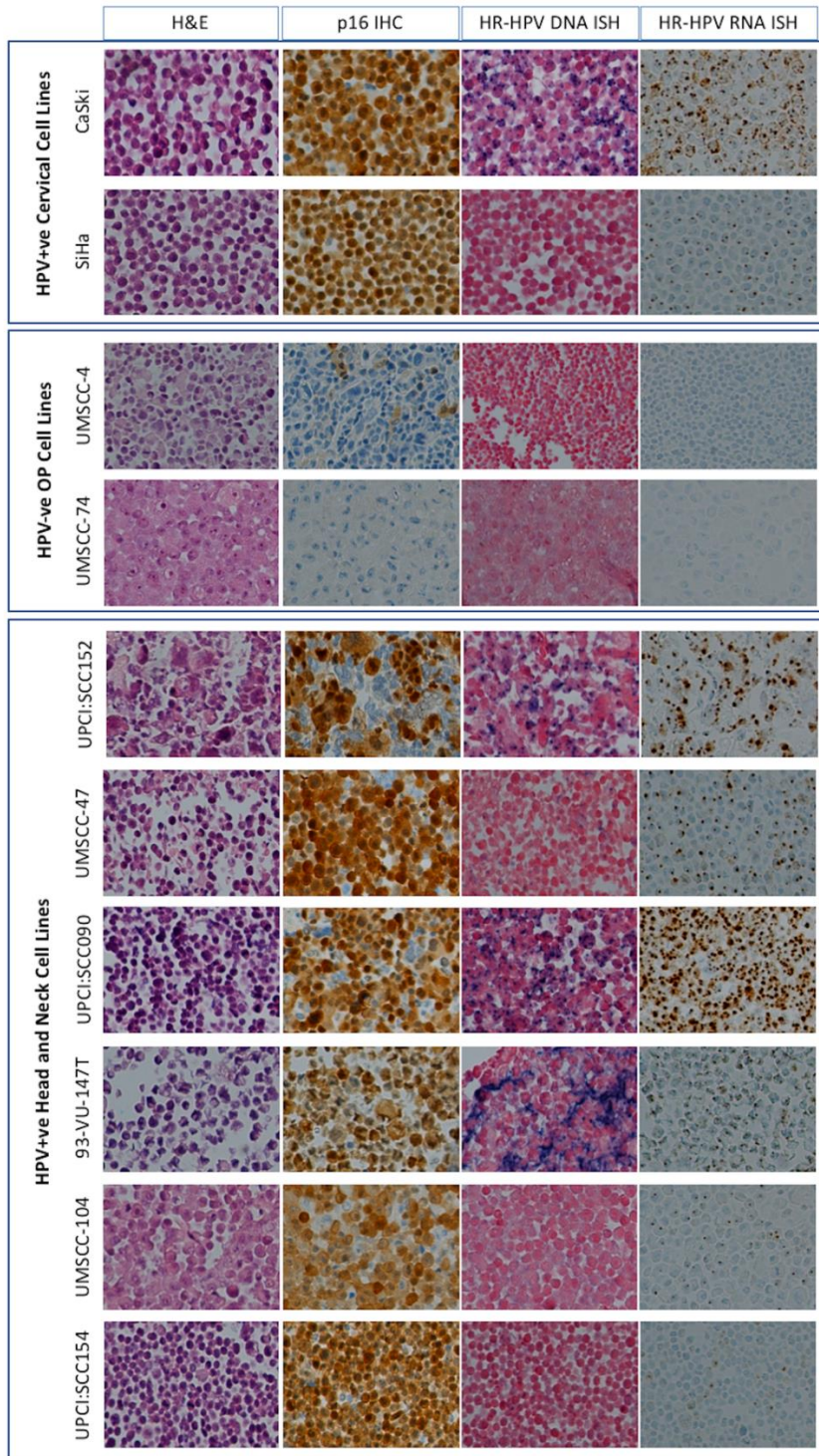


Figure 5.5 HPV diagnostic testing on fixed cell pellets. H&E staining, p16 IHC, HR-HPV DNA ISH and HR-HPV RNA ISH results. p16 IHC positive: brown stain; HR-HPV DNA ISH positive: blue stain; HR-HPV RNA ISH positive: brown stain

5.2.6 IHC on fixed cell pellets for invasion proteins and epithelial-mesenchymal transition markers

Using the cell pellets from 5.2.5, a TMA was constructed containing 1mm cores from all cell lines. Although entire cores were not achievable for all cases, as the starting sample was a single cell population a fragmented core was still representative for the whole cell line population, however no cells were obtained from the 93-VU-147T pellet.

Each section was stained with the antibodies podoplanin (PDPN); E-cadherin and vimentin (methods section 3.11.2) and imaged on Aperio ImageScope (Figure 5.6).

All cell lines had positive expression for the epithelial cell marker E-cadherin, however UPCI:SCC154 and UMSCC-74A had exclusively cytoplasmic staining.

Data collected during migration analysis determined cell lines expressing podoplanin had collective cell migration (CaSki, UMSCC-104 and UMSCC-4), with cells remaining in contact with each other and moving in a 'sheet' formation. The two fastest gap closing cell lines CaSki and UMCC-74A had positive vimentin staining (Table 5.4)


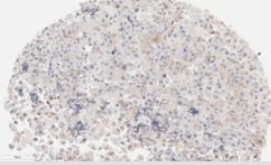

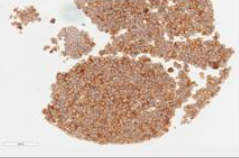
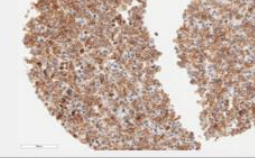
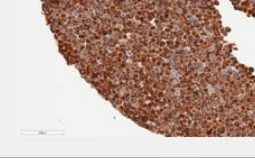
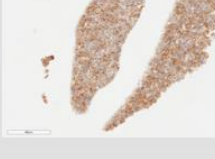
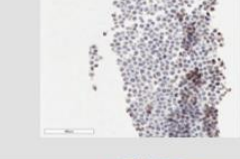










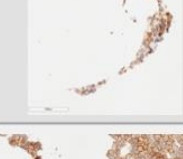
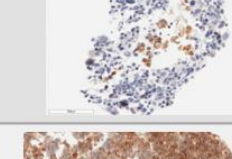



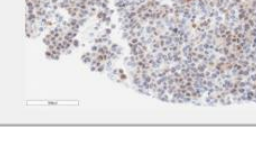
CELL LINE	E-CADHERIN	PODOPLANIN	VIMENTIN
UMSCC-74A			
CaSki			
SiHa			
UMSCC-104			
UPCI:SCC154			
UMSCC-4			
UPCI:SCC152			
UMSCC-47			

Figure 5.6. Examples for each cell line on expression of E-cadherin, podoplanin and vimentin.

Cell line	Speed of migration	Type of migration	E-cadherin expression	Podoplanin expression	Vimentin expression
CaSki	Fast	Collective	Positive(membrane)	Positive	Positive(strong)
UMSCC-74A	Fast	Single cells	Positive(cytoplasm)	Negative	Positive(strong)
SiHa	Moderate	Single cells	Positive(membrane)	Negative	Negative
UMSCC-4	Moderate	Collective	Positive(membrane)	Positive	Negative
UMSCC-104	Moderate	Collective	Positive(membrane)	Positive	Negative
UPCI:SCC154	Slow	Single/collective	Positive(cytoplasm)	Negative	Negative

Table 5.4 Description of each cell line and IHC expression

5.3 Discussion

The robust diagnostic profiling of these cell lines, combined with complete phenotypic and behavioural observations, provided the first report fully characterising the only available cell lines for HPV-positive head and neck cancer, creating an essential reference point for future *in vitro* HPV-positive HNSCC research.

The results draw parallels with the difficulties sometimes faced when determining HPV status clinically; namely through the variation in detection methods on fixed cells and qPCR results from DNA extracts from non-fixed cells. The RNA ISH technique, RNAScope¹⁶⁵ is more sensitive and specific compared to conventional RNA ISH techniques, and subsequent analysis of all expected positive cell lines yielded positive results from this single test. Although transcript detection in fresh tissue by way of cDNA rt-qPCR may be seen as the 'gold standard', this is potentially more time consuming compared to RNA ISH methods.

Rt-qPCR allowed the assessment of both the integrity of the viral genome and its activity in each cell line. Although the previously

designated HPV status was confirmed in all cell lines tested, the novel finding of variation in both the detection of E6 and its expression was observed in 2 HPV-positive cell lines (UMSCC-47 and UPCI:SCC152). In contrast, the loss of the E2 gene in UPCI:SCC154 and UMSCC-47 is similar to observations in SiHa which have previously been described^{166,167}. The application of the histopathological tests recommended by national guidelines for HPV status determination to each cell line is unique and again demonstrated not only a confirmation of HPV status retained over time in culture and through multiple passages, but also the degree of variability that can be observed in a homogeneous cell population. Whether this variability can be linked to individual gene presence/expression or the virus life cycle requires further experimentation and may allow researchers to gain understanding into the role of individual viral genes in both initiation and maintenance of HNSCC.

Although HPV-positivity has been confirmed in these cell lines, it is worth noting the atypical clinicopathological and demographical features of the patients from which they were derived, primarily the anatomical site and usage of tobacco and alcohol²⁴. Whilst

their parent tumour characteristics may not fully represent the average HPV positive tumour, smokers still develop HPV-positive OPSCC and small T1 tumours are common. A pronounced benefit of these cell lines is their derivation from tumour tissue and have gone through carcinogenesis *in vivo*, arguably producing a better viral model of HPV-positive cancer compared with experimental transfection of E6/E7 into normal epithelial cell lines e.g. NOK^{168,169}. Many previous studies, primarily in cervical cancer, have concluded that transformation results from persistent viral infection combined with insufficient clearance by the immune system¹⁷⁰. Although HPV-positive OPSCC has yet to be considered in the same way, the benefit of using cell lines which have been subjected to natural selective pressures before, during and after carcinogenesis may more accurately represent HPV-related disease in this anatomical site and could allow more clinically-relevant *in vitro* modelling. This paradox between demonstrable HPV status and the irregular patient factors associated with source tumour tissue should encourage a degree of critique, particularly when research utilising these cell lines seeks direct clinical correlates. However, by contrast, the profound difficulties in deriving primary cell cultures (as discussed in Chapter 4) from HPV positive tumours make these cells a

critical and essential model for HPV-HNSCC research in the absence of viable alternatives.

As previously discussed, the development of primary cell lines from naturally infected HPV-positive OPSCC tumours is rare¹⁷¹ and a recent success from Lars Ekblad's group in establishing an oropharyngeal HPV-positive cell line (LU-HNSCC-26) highlights this point¹⁷². They report a success rate of HPV-positive OPSCC cell line establishment of <5% and the requirement for the use of xenografts in nude mice. The cell line they finally produced was very slow to initiate, with a doubling time 3 times slower than those in other HNSCC cell lines. The exact reasoning for poor *in vitro* culturing of HPV-positive, or oropharyngeal cells in general, is unknown and exactly how the cell lines that are available were able to be selected in culture is not clear. HPV-positive tumours from non-smokers have been shown to have very low mutation rates^{173,174} which may imply that apoptotic pathways are still active when the cells are removed from the *in vivo* environment and may partially explain why they are difficult to culture while the currently available cell lines proliferate well.

Nodal progression is observed in the majority of HPV-positive OPSCC cases¹⁷⁵, and the hypothesis that cancer cell migration may be altered in these tumours was explored. Although previous literature has suggested a role for the tumour microenvironment in HNSCC cell migration¹⁷⁶, only HPV-negative cell lines were used in those studies. The in-depth characterisation and real-time analysis of wound healing in these cell lines provides evidence that there is no universal pattern of migration, nor is speed of migration linked to HPV status. A review by Friedl and Gilmour categorised cell migration into collective and singular patterns¹⁷⁷. Collective migration involves cells remaining connected to one another, migrating as 'sheets' of cells moving towards each other in 2D assays and as clusters of cancer cells penetrating tissue or tissue matrix in 3D assays. This data indicated that both CaSki and UMSCC-104 exhibit collective migration, closing the gap with a single sheet-like unidirectional movement. The movement of 93-VU-147T, UMSCC-4 and UPCI:SCC154 can also be described as collective cell migration, with an increased range of direction and variable speed. Protrusions into the gap observed in assays using these cell lines appear to be led by individual cells capable of changing direction but not clearly displaying cellular tropism. Individual, single cell movement was demonstrated by SiHa and

UMSCC-74A. The rates of wound closure appeared to be related to the pattern of cell movement rather than the HPV status, with the 'sheet formation' and 'single cell' migration patterns being the fastest to close and the 'led' migration being the slowest, either due to very slow movement initially or the multi-directional movements of the protrusions reducing the speed of gap filling. The rate of wound closing was not related to cell doubling time.

Cell pellet IHC staining with proteins involved with migration and invasion allowed comparison with cell movement and expression. Surprisingly UMSCC-74A and CaSki were both strongly positive for the mesenchymal marker vimentin. Although it is unclear whether vimentin causes increased migratory rates or is just a marker for mobile cells recent studies have hypothesized vimentin modulates the intracellular network of actin and microtubules to promote single cell migration¹⁷⁸. Although all cell lines expressed E-cadherin, UMSCC-74A was exclusively cytoplasmic, indicating possible evidence this cell line has lost its epithelial properties and gained those of mesenchymal cells; gaining an epithelial-mesenchymal transition (EMT)-Associated phenotype. Furthermore, the positive expression of podoplanin in UMSCC-4,

CaSki and UMSCC-104 could explain the phenotypic collective cell migration observed in these cell lines. Wicki et al demonstrated cells that expressed podoplanin had increased migratory properties by altering their polarity and actin cytoskeleton to migrate with collective migration opposed to single cells^{117,135}. The data in this thesis agrees with their findings and allows functional analysis with specific protein expression. This generates the hypothesis that cells that have an EMT-associated phenotype or overexpression of podoplanin have increased migratory capabilities and pathologically this could indicate invasive disease capable of metastasis. To test this hypothesis a larger cohort of OPSCC patient samples were obtained and stained for these markers to find a cause of increased lymph node metastases seen in HPV-positive OPSCC.

Chapter 6: Epithelial to Mesenchymal Transition (EMT) and expression of the invasive marker Podoplanin (PDPN) in Oropharyngeal Squamous Cell Carcinoma (OPSCC)

6.1 Introduction

The preceding chapters address the need, availability and management of an *in vitro* head and neck cancer cell model, however many problems are associated with the use of primary and secondary cell lines for translational experiments including cell line misidentification, mycoplasma contamination, viability in culture, storage procedures and the overall time and resources involved in maintaining multiple cell lines simultaneously¹⁷⁹. To observe genomic, morphological and proteomic properties within a disease population, formalin-fixed paraffin embedded (FFPE) tissue provides a readily available resource that maintains DNA, total RNA and totally protein quality and quantity for years at room temperature¹⁸⁰, and therefore can be used retrospectively for many research projects.

Preliminary functional assays in the previous chapter showed CaSki, UMSCC-104 and UMSCC-4 had increased expression of podoplanin and all exhibited a collective migration profile *in vitro*.

Research by Wicki et al¹¹⁷ determined podoplanin promoted cancer cell invasion in breast cancer and pancreatic cancer *in vivo* and *in vitro* and described similar cellular movements as CaSki and UMSCC-104. Additional research by this group highlighted the potential of podoplanin as a marker for cancer invasion¹³⁵. The protein is also thought to have a role in lymphangiogenesis and could be a major component for tumour metastasis to the nodes as the formation of new lymphatic vessels provides an escape route for tumour cells¹⁸¹. Studies have concluded tumour cells with upregulated podoplanin have increased incidences of lymphangiogenesis¹⁸², and conversely is significantly reduced in *Pdpr⁻/Pdpr⁻* mice¹⁸³.

It was observed the HPV-negative cell line UMSCC-74A had lost membranous E-cadherin and subsequent cell migration was by the movement of single cells. This cell line was strongly positive for the mesenchymal marker vimentin implying this particular cell line could have gained an EMT-associated phenotype. Similarly, the HPV-positive cervical cell line CaSki was strongly positive for vimentin and as it still expressed membrane E-cadherin, cells moved collectively, yet at a faster rate. Implying the gain of vimentin could impact on the migratory properties of cells *in vitro*.

However, the literature is mixed with conflicting results in oropharyngeal tumours and only a couple of papers have included sufficient HPV-positive OPSCC tumour samples to provide statistical analysis on vimentin, E-cadherin and podoplanin expression^{126,128,184}.

The model of epithelial-mesenchymal transition is portrayed differently throughout the literature and includes single markers i.e. epithelial cells that have gained the mesenchymal marker vimentin or lost expression of E-cadherin. Alternatively, the combination of the expression pattern of these two proteins and is termed as an 'EMT-associated phenotype' in this thesis. This is due to the clear staining categories available for E-cadherin and vimentin in oropharyngeal tissue.

Although it is accepted HPV-negative OPSCC is a different disease to HPV-positive OPSCC in relation to demographics, presentation and prognosis, comparison between these two groups will allow for further characterisation on a molecular level, differentiating them further or connecting them with a common method of invasion. It is hypothesised that the tumours with the invasive profile of epithelial-mesenchymal transition and/or the

overexpression of podoplanin will have a more clinically invasive phenotype; demonstrated by progression to the lymph nodes.

6.2 Results

6.2.1 Patient Demographics

A total of 145 FFPE blocks (n=97 primary tumour tissue; n=48 nodal tissue) from 99 patients who had surgically managed OPSCC from 1988 to 2014 at Aintree University Hospital and had relevant consent for their samples to be used in research were collected (Ethical approval numbers: EC47.01; 10/H1002/52 & 09/H1010/54). Tumour staging was classified by the reporting pathologist during diagnosis following TNM7 guidelines¹⁷. Tonsil was the predominant site for primary tumour and there was no significant difference between HPV-positive (n=54) and HPV-negative (n=45) patient demographics (Table 6.1). HPV status was confirmed by p16/ISH positivity in previous publications^{32,33}.

6.2.2 Antibody Optimisation

Antibodies were optimised by methods described in section 3.11.2. There was good staining at 1:200 dilution for podoplanin, E-cadherin and vimentin and initially N-cadherin. However, when TMAs were stained, the pattern of N-cadherin staining was not consistent across the slides with occasional nuclear staining and

varying levels of intensity across slides, not repeatable in duplicates or staining procedures. Therefore, this marker was removed from the testing cohort.

A single TMA core stained with each antibody is represented in Figure 6.1. Figure 6.2 depicts a normal epithelial stained with all marker.

Characteristics	Total (n=99)	HPV- negative (n=45)	HPV- positive (n=54)	<i>P</i>
Gender				
Male	64	29	35	0.88147
Female	19	11	8	
Unrecorded	16	5	11	
Anatomical site				
Tonsil	56	20	36	0.0992
Base of Tongue	22	11	11	
Soft Palate	10	7	3	
Unknown	11	7	4	
TNM* staging				
<i>Tumour staging</i>				
Cis	1	0	1	1
T1-T2	43	18	25	
T3-T4	41	17	24	
Unrecorded	14	10	4	
<i>Nodal status</i>				
N0	17	8	9	0.5844
N1-3	71	27	44	
Unrecorded	12	11	1	
Extracapsular spread (ECS)				
Negative	15	8	7	0.7627
Positive	40	18	22	
Unrecorded	16	1	15	

Table 6.1 Patient cohort and clinicopathological features in relation to HPV status. Fisher's exact t-test, significance <0.05

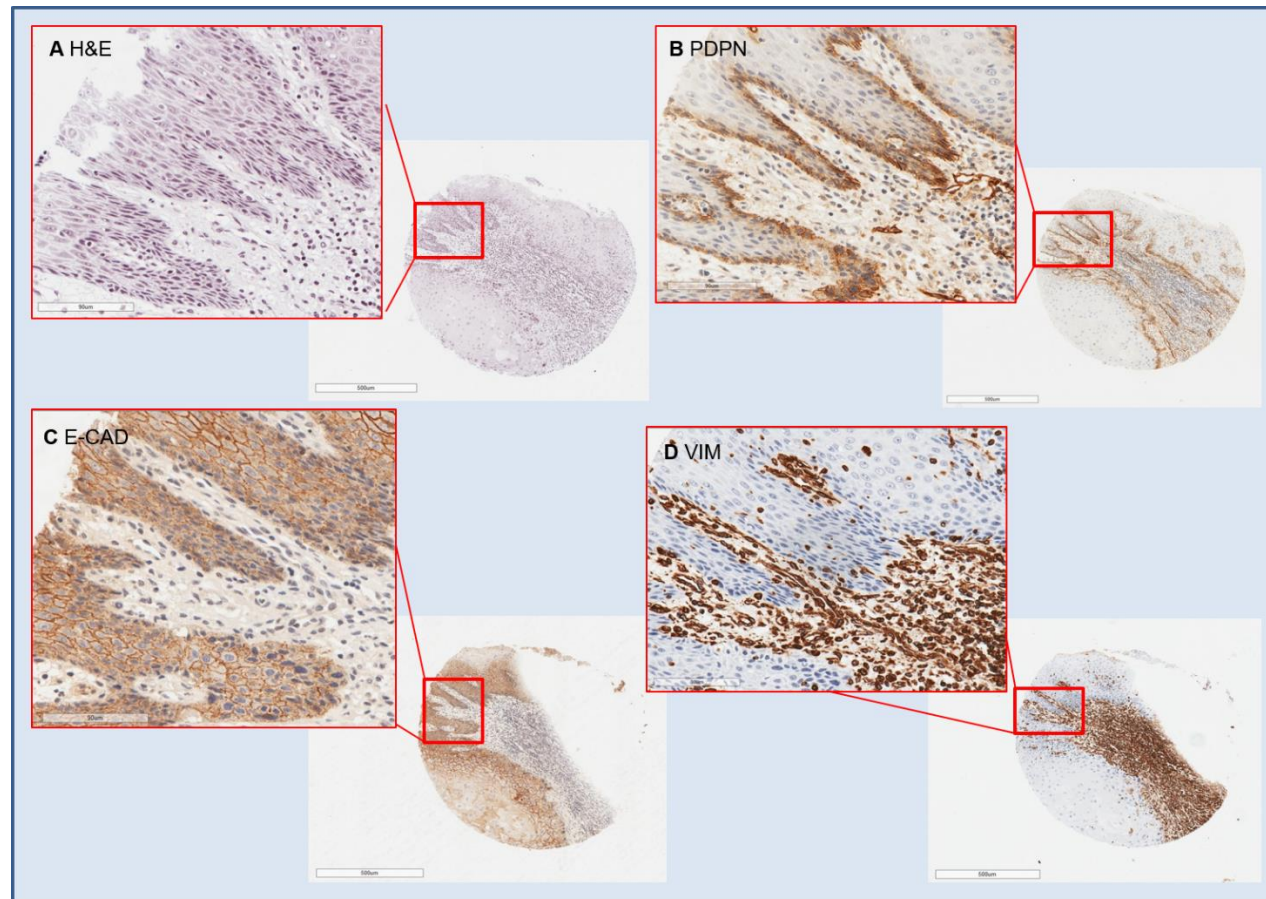


Figure 6.1 Representative of H&E (A), Podoplanin (B), E-cadherin (C) and vimentin (D) on a repeated TMA core.

Scale bar = 500µM

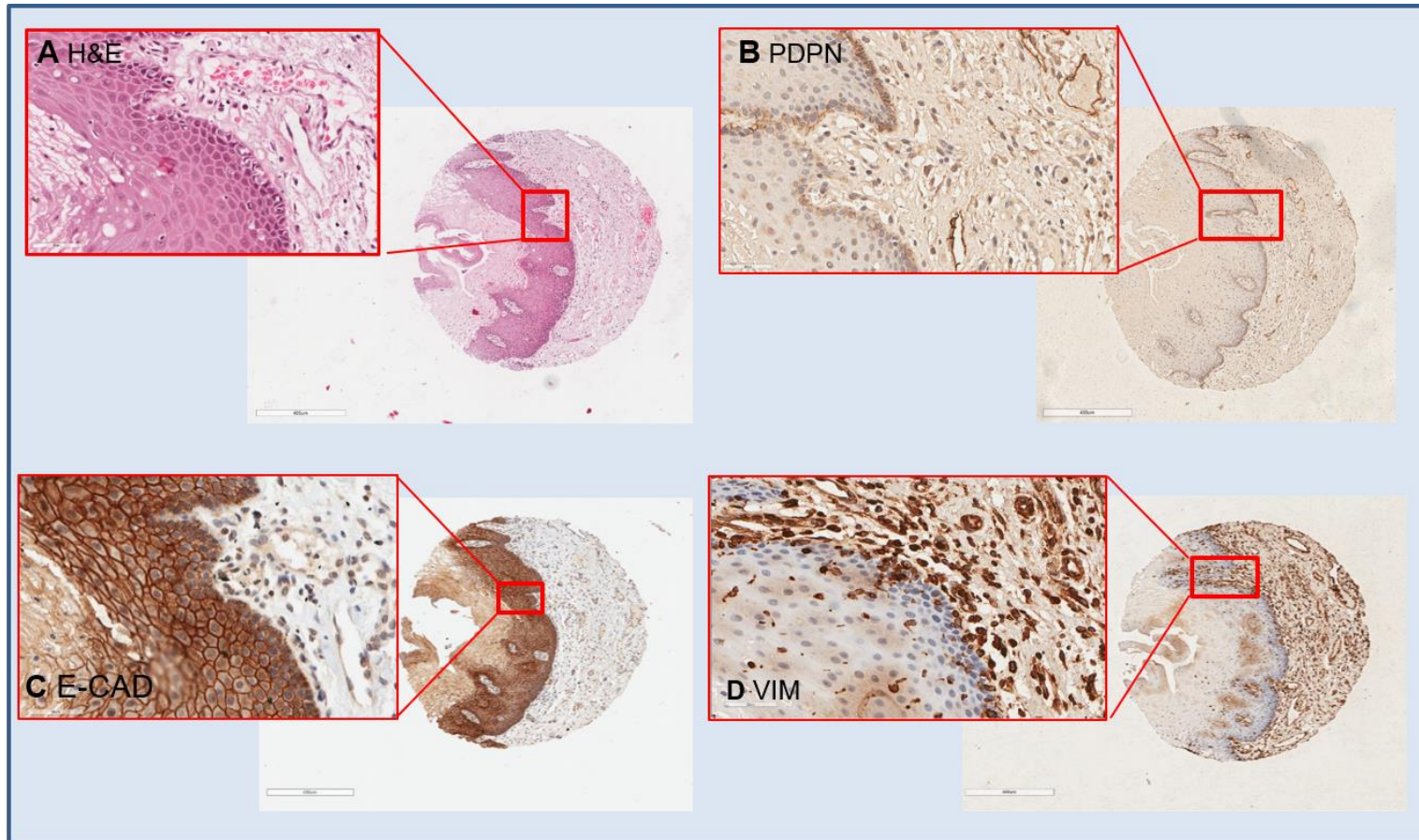


Figure 6.2 Staining patterns of normal tissue with H&E (A), Podoplanin (B), E-cadherin (C) and vimentin (D) on a repeated TMA core. Scale bar = 500 μ M

6.2.3 Primary Tumour

97 patients with confirmed HPV status had available tumour tissue. Areas of interest were marked on corresponding H&E slides by a head and neck pathologist (Dr Asterios Triantafyllou). For each case, three cores were sampled from the tumour centre and a further three cores from the advancing front (Material and Methods Chapter 3.10.1). Subsequent H&E staining of TMA sections highlighted most cores from the centre of the tumour had stroma sampling, and conversely rarely did the advancing front include tumour cells. This highlighted the microscopic nature of the tumour invasive front and the mixed population of tumour and stroma seen in oropharyngeal cases. As the interest in the advancing front lies in the interaction with tumour-associated stroma, it was possible to assign a score for both tumour cores and tumour advancing fronts from the single central core. Initially a scoring system for each marker was determined by Dr Asterios Triantafyllou and a single TMA scored by Frances Greaney, Dr Risk and Dr Schache together. Subsequent scoring of additional TMAs was performed by a single user (FG). Triplicate scores were consolidated to a single consensus score, if triplicates were unattainable due to missing cores or no tumour cells in the sample, cores from the advancing front samples were added to

the cohort. 88/97 (90.72%) patients received a score for all the markers; podoplanin, E-cadherin and vimentin.

6.2.4 Nodal Tissue

48 patients had available nodal tissue, with the majority originating from HPV-positive patients (32/48; 66.67%). To deduce whether nodal scores could be substituted for missing primary tumour cases, the level of agreement between available nodal and primary tissue scores was assessed for each marker using Kendall's concordance coefficient (W) where a score of 1 shows perfect agreement and a score of 0 indicates perfect disagreement (Table 6.2). Only vimentin and podoplanin appeared to show strong agreement between primary and nodal tumour, yet this was not as strong when comparing the advancing front scores with nodal advancing front. Therefore, any missing cores from primary tumour were not substituted with nodal scores. However, this could give an indication on the expression levels of each protein through the cycle of metastasis.

Marker	Primary tumour core vs Nodal core Kendall's W	Relationship	Primary advancing front vs nodal advancing front Kendall's W	Relationship
Vimentin	0.703	Strong agreement	0.615	Moderate agreement
Podoplanin	0.828	Strong agreement	0.648	Moderate agreement
E-cadherin	0.649	Moderate agreement	0.427	Weak agreement

Table 6.2 Relationship of scores for vimentin, podoplanin and E-cadherin between primary and nodal tissue

6.2.5 Vimentin staining

A vimentin score was obtained for 91/97 (93.81%; 43 HPV-negative; 48 HPV-positive) primary tumours and 45/48 (93.75%; 15 HPV-negative; 30 HPV-positive) nodal tissue. As a mesenchymal marker¹⁸⁵, vimentin is present on the intermediate filaments attached to the nucleus, endoplasmic reticulum and mitochondria of all stroma cells, therefore only stained cells within the body of the tumour were included in the scoring, and stroma cells excluded. Staining of normal tissue is shown in Figure 6.2

where the stroma is strongly stained and the epithelium is negative with single positive cells.

Tumour cells were assigned low (<10% cells positive), medium (10-50% cells positive) or high (>50% cells positive); Categories 1,2 or 3 respectively. Figure 6.3 denotes each scoring category for the tumour centre. For analysis and comparison between HPV groups, categories 2 and 3 were combined as the vimentin-positive group and compared to category 1 as the vimentin-negative group.

There was an additional scoring category if the tumour cells closely associated with surrounded stroma, termed 'the advancing front', were positive (score of 1), either partially or in its entirety, or had absent staining (score of 0). Figure 6.4 denotes positive and negative 'advancing fronts' and shows partial and entire staining.

Different patterns of staining were present across cores and examples are illustrated in Figures 6.2-6.4 with one case showing 'finger-like' projections of vimentin extending from the stroma into the centre of the tumour.

In all cohorts, a tumour score of 1 was most commonly observed, and tumour scores of 3 were most often associated with staining at the advancing front (Table 6.3). There was no significant difference between HPV-negative and HPV-positive patients in terms of proportion of the population that were vimentin positive in either the primary tumour ($p=0.913$), nodal tissue ($p=0.538$) or presence of advancing front ($p=1$).

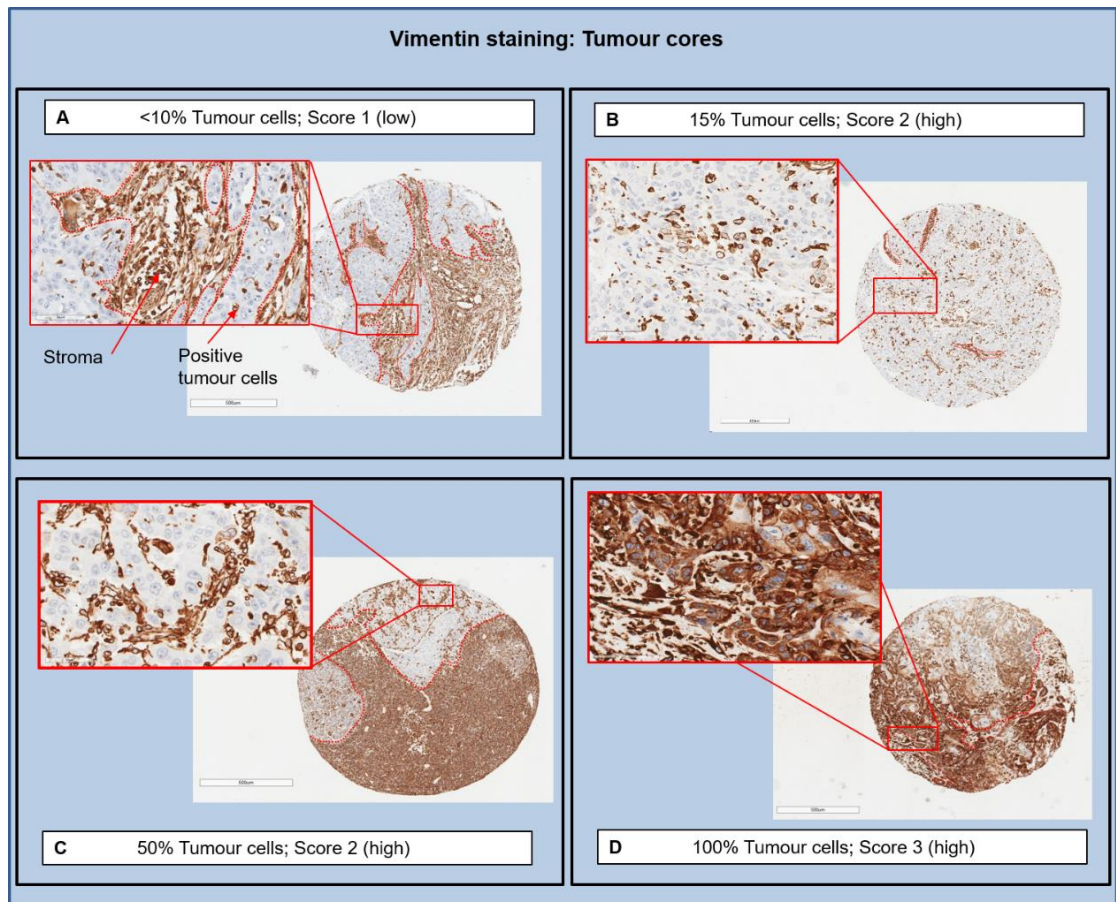


Figure 6.3 Representation of each vimentin scoring category for primary tissue. Tumour populations outlined in red with higher magnification (x40) boxes to show individual cells (A) Score 1 (<10% tumour cells positive) (B) Score 2 (15% tumour cells positive) (C) Score 2 (50% tumour cells positive) (D) Score 3 (>50% tumour cells positive). Magnifications 6x and 40x.

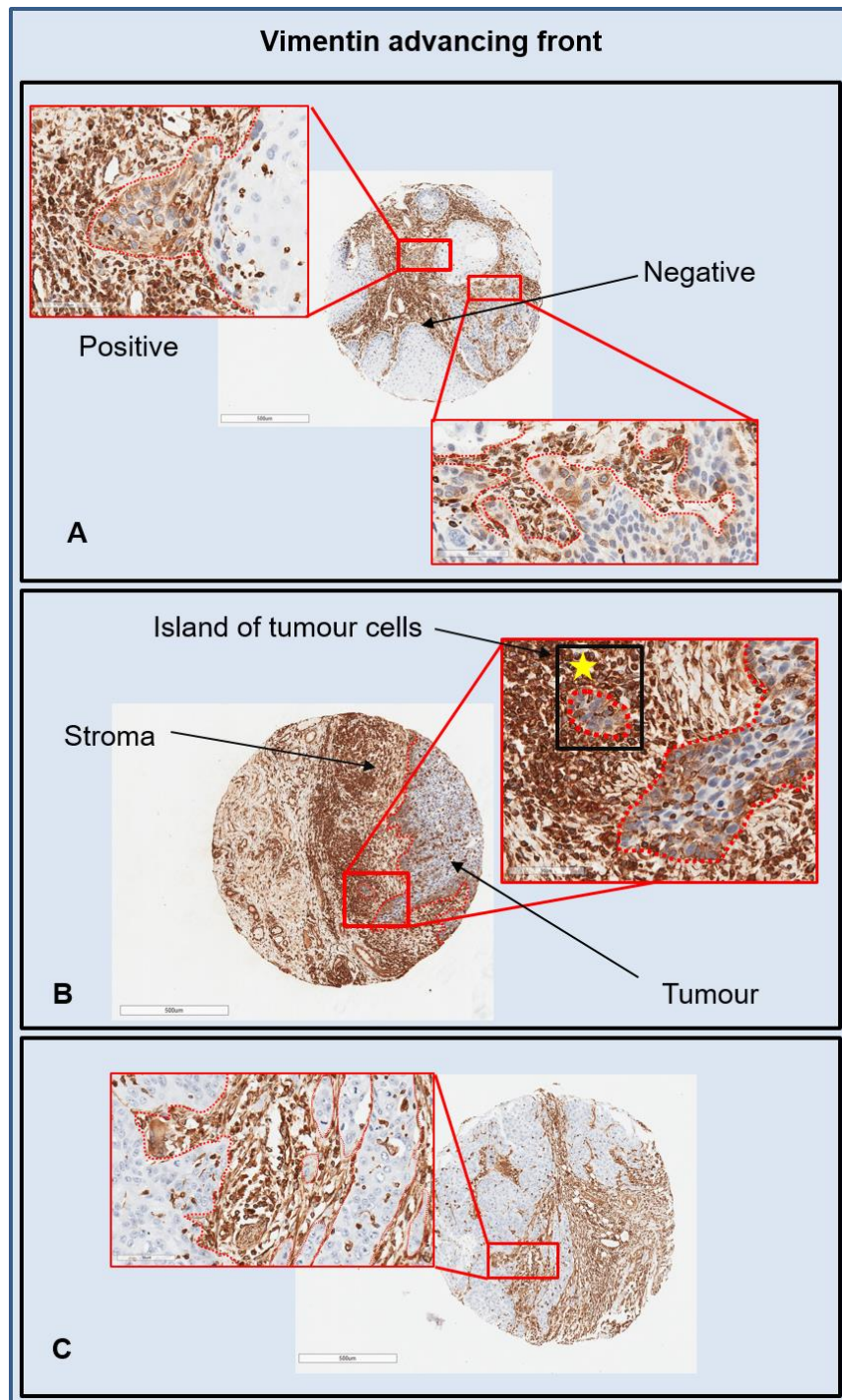


Figure 6.4 Representation of vimentin-positive staining for (A) partial (B) entire and (C) negative advancing fronts. Star represents tumour island migrating away from main specimen. Magnification at 6x and 40x.

Vimentin Score	HPV-negative		HPV-positive		<i>P</i>	
	Primary Tissue					
	N=43		N=48			
	Total number	Positive advancing fronts	Total number	Positive advancing fronts	Total number	Positive advancing front
1	28	6	22	8	.913	1
2	3	1	12	3		
3	12	10	14	13		
	Nodal Tissue				<i>P</i>	
	N=15		N=30			
	1	8	1	19	4	.538
2	3	0	4	1		
3	4	3	7	7		

Table 6.3 Vimentin scores for primary and nodal tissue. Fisher’s exact t-test

6.2.6 Podoplanin

A podoplanin score was obtained for 90/97 (92.78%; 43 HPV-negative, 47 HPV-positive) primary tumours and 46/48 (95.83%; 16 HPV-negative, 30 HPV-positive) nodal tissue. Podoplanin is expressed on lymphatic endothelium, but not blood vessel endothelium and is a cytoplasmic stain, although can sometimes be membranous, as described on the data sheet. There was a significant difference between the number of cases with membranous staining depending on HPV status as 2/43 HPV-negative cases and 10/47 HPV-positive cases had additional

membranous and cytoplasmic staining ($p=0.0286$). The scoring criteria was determined by the intensities of staining within tumour cells and categorised as; absent, + or ++ with scores of 0, 1 or 2 respectively and illustrated in Figure 6.5. Examples of stains within nodal tissue are illustrated in Figure 6.6. Cases which had a stronger staining across the advancing front (Figure 6.5) were noted and there were 29 cases with a positive advancing front in both the HPV-negative and HPV-positive primary tumour cohorts and therefore no significant difference between groups ($p=0.6611$). Nodal tissue also showed no significant difference for staining intensity ($p=.894$), advancing front staining ($p=1$) or membranous staining ($p=0.282$) however, there was a significantly greater proportion of HPV-positive tumours with intense staining ($p=.0432$) (Table 6.4).

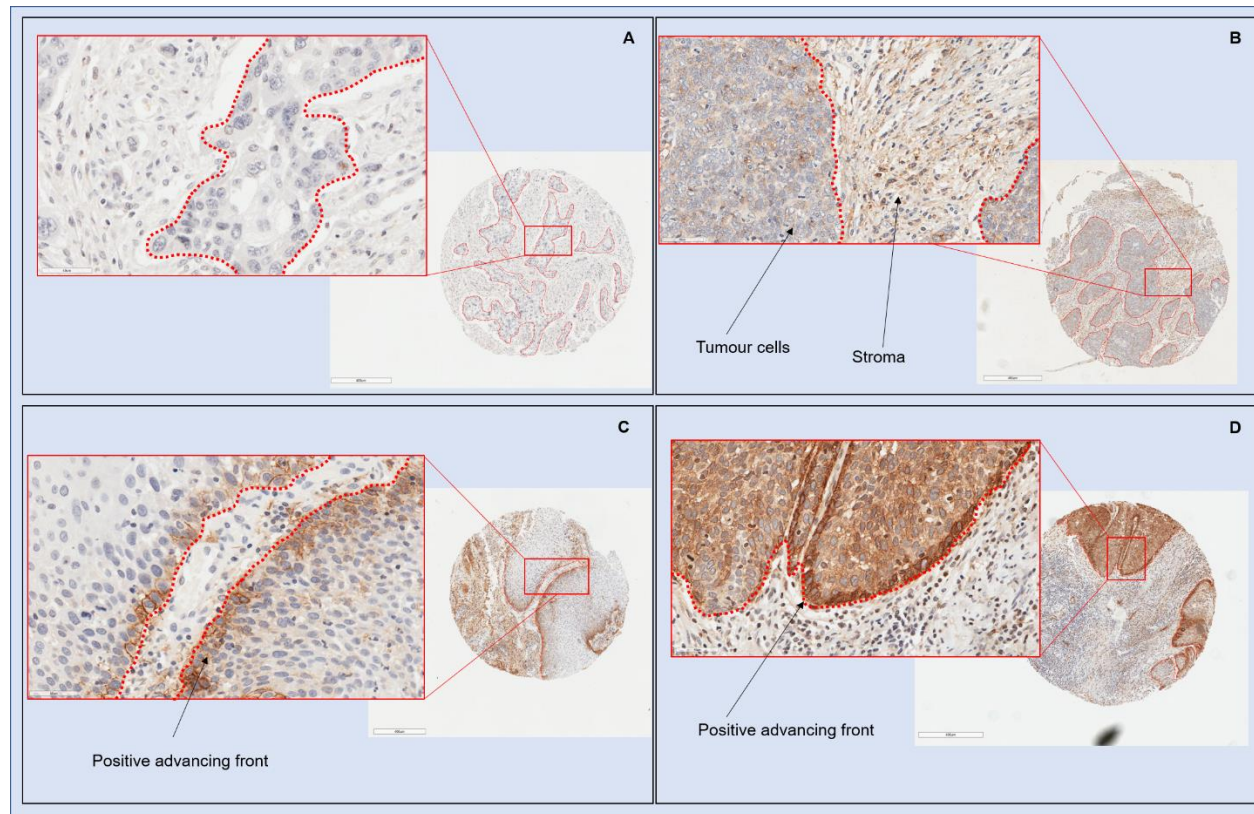


Figure 6.5 Examples of podoplanin cores with each scoring criteria. Absent; Score=0 (A) Weak cytoplasmic staining with negative advancing front; Score=1 (B) Staining in advancing front only; Score=1 (C) Strong staining throughout tumour cells and positive advancing front; Score=2 (D). Magnification at 40x and 6x

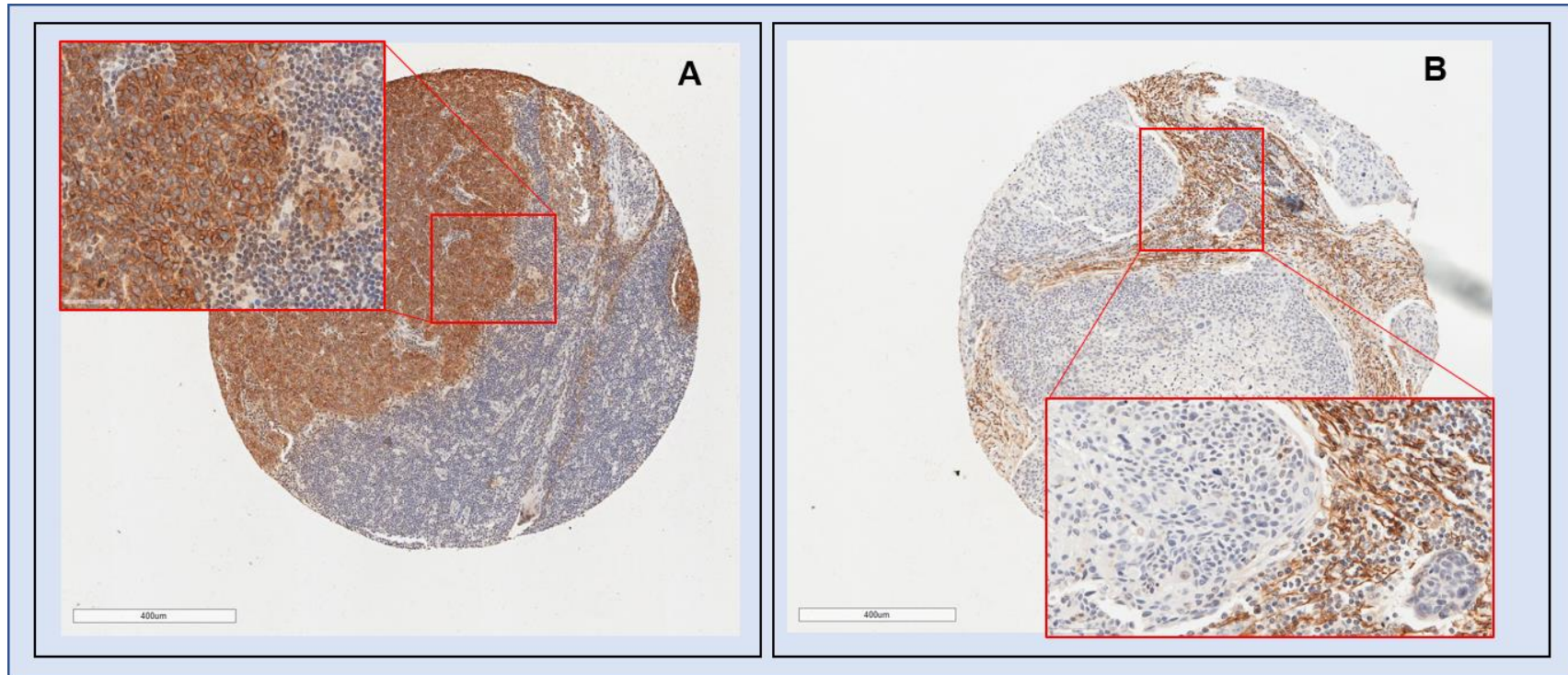


Figure 6.6 Nodal tissue with positive (score 2) podoplanin staining (A) and negative (score 0) staining (B)

Podoplanin Score	HPV-negative		HPV-positive		<i>P</i>	
	Primary Tissue					
	N=43		N=47			
	Total number	Membrane staining	Total number	Membrane staining	Total number	Positive advancing front
0	10	0	11	0	.0432	.6611
1	20	2	11	0		
2	13	0	25	10		
	Nodal Tissue				<i>P</i>	
	N=16		N=30			
	0	2	0	4	0	.894
1	7	0	11	1		
2	7	0	15	3		

Table 6.4 Podoplanin scores for primary and nodal tissue. P values denote Chi-squared calculation between all groups.

6.2.7 E-cadherin

An E-cadherin score was obtained for 89/97 (91.75%; 42 HPV-negative 47 HPV-positive) primary tumour samples and 47/48 (97.92%; 15 HPV-negative 31 HPV-positive) nodal samples. Due to E-cadherin being a transmembrane protein, staining in controls was membranous, however cytoplasmic staining was observed and has been shown to be present in oral SCC¹⁸⁶. There was a

correlation between HPV-negativity and cytoplasm staining and HPV-positivity and membranous staining in primary tissue ($p < .00001$) (Table 6.5). Tumour cells were given a score based on the intensities of cytoplasmic and/or membranous staining ranging from absent, +, ++ or +++ with scores 0,1,2 or 3 respectively (Figure 6.7). Although the majority of HPV-negative cases were all cytoplasmic (65.63%), there were isolated cases where the advancing front of the tumour had a different expression or pattern of staining compared to the tumour core, either by change in intensity or the loss of membranous staining towards the advancing front as demonstrated in Figure 6.8. HPV-positive primary tissue showed significantly more intense staining than HPV-negative primary tissue ($p < .00001$), however this was not correlated in nodal tissue ($p = .5156$).

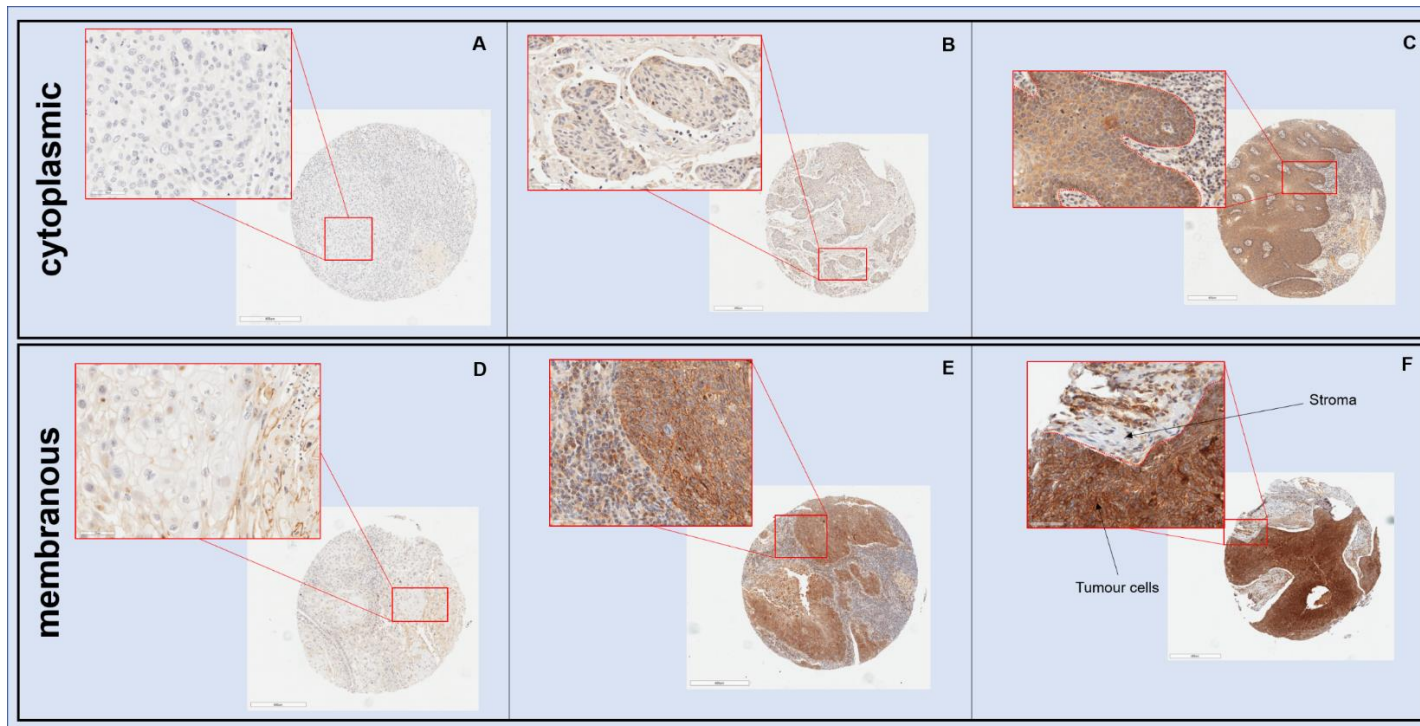


Figure 6.7 Representative cores for each scoring criteria for E-cadherin both cytoplasmic (A-C) and membranous staining (D-F). Absent; Score 0 (A) + cytoplasmic stain (B) ++ cytoplasmic stain (C) + membrane stain (D) ++ membrane stain (E) +++ membrane stain (F). Stroma cells negative staining. Magnification 6x and 40x

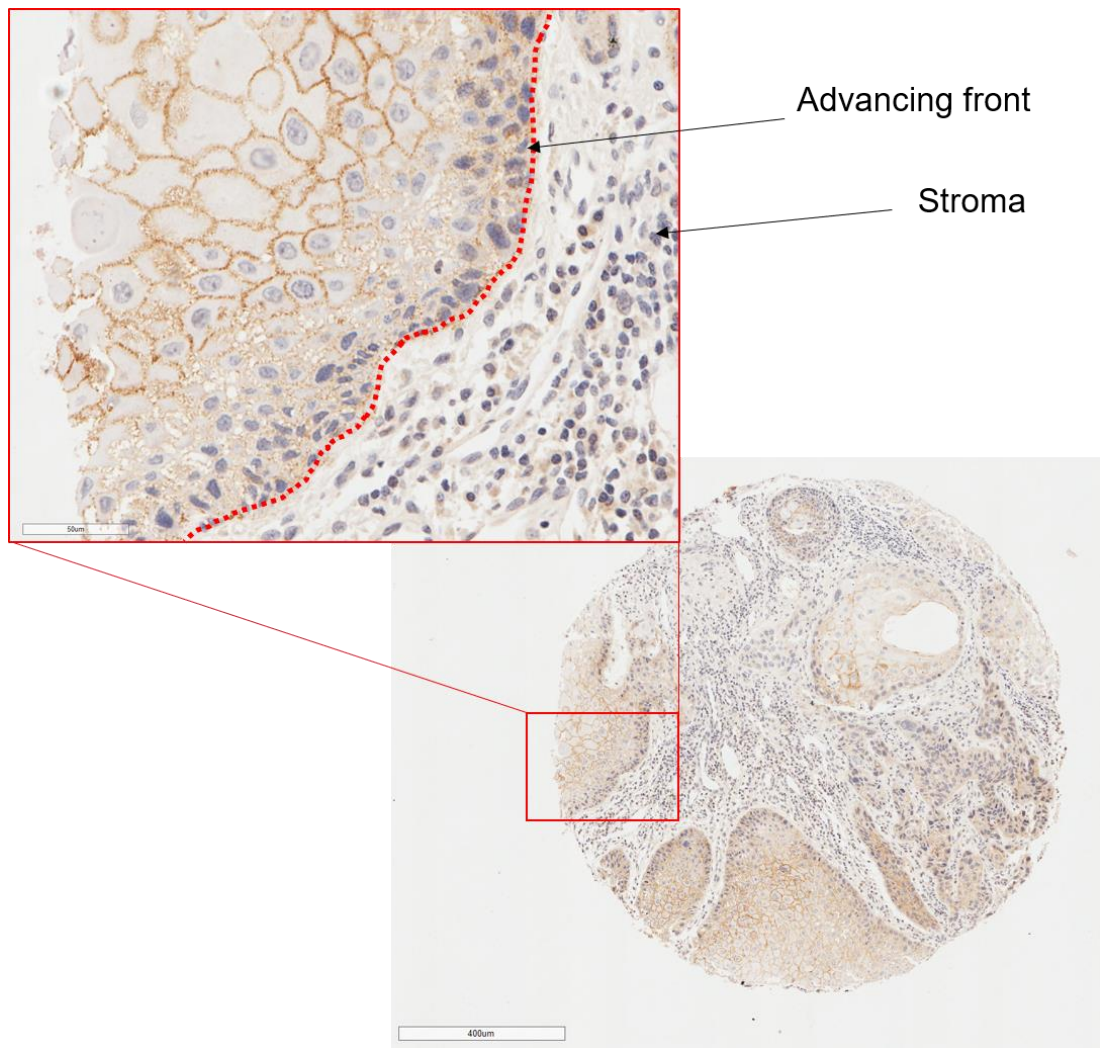


Figure 6.8 Example of loss of membrane staining at advancing front in tumour. Magnification x6 and x40

Max E-cadherin Score	HPV-negative		HPV-positive		<i>P</i>	
	Primary Tissue					
	N=42		N=47			
	Total number	Number of cytoplasm staining (%)	Total number	Number of cytoplasm staining (%)	Total number	Cytoplasm staining
0	10	21/32 (65.63)	0	10/47 (21.28)	<.00001	<.00001
1	19		9			
2	11		26			
3	2		12			
	Nodal Tissue				<i>P</i>	
	N=15		N=30			
	Total number	Number of cytoplasm staining (%)	Total number	Number of cytoplasm staining (%)	Total number	Cytoplasm staining
0	4	7/11 (63.63)	3	8/27 (28.57)	.5156	0.0733
1	3		7			
2	8		12			
3	0		9			

Table 6.5 E-cadherin scores for primary tumour and nodal tissue.

Scores 1, 2 and 3 represent the highest intensity of E-cadherin staining regardless of membrane/cytoplasm staining. Proportion of total cases stained with only cytoplasm staining. T-test significance <.05

6.2.8 Epithelial-Mesenchymal Transition (EMT)-

Associated Phenotypes and Invasiveness

The combination of the loss the epithelial marker of E-cadherin and gain of the mesenchymal marker vimentin could indicate cells have transitioned from static epithelial cells to more mobile mesenchymal cells. Increases in podoplanin expression could indicate a more invasive phenotype and the number of cases with these proteins in combination are demonstrated in Table 6.6.

To re-score depending on high/low expression, E-cadherin, podoplanin and vimentin scores >1 were labelled as high expression. A positive EMT-Associated phenotype was defined as the combination of high vimentin and low E-cadherin expression and although not statistically significant, there was a strong trend towards HPV-negative tumours having more EMT-positive phenotypes ($p=0.0679$) (Table 6.6). This was not replicated in the nodal tissue ($p=1$), however the number of cases with dual opposing stains was much lower. Only 21/42 (50%) HPV-negative and 25/47 (53.19%) HPV-positive primary tumour cases and

10/15 HPV-negative and 18/30 HPV-positive nodal cases had clear opposing expression levels. The remaining scores were either low or high expression for both proteins.

Low E-cadherin staining combined with high demonstrates a possibly more invasive phenotype and HPV-negative cases showed a significantly more invasive phenotype with this classification ($p=.0359$) yet conversely when high podoplanin combined with high vimentin was used to define an invasive phenotype, HPV-positive cases were significantly more invasive ($p=.0102$).

6.2.9 Impact on Nodal status

Each marker was analysed individually and in combination to observe if varying expression levels had an impact on nodal status of the patient. Due to the majority of HPV-positive patients presenting with node positive disease (27/45 recorded node-positive) comparisons were made within HPV-status groups. Table 6.7 demonstrates that expression of podoplanin, E-cadherin or vimentin did not significantly impact nodal status. Statistical power reduces when additional markers are included and

although EMT-associated markers and invasions markers are included in Table 6.7 the total number of cases with all the required information is reduced to a smaller overall number (HPV-negative N=9; HPV-positive N=16).

Criteria	HPV-negative	HPV-positive	<i>P</i>
	Primary Tissue		
	Total number of cases	Total number of cases	
EMT-Associated phenotype	N=21	N=25	
Negative (High E-cadherin/low vimentin)	10	19	.0679
Positive (Low E-cadherin/high vimentin)	11	6	
Invasion phenotype	N=15	N=17	
Low invasiveness (Low podoplanin/high E-cadherin)	3	10	.0359
High invasiveness (High podoplanin/Low E-cadherin)	12	7	
	N=28	N=22	
Low invasiveness (Low podoplanin/low vimentin)	17	5	.0102
High invasiveness (High podoplanin/high vimentin)	11	17	
Criteria	HPV-negative	HPV-positive	<i>P</i>
	Nodal Tissue		
	Total number of cases	Total number of cases	
EMT-Associated phenotype	N=9	N=14	
Negative (High E-cadherin/low vimentin)	6	9	1
Positive (Low E-cadherin/high vimentin)	3	5	
Invasion phenotype	N=10	N=18	
Low invasiveness (Low podoplanin/high E-cadherin)	3	5	1
High invasiveness (High podoplanin/Low E-cadherin)	7	13	
	N=8	N=16	
Low invasiveness (Low podoplanin/low vimentin)	5	10	1
High invasiveness (High podoplanin/high vimentin)	3	6	

Table 6.6 Combination of EMT and invasion markers in primary and nodal tissue. T-test significance <.05

	HPV-Negative			HPV-Positive		
	N0	N+	<i>p</i>	N0	N+	<i>p</i>
E-cadherin expression						
Low	5	14	1	2	7	0.6585
High	3	10		6	29	
E-cadherin membrane staining						
Negative	5	19	0.3346	3	10	0.6689
Positive	3	4		5	28	
Podoplanin expression						
Low	4	11	1	1	12	0.4088
High	4	14		7	26	
Vimentin expression						
Low	7	16	0.382	5	16	0.4372
High	1	9		3	23	
EMT-Associated phenotype						
Negative	1	2	0.333	4	6	0.5879
Positive	0	6		1	5	
Invasion Profiles						
Low (high ECad/low PDPN)	2	8	0.5	0	2	1
High (low Ecad/high PDPN)	0	6		6	21	
Low (low PDPN/low Vim)	4	8	0.6027	1	14	0.0766
High (high PDPN/high vim)	1	6		3	4	

Table 6.7 Effect of protein expression on nodal status. Fisher

Exact t-test significance <0.05

6.2.10 Overall survival and Disease-free survival

HPV Status

Initially overall survival (OS) and disease-free survival (DFS) at 3 years (36months) was calculated for HPV-positive and HPV-negative cohorts (Figure 6.9). HPV-negative patients had significantly worse outcome compared to HPV-positive patients (69% n=12 vs 94.3% n=3 total n=95) ($p < .001$).

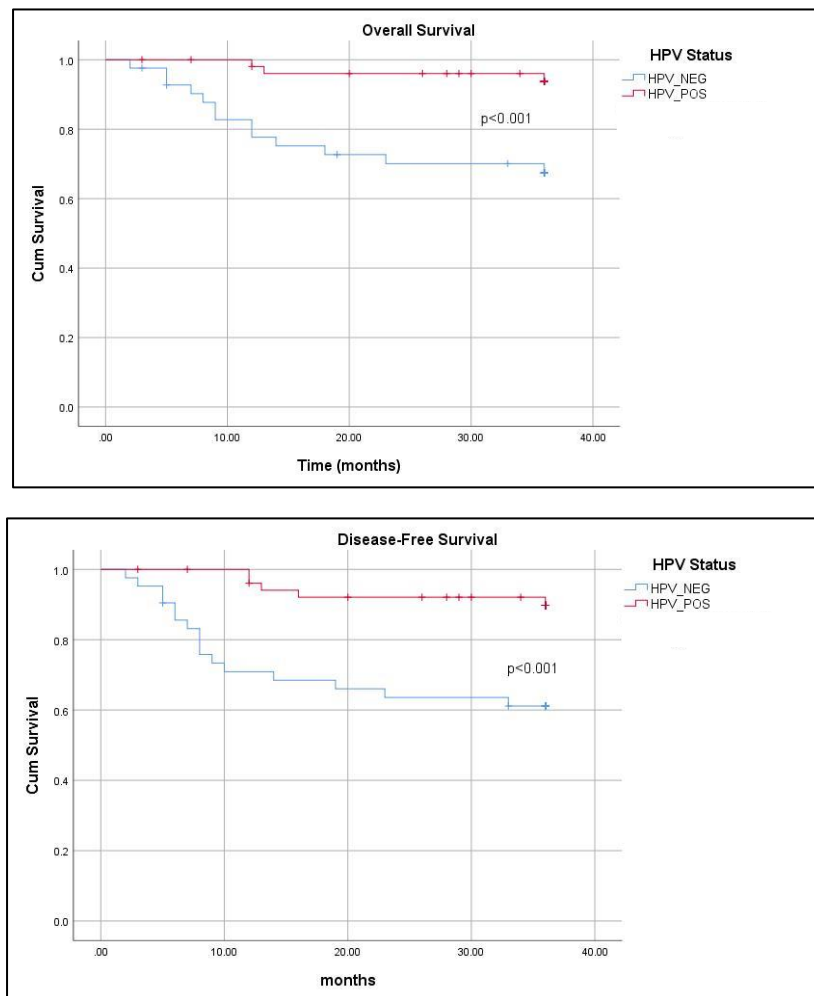


Figure 6.9 Overall and Disease-free survival for HPV-positive and HPV-negative patients. Significance for overall survival and disease-free survival $P < 0.001$ between HPV groups

Node Status

Nodal status was a prognostic factor for HPV-negative patients (OS $p=.062$; DFS $p=.048$) but node-negative status was associated with poor disease-free survival in HPV-positive patients (OS $p=.512$; DFS $p=.051$) (Figure 6.10).

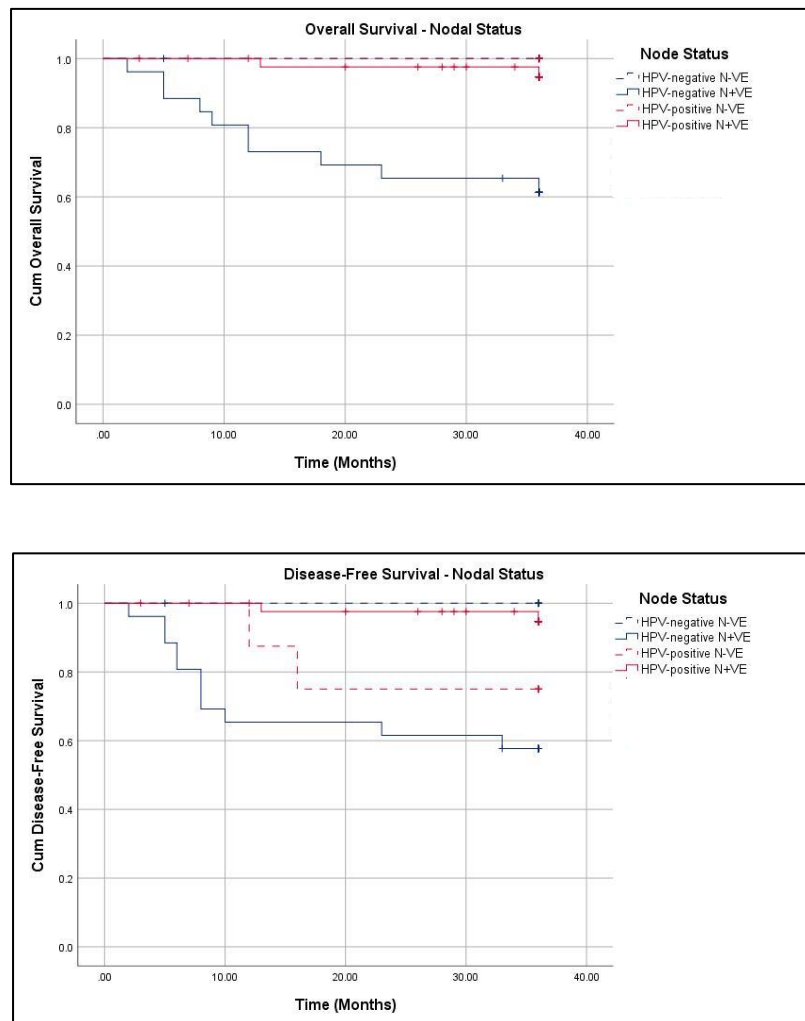


Figure 6.10 Nodal status as a prognostic indicator in HPV-negative (OS $p=.062$; DFS $p=.048$) and HPV-positive overall (OS $p=.512$; DFS $p=.051$) and disease-free survival.

Invasion markers and outcome

Due to the strong-moderate correlation between primary and nodal tissue (Table 6.2) and the increased numbers of stained cases available, only staining in the primary tissue was correlated with outcome.

Vimentin

Vimentin had no significant impact on overall or disease-free survival in either HPV-negative (OS $p=.514$; DFS $p=.255$) or HPV-positive (OS $p=.465$; DFS $p=.121$) patients (Figure 6.11)

E-cadherin

E-cadherin expression had no significant effect on HPV-positive overall or disease-free survival (OS $p=.374$; DFS $p=.243$), but low E-cadherin expression was strongly correlated with poor 3-year overall and disease-free survival in HPV-negative patients (Low ECAD=57.7% $n=11$ vs High ECAD=92.3% $n=1$; total $n=39$) but not in the HPV-positive tumours (Low ECAD=100% $n=0$ vs High ECAD=92.1% $n=3$; total $n=47$) (OS $p=.022$; DFS $p=.006$) (Figure 6.12).

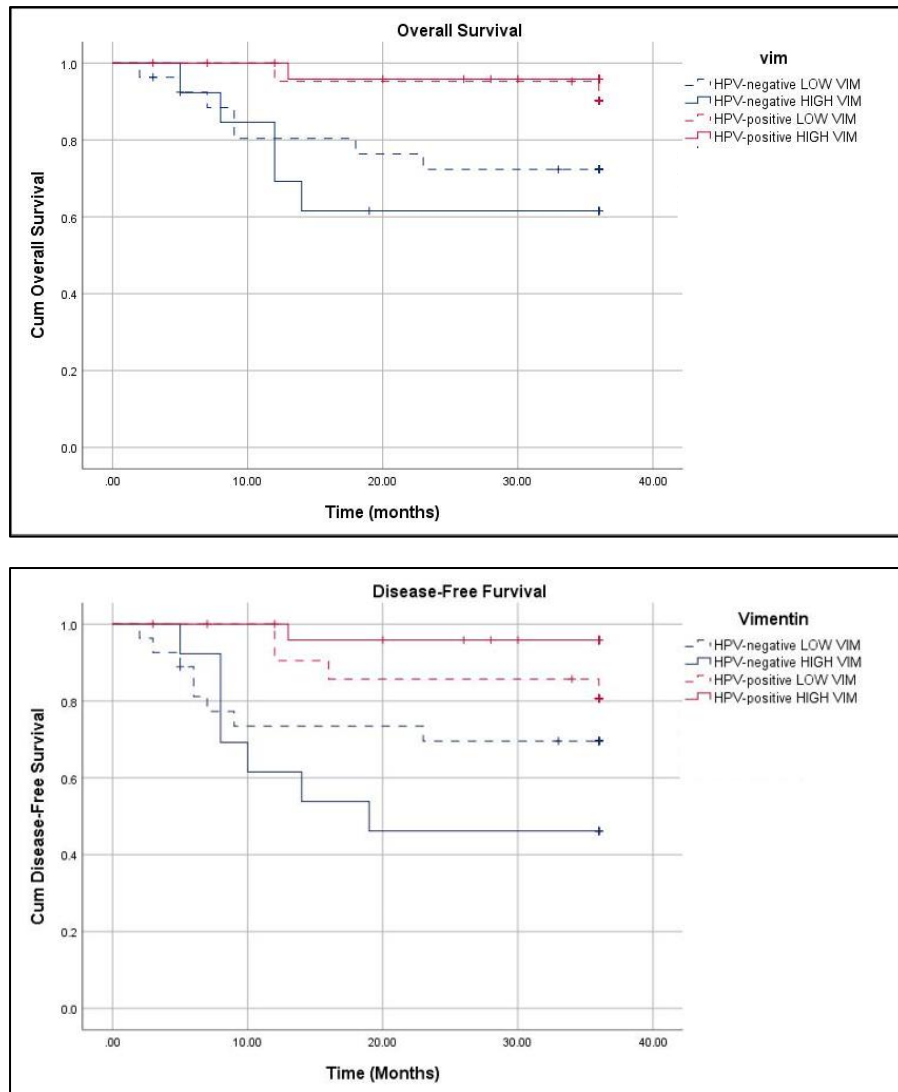


Figure 6.11 Vimentin expression on overall and disease-free survival. HPV-negative (OS $p=0.514$; DFS $p=0.255$) HPV-positive (OS $p=0.465$; DFS $p=0.121$)

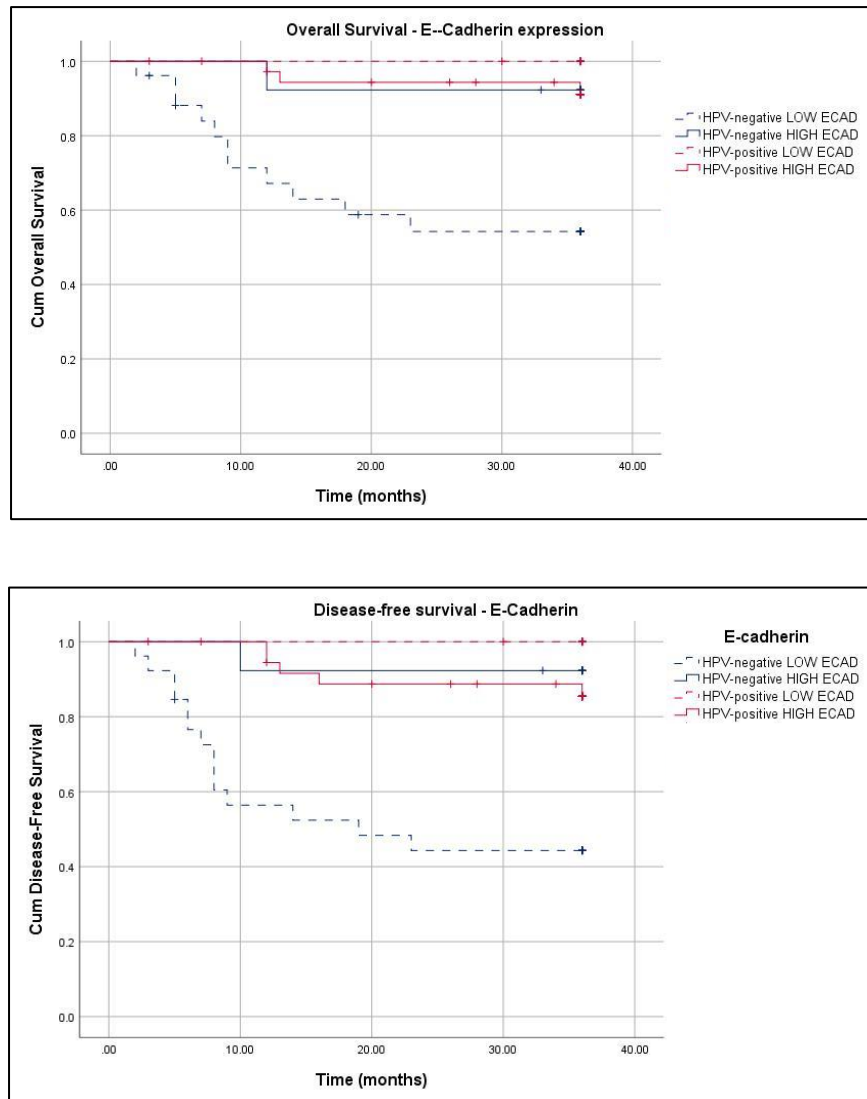


Figure 6.12 Effect of E-cadherin on overall and disease-free survival. HPV-negative (OS $p=.022$; DFS $p=.006$) HPV-positive (OS $p=.374$; DFS $p=.243$)

Podoplanin

Podoplanin expression had no significant effect on overall or disease-free survival in HPV-negative patients (OS $p=.122$; DFS $p=.277$) or HPV-positive patients (OS $p=.322$; DFS $p=.185$) (Figure 6.13).

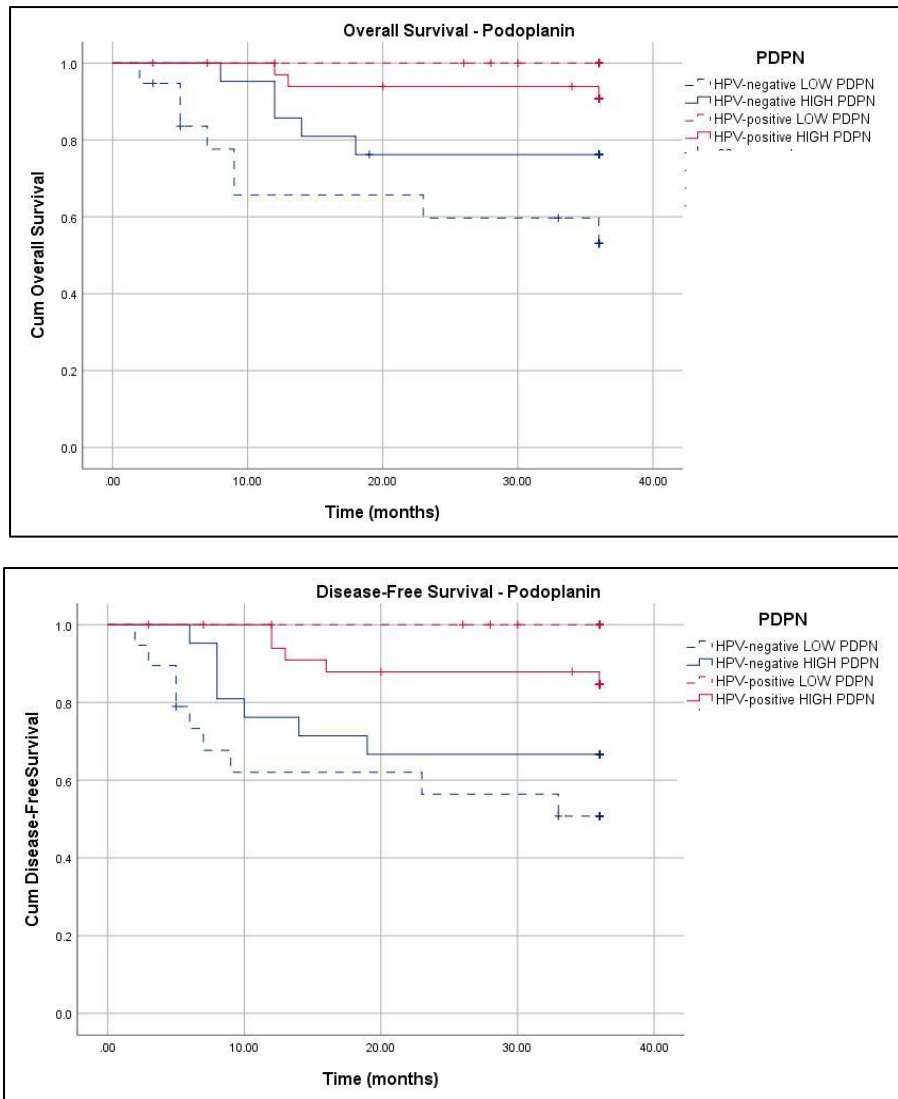


Figure 6.13 Effect of podoplanin on overall and disease-free survival. HPV negative (OS $p=.122$; DFS $p=.277$) HPV-positive (OS $p=.322$; DFS $p=.185$)

Classical EMT

Classical EMT was defined as per Table 6.6 as cases expressing high vimentin with low E-cadherin. Although EMT had no effect on HPV-positive patients, with EMT-negative patients actually having poorer outcome (OS $p=.504$; DFS $p=.379$), EMT-positive patients

who were also HPV-negative tended towards worse disease-free survival (OS $p=.313$; DFS $P=.071$) (Figure 6.14).

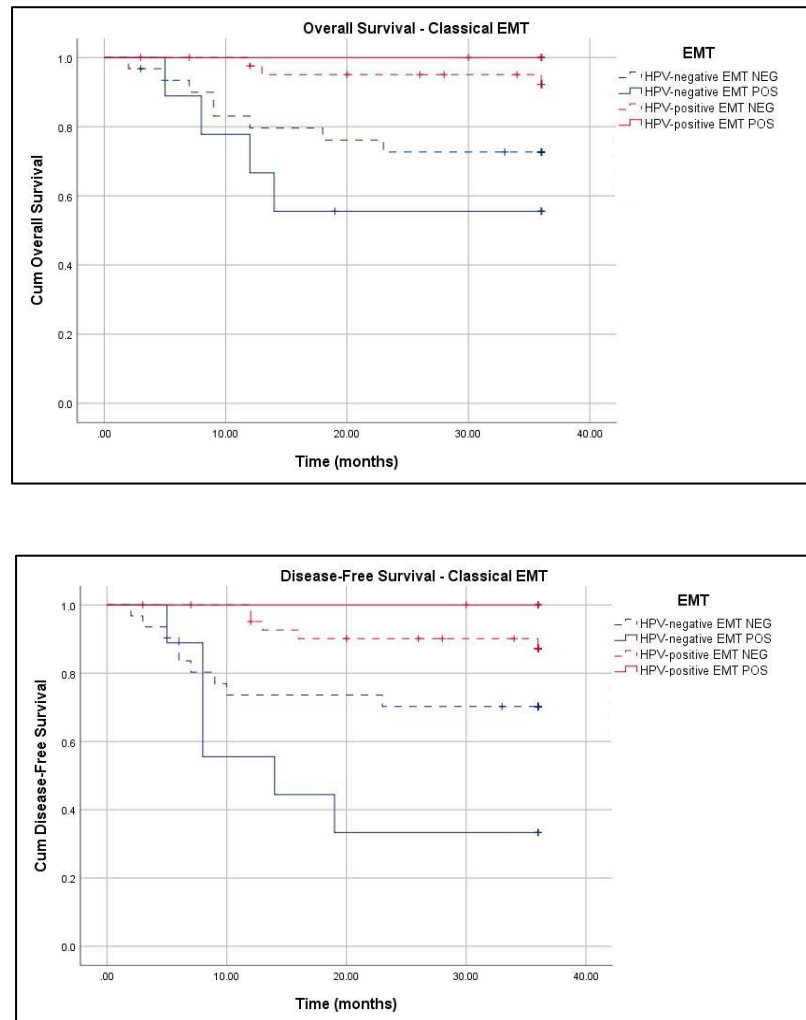


Figure 6.14 Effect of ‘Classical EMT’ on overall survival and disease-free survival. HPV-negative (OS $p=.313$; DFS $P=.071$) HPV-positive (OS $p=.504$; DFS $p=.379$)

Invasiveness

Previously, cases were assigned an invasive phenotype via two separate criteria; both with increased expression of podoplanin but either with low E-cadherin or increased vimentin (Table 6.6).

Figure 6.15 demonstrates OS and DFS in cases with reduced E-cadherin and increased podoplanin. There was no significant impact on OS or DFS in either HPV-negative (OS $p=.841$; DFS $p=.331$) or HPV-positive (OS $p=.434$; DFS; $.310$) cohorts.

Figure 6.16 demonstrates OS and DFS for patients with high vimentin and high podoplanin. Similar to the previous definition of invasiveness, there was no significant association with increased invasiveness and poor overall or disease-free survival in HPV-negative (OS $p=.612$; DFS $p=.245$) or HPV-positive (OS $p=.899$; DFS $p=.425$) patients.

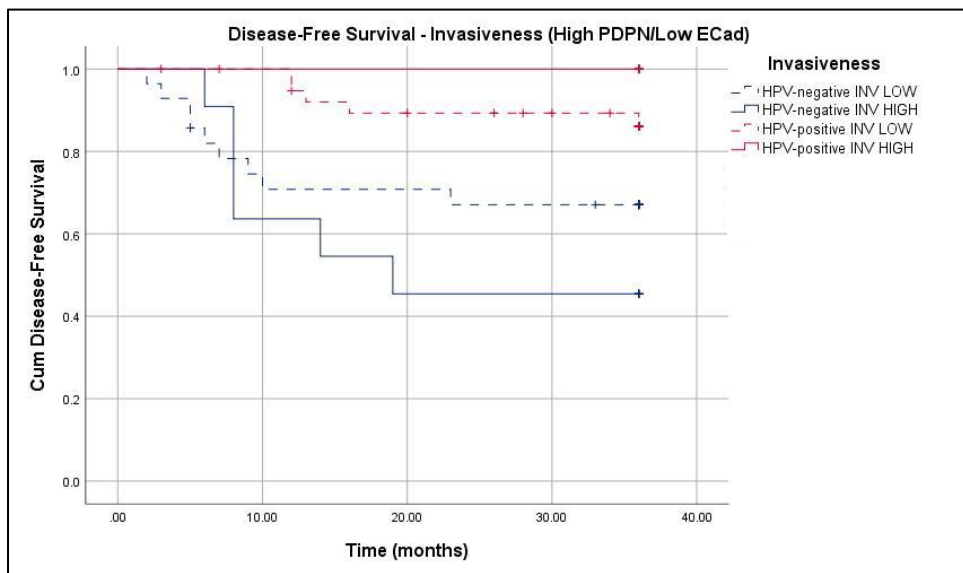
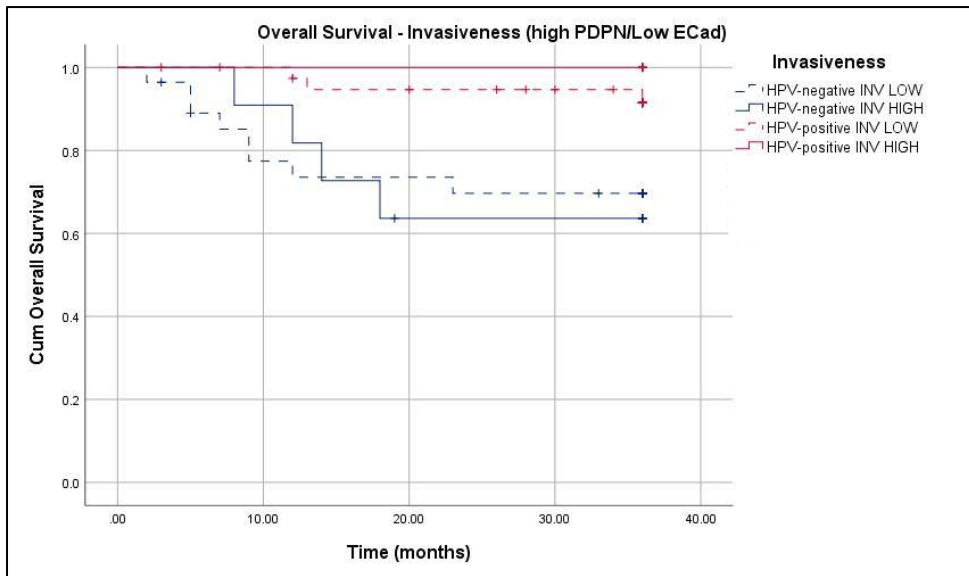


Figure 6.15 Defining invasiveness by high podoplanin and low E-cadherin and its effect on overall survival and disease-free survival. HPV-negative (OS $p=0.841$; DFS $p=0.331$) HPV-positive (OS $p=0.434$; DFS; 0.310)

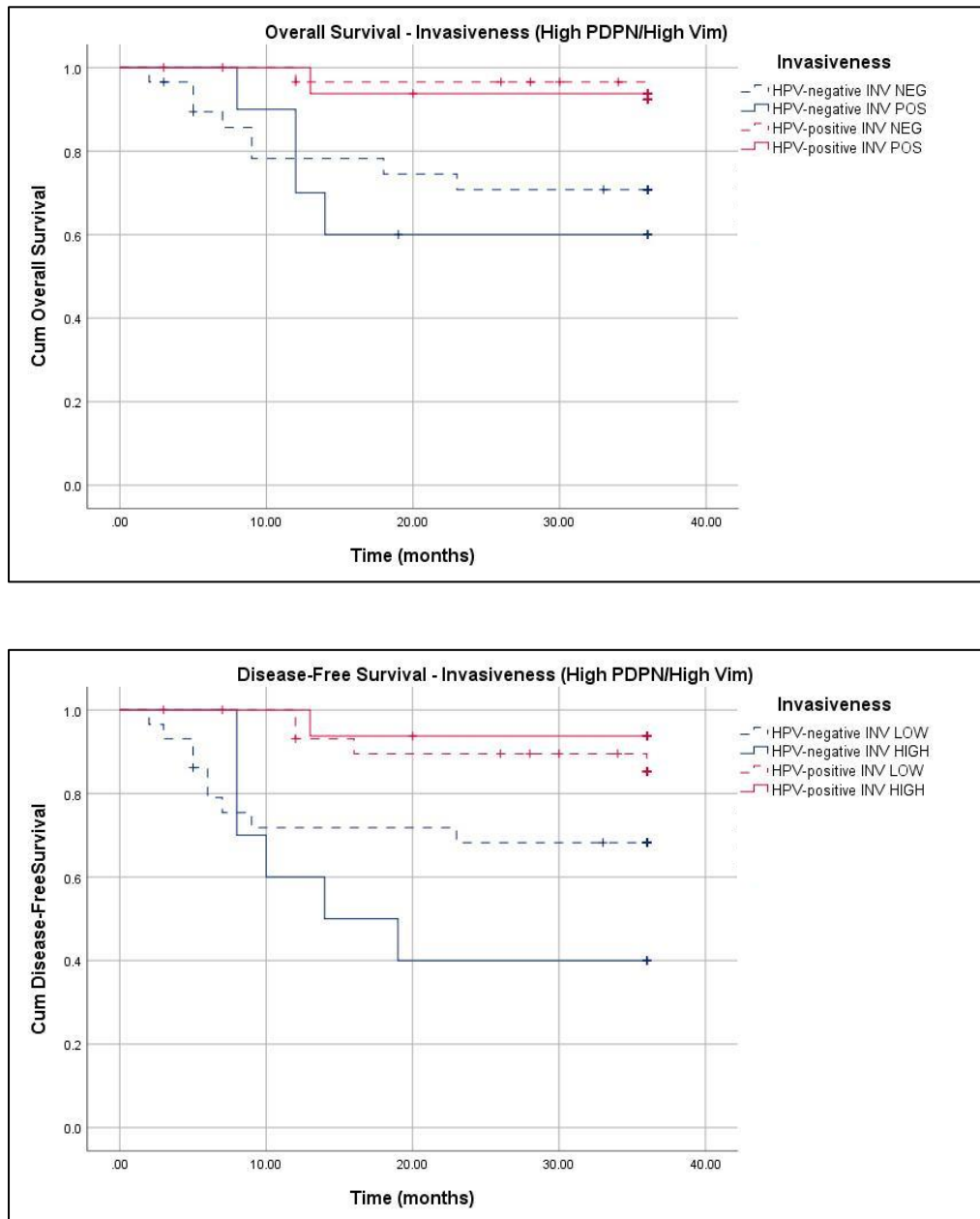


Figure 6.16 An alternative criterion for invasiveness: High podoplanin with high vimentin and its effect on overall survival and disease-free survival. HPV-negative (OS $p=.612$; DFS $p=.245$) HPV-positive (OS $p=.899$; DFS $p=.425$)

Discussion

The current understanding of invasion in HPV-positive OPSCC is limited and although the proteins E-cadherin, podoplanin and vimentin have been examined in various HNSCC research papers^{118,121-124}, studies focusing on oropharyngeal SCC are scarce, and HPV-positive OPSCC are even less so.

The results in this chapter have shown for the first-time HPV-positive OPSCC tumours have significantly higher expression of the invasive marker podoplanin. This is in marked contrast to the results presented by Wakisaka et al that observed HPV-positive tumours have lower E-cadherin and podoplanin expression compared to HPV-negative patients and this is correlated with nodal status¹²⁶ and Preuss et al who found no significant difference in HPV-positive tumours¹²⁸. Additionally, this data shows HPV-negative OPSCC tumours lose the ability to retain membranous E-cadherin and although this does not correlate with nodal metastasis, those patients have significantly worse prognosis (Overall survival $p=0.022$; Disease-free survival $p=0.006$). This is a novel finding for HPV-negative OPSCC as

previously low E-cadherin expression has not been linked to poor prognosis¹²¹. HPV-negative patients who exhibited the 'classic EMT'-associated phenotype of low E-cadherin in addition to high vimentin expression tended towards worse disease-free survival ($p=0.71$).

The presented data shows similar vimentin results to Hatakeyama et al, who also found no significant difference in vimentin expression depending on HPV status, nor did it impact prognosis¹⁸⁴, however this data set disagrees with the results from the papillophar study that showed HPV-positive patients had increased vimentin staining correlating with nodal metastasis¹²⁷.

In comparison to previous studies, this HPV-positive dataset is larger than previously observed with paired nodal tissue that shows close correlation to primary tissue protein expression (strongest for podoplanin and vimentin $W=0.828$ and 0.703 respectively). Clinically, although it appears 'classic EMT' or deregulation of E-cadherin is not the cause for increased incidence of nodal metastasis in HPV-positive OPSCC, podoplanin expression could be involved. The statistical tests to

differentiate between node positive and negative cases and those with poor prognosis is limited in the HPV-positive cohort due to the small numbers available in this data set. Individual cases that exhibit poor survival do not appear reliant on nodal status as poor prognosis was correlated with node negative disease in HPV-positive patients, supporting El Asmar et al⁴¹ and Meyers et al⁴². Individual case observations show that only the HPV-positive patients with high levels of podoplanin have poor outcome. Although this biomarker is not defined to those who have bad outcome, a larger data set could allow for a more sensitive predictive model.

It is important to clarify the limited number of patients with poor overall survival (n=12 in HPV-negative cohort vs n=3 in HPV-positive cohort) and additional samples will provide greater statistical power behind the significant findings of E-cadherin and EMT-associated phenotype.

Chapter 7: Discussion, Limitations and Future Works

The incidence of oropharyngeal squamous cell carcinoma (OPSCC) has been increasing significantly more rapidly in the last 40 years in countries around the world compared to oral cavity^{22,187,188}, and it is estimated around 70% of all cases are driven by Human papillomavirus (HPV), predominantly type HPV16¹⁴. HPV is becoming a huge burden worldwide and it is estimated 5% of all cancers are attributed to the virus¹⁸⁹. The introduction of prophylactic vaccines (Cervarix, Gardasil and Gardasil 9) is expected to drastically reduce incidence numbers and initial reports have reported up to a maximum 90% reduction in HPV6/11/16/18 infection during the first 10 years of vaccination with Gardasil^{62,152}.

HPV-positive OPSCC is now classified as a separate disease to HPV-negative OPSCC due to the differences in prognosis and presentation. The new TNM8 staging released in 2017 accounts for the changing landscape of head and neck cancer and accounts for the good prognosis seen in HPV-positive patients regardless of lymph node involvement and consequently

downstages patients compared to TNM7³⁶. Although clinicians are beginning to adapt their treatment plans to account for this subset of patients, including trials aimed directly at HPV-positive head and neck patients (De-ESCALaTE HPV, NRG Oncology RTOG 1016) the consequences of substituting cisplatin with the less-toxic cetuximab has actually been detrimental to tumour clearance^{190,191}. Until a greater understanding of the underlying biology of this disease is achieved, the standard of care remains the same as HPV-negative disease.

Research should be focusing on the determinants of improved prognosis in 82.4% of patients with HPV-positive OPSCC, and perhaps more importantly why the remaining 17.6% do not share this advantageous outcome, allowing clinicians to confidently prescribe personalised treatment with minimal toxicities⁴⁷. The stark difference in prognosis observed in HPV-driven cancers at other anatomical sites, such as cervical carcinoma of which 99% are HPV-driven and 5-year survival is lower at 67.4%¹⁹², implies that HPV infection alone is not accountable for improved responses to treatment in OPSCC¹⁹³. Furthermore, the mechanisms of disease progression are still to be elucidated, as it

is unknown why the majority of HPV-positive head and neck cancer patients present with advanced nodal disease and why recurrence risk is so low.

The primary aim of this thesis was to establish a suitable *in vitro* HPV-positive head and neck cancer cell model to provide the resource to investigate these questions. Currently, the majority of *in vitro* studies utilise the small number of continuous cell lines which have not been characterised or confirmed as a reliable model for HPV-positive head and neck cancer.

A second aim was to consider epithelial-mesenchymal transition (EMT) and the expression of the invasion-related protein podoplanin as a measure of carcinoma cell migration. This offers the potential to identify biomarkers which could predict patient response and would, for the first-time, allow stratification of HPV-positive tumours to a different treatment regimen based on anticipated outcome.

There are a number of limitations and potential biases within the process of this thesis, including initially the patient sample demographics. All samples collected for primary cell culture were selected from patients undergoing primary surgery as treatment and although the exclusion criteria were narrow, only patients fit for surgery were included. This could lead to a bias towards 'healthier' patients donating samples and potentially do not represent HPV-positive disease overall. This was mitigated by the range of TNM stages, gender and ages of donors to provide a varied demographic for sampling.

The Model of HPV OPSCC: Primary and Secondary Cell Lines

32 attempts to produce an immortal primary cell line derived from an HPV-positive oropharyngeal tumour, which still retained HPV16 E6 or E7 oncogene integration were ultimately unsuccessful. However, it is worth noting the delicate balance of this process, as fungal contamination from the oral cavity remains an obstacle to culture and this is heightened when antimycotics are removed to promote virally-infected cell growth; and as such a compromise was made to avoid loss of all material due to fungal contamination. Furthermore, explants which were successfully

grown direct on plastic surfaces had a reduced ability to reach sufficient confluency for functional assays. This outcome is not exclusive to our methods as other labs have also documented the difficulty they face when attempting to produce continuous cell lines from oropharyngeal tumours, including Prof Suzanne Gollin's lab who derived the UPCI:SCC cell lines and state a 18.8% oropharyngeal tumour success rate compared to 51.1% from other head and neck sites¹⁵⁶. Their paper, along with HPV-positive cervical cell lines and previous results from oral cavity cell lines implied successful cell line establishment is biased towards poor prognosis and could be the factor missing from HPV-positive OPSCC tissue^{137,156}.

Furthermore, the eight cell lines from HPV-positive tumours which did proliferate on plastic failed to retain the viral oncogenes, generating a hypothesis that the normal cells within a heterogenous tumour out-competed those which are virally infected. Few studies have looked at intra-tumour heterogeneity within OPSCC or described normal:tumour ratios in these tissues, however it is worth highlighting that the samples taken from oropharyngeal FFPE blocks detailed in Chapter 6 were rarely exclusively tumour tissue even when it was sampled from the

tumour core supporting the evidence of normal cell 'contamination' in the starting material. Thus, further characterisation of the 'successfully cultured' cells should be implemented to confirm they are of tumour origin, potentially by full transcriptome analysis in comparison to parent tumour and adjacent tissue. Alternatively, xenograft models with the newly established cell lines would confirm carcinogenic potential. Although real-time qPCR has been confirmed as a highly sensitive test for detecting low amounts of HPV DNA, the visual component of p16 IHC, HR-HPV DNA ISH and RNAScope could have provided further information on the cell population in the cell lines^{146,194}. Unfortunately, the delicate nature of low passage cells that were obtained did not result in a robust enough cell pellet for embedding and sectioning for these assays, potentially future application will allow for alternative material to FFPE to be processed.

Possible other causes for a lack of tumour cell growth include the relative lack of somatic mutations in HPV-positive tumours, with studies showing the mutation rate for HPV-positive HNSCC tumours was half that seen in HPV-negative HNSCC tumours¹⁷³,

consistent with the demographic of many non-smokers developing this disease and this could be the cause of successful cell lines being derived from tumours with a high mutational burden.

Although not covered in this research, the methods by which HPV evades apoptosis *in vivo* could supply additional information on the cause of unsuccessful cell line development. Viruses require the ability to avoid a host's apoptotic pathway to ensure survival and HPV does so via its oncogenes E5, E6 and E7. Each have different anti-apoptotic properties including downregulating Fas expression, a protein essential in the death-inducing signalling complex¹⁹⁵ and importantly, degradation of p53 by ubiquitination caused by the binding of E6⁷⁴ and binding of retinoblastoma protein (Rb) by E7, thus freeing E2F to bind to DNA and promote entrance into S phase of cellular proliferation¹⁹⁶. In relation to cell line immortalization, it was proven cells require E6 and E7 to cooperate to maintain cell proliferation *in vitro*¹⁵⁵. Conversely, the splice isoform of E6, E6* potentially has pro-apoptotic properties by binding and thus inactivating E6 supported by a study observing over-expression of E6* in SiHa and the increased

sensitivities to Fas-induce apoptosis¹⁹⁷ This generates the hypothesis that other oncogenes not tested for in this research could influence the outcome of primary cell culture and quantitative analysis of E6* in primary tissue could predict cell line outcome.

In conclusion it is clear that HPV-positive OPSCC cells cannot transition directly to growth on plastic: only two labs worldwide have successfully cultured OPSCC cell lines which still retain HPV16. One successfully established a cell lines with episomal HPV16 yet the doubling time was almost three times that seen in other primary head and neck cell lines at 84 hours¹⁷², making proliferation functional assays difficulty and not applicable for translational research. However, this finding could have an implication on the cell cultures in the current project which were discarded after four weeks of no visible growth and perhaps longer incubation times were necessary. The second lab successfully implemented the feeder cell technique first developed by Prof Margaret Stanley for isolation of cervical carcinoma cells^{96,97}. This supports the need of an *in vitro* model with a more intricate cell culture environment which utilises

stromal cells as an anchor and feeder layer. 3D cultures¹⁹⁸, raft models¹⁹⁹ and/or additional culture supplements (e.g. EGF)²⁰⁰ are probably necessary for the isolation of HPV-positive OPSCC cell lines. The preliminary results presented in this thesis showed that patient-derived fibroblasts are much easier to work with than the conventional mouse 3T3 fibroblasts in this regard and would be a useful starting material for future efforts.

The thesis aim to isolate and maintain an HPV-positive *in vitro* primary OPSCC cell lines was ambitious, yet a large resource of other material was established over the course of this thesis which included HPV-negative cell lines from the oropharynx and oral cavity; paired fibroblasts from tumour and normal tissue and normal keratinocytes from HPV-positive and HPV-negative patients; keratinocytes and fibroblasts from involved lymph nodes and paired frozen tissue and/or bloods from time of surgery. These valuable resources can be utilised in an array of future experiments to develop advanced 3D cell culturing environments, investigate the influence of the tumour stroma or the impact of immune cells and to observe treatment response²⁰¹. Indeed, the initial attempts at organotypic cell culture in this research were

worthwhile for any future researchers who wish to pursue this culture method, however changes should be made to the processing step to avoid loss of seeded keratinocytes, frozen sectioning for example could be more suitable for organotypic dissection. It could also be a method for initiation of HPV-positive explants but may prove difficult to produce a homogenous cell population of keratinocytes. Although an exact reason viable cells did not retain the HPV16 viral genome could not be identified, it could be postulated the viral-positive cells could not compete with non-transformed cells in the initial explant growth stage, evidence of which lays in the similarities in morphology and viability to corresponding normal sample cell culture. Visualisation of HPV DNA integration by fluorescent in situ hybridisation (FISH) could also aid future attempts for successful cell line initiation.

To further investigate a model for HPV-positive OPSCC, the full characterisation of available HPV-positive secondary cell lines provided the first complete profiling of cells which are used worldwide as a tool to investigate HPV-positive head and neck cancer *in vitro*. A major concern for the use of these cell lines are the clinicopathological and demographic features of the patients from which the cell lines were sourced. All primary tumours

originating outside the oropharynx and the single base of tongue tumour presented as a recurrence. Similarly, all patients were smokers and drinkers, which is less common in HPV-positive disease, and subsequently these cell lines may contain higher mutation rates to those seen in the clinical HPV-positive cancer population. This could again strengthen the evidence that establishment of new cell lines is dependent on prognosis/mutational burden.

Regardless of ill-fitting demographics, all six cell lines; UMSCC-47, UMSCC-104^{160,161}, UPCI:SCC152, UPCI:SCC154, UPCI:SCC090^{156,162} and 93-VU-147T¹⁶³ and two cervical cell lines; CaSki and SiHa were confirmed to be HPV-positive by p16 IHC, HR-DNA ISH, RNAScope and the gold standard rt-qPCR for quantitating oncogene expression. Variability between cell lines was observed for the expression of the oncogenes E2, E6 and E7 and for HR-DNA ISH, where SiHa, UMSCC-104 and UPCI:SCC154 gave a negative DNA ISH result, possibly defining RNAScope as a superior testing method. Although not fitting the typical demographic of HPV-positive head and neck disease, these cell lines are still demonstrably HPV-positive and remain an

essential tool for cancer biology studies, especially as they harbour the natural integration of HPV DNA and oncogene expression and do not rely on *in vitro* manipulation. Further mutational analysis of these cell lines could provide insights into why these patient samples led to successful cell culture such as altered apoptotic pathways as described previously, or if common mutational profiles can be observed via sequencing analysis and comparison to the TCGA database that holds data for over 20,000 primary cancer samples²⁰².

The functional analysis of these cell lines utilising individual chambers for migration assays provided a novel insight into the mechanisms of cell movement, without the impact of cell damage usually caused by a scratch assay. Although there was not an obvious difference between the HPV-positive and HPV-negative cell lines, unique patterns emerged for cell movement including single cell movement, collective 'sheet-like' and 'protrusion-led' closure and these data suggest that 2D cell movement is not dependent on HPV status¹⁷⁷. The use of these chambers to observe co-cultures could allow future studies observe the complex relationship between tumour and stroma quite simply.

The observation of instable mitosis, a hallmark of cancer, was captured in SiHa cells and provides confirmation of tripolar mitosis²⁰³. Real-time imaging allows visualisation of cell growth discrepancies and could be implemented in future primary cell culture to confirm cultured explants from tissue are cancer cells with chromosome instability^{204,205}.

IHC on cell line pellets showed unexpectedly strong vimentin staining, a marker for mesenchymal cells, in CaSki and UMSCC-74A which may account for the increased mobility of these cells in the migration assay. However, although vimentin is a marker of mesenchymal cells, it is unclear what direct role it has in migration^{206,207}. All of the cell pellets tested were positive for E-cadherin, but UMSCC-74A had lost membrane staining, implying that these cells had an EMT-associated phenotype¹²⁶ which may account for the quick wound closure time observed in the migration assays. Furthermore, CaSki, UMSCC-4 and UMSCC-104 were podoplanin positive in culture and were the only cell lines to show collective cell movement, particular CaSki and UMSCC-104 that had exclusively 'sheet-like' closure. This agrees with Wicki et al who have shown that podoplanin expression is

linked to the remodelling of the actin cytoskeleton which leads to sheet-like collective cell migration¹¹⁷.

These data on cell line pellets represent static measurements of protein expression, while future experiments with fluorescent protein tagging could allow for observational changes in expression patterns in real time.

The discovery of podoplanin as a potential marker for invasion, together with the observation that an EMT-associated phenotype may lead to increased migration rates *in vitro*, led to the hypothesis that patients with either increased podoplanin expression or an EMT-associated morphology expression at the advancing front had a more aggressive, and therefore more invasive tumour type. A large cohort of FFPE OPSCC samples were collected, arranged into tissue microarrays (TMAs) of the tumour core and advancing front, analysed for these markers and correlated with clinicopathological and survival outcomes.

TMA constructs were utilised due to the advantages over whole stain sectioning and staining, including the ability to analyse large numbers of patients under the same experimental conditions in a timely manner with little wastage of precious tissue^{101,102}.

Sampling of the oropharyngeal tumour cores yielded 100% tumour in only a few cases and tumour stroma was commonly involved. This is worth consideration for future construction of OPSCC TMAs as information on both tumour core and advancing front could be gained from each core allowing for a halving of sampled cores thus preserving precious tissue.

EMT and Podoplanin: potential biomarkers for invasion in HPV-positive OPSCC

A number of studies have clarified the requirements for a prognostic biomarker to be deemed useful and accurate, and indeed many clinical trial focus intently on the study design to ensure thorough statistical power is achieved within their sample collection^{208,209}. Exploratory research, represented by this thesis demonstrates statistical significance may not be achieved with the given sample numbers and this does call for a bigger study to increase statistical power and confirm the statistical significance

seen in some of the markers for overall and disease-free survival. Additionally, similar to the samples selected for primary cell culture the source material originates from patients who have undergone primary surgery as their initial treatment strategy and could pose some bias towards 'healthier' patients rather than the disease population on a whole.

The data in this thesis demonstrated a significant difference between the expression of E-cadherin in HPV-positive and HPV-negative tumours ($p < 0.0001$) with 23% of HPV-negative tumours retaining a high intensity score for E-cadherin versus 81% of HPV-positive tumours. The data shows low E-cadherin has a significant effect on prognosis in HPV-negative oropharyngeal tumours (OS $p = .022$; DFS $p = .006$). Previous meta-analysis has shown this to be true for all HNSCC however only one study that included oropharyngeal tissue was included in their analysis¹²². A study that only focused on HPV-negative oropharyngeal tissue concluded that only low β -catenin, another adheren protein, and not low E-cadherin had an impact on prognosis¹²¹. Therefore, the results from this thesis is the first-time low E-cadherin had been linked to poor overall and disease-free survival in HPV-negative OPSCC.

Furthermore, significantly more HPV-positive samples expressed high podoplanin levels (52.1%) compared to HPV-negative (30.23%) ($p=0.00399$). The results imply that HPV-positive OPSCC cells are not undergoing 'classical' EMT but maintain their epithelial characteristics, yet harbour potentially invasive capabilities due to the overexpression of podoplanin. This is a novel result that contradicts those of Wakisaka et al and Hatakeyama et al who determined that HPV-positive cells showed increased EMT phenotype and downregulation of podoplanin which unexpectedly led to nodal metastasis^{109,164}. Both papers defined the EMT-associated phenotype as E-cadherin negative and vimentin positive and when this definition was applied to our dataset, the results from the two groups tended towards HPV-negative tumours being more EMT-like ($p=0.0679$). Similar to low E-cadherin, this cohort of patients tended towards worse disease-free survival chances (OS $p=.313$; DFS $P=.071$) which has not been correlated in the literature before. Alternative indicators of EMT have been defined in the literature as exclusively the gain of vimentin, and the study that utilised sample data from the papillophar study in France concluded 20.3% HPV-positive

OPSCC samples had increased levels of vimentin and this tended towards worse prognosis¹¹⁰. However, vimentin expression was not significantly different between HPV groups in this thesis and regardless of a higher percentage of HPV-positive tumours scoring the highest vimentin score (>50% tumour cell staining) 14/48 (29.2%), this did not affect overall or disease-free survival. This result is mirrored Hatakeyama et al who also found vimentin was not correlated to HPV status¹⁶⁴.

Podoplanin has been a protein of interest in HNSCC and has been shown as a biomarker for lymph node metastasis in both oral cavity and oropharynx, however this study did not differentiate between sites or HPV-types¹⁰⁷. Additionally, podoplanin-positive cells were described as having partial-EMT (p-EMT) by Parikh et al and they concluded tumours from the oral cavity expressing p-EMT were associated with nodal metastasis but it did not influence overall or disease-free survival.

These previous studies generated the initial hypothesis that HPV-positive tumours would exhibit a more aggressive phenotype, explaining the high nodal metastasis documented in this disease

cohort and it is supported by the data showing HPV-positive tumours significantly over express podoplanin compared to HPV-negative OPSCC. HPV-positive tumours still retained their E-cadherin expression, significantly more than HPV-negative tumours which could impact their migratory abilities as they maintain their epithelial polarity and integrity. Pathological outcome data in our cohort showed that although 70.27% node-positive HPV-positive patients expressed high podoplanin, there was no significant difference to node-negative podoplanin expression ($p=.4186$). The statistical analysis is underpowered for HPV-positive tumours with disease-free nodes and/or poor outcome in our cohort and therefore there was no significant difference in overall survival or disease-free survival in HPV-positive patients depending on podoplanin expression or E-cadherin intensity. This is supported by the interesting observation that of the eight HPV-positive patients who did not survive; three were pN0 yet all had increased podoplanin expression in their primary tumours, one with decreased E-cadherin expression and the other two retaining their epithelial phenotype. Further research is required to determine whether podoplanin is a suitable biomarker for poor prognosis in HPV-positive patients and if other proteins are also affected e.g. β -

catenin. This would require a much larger cohort of patients, especially HPV-positive patients with poor outcome. A supply for such a resource could potentially be PATHOS, a UK trial in which 1000s of HPV-positive OPSCC tissue is being currently collected during surgery with robust clinicopathological, demographic and therapeutic information²¹⁰.

As previous discussed, cells that express podoplanin migrate collectively, as demonstrated in *in vitro* cell line assay (section 5.2.6) and in connection to more HPV-positive tumours expressing this protein it could imply these cells could retain the ability to remain attached to neighbouring cells, therefore reducing single cell metastasis and improving surgical and chemoradiotherapy clearance. The HPV-positive cell lines CaSki and UMSCC-104 both express high podoplanin and retain their membranous E-cadherin expression and therefore would be a good model to test this hypothesis as well as knock out experiments to observe the impact on migratory rates. Additionally, UMSCC-4 would be a good HPV-negative control that still expresses podoplanin and E-cadherin.

In conclusion, this research has provided vital methodology in developing a novel *in vitro* HPV-positive OPSCC model with future emphasis on the need to develop more sophisticated 3D cell cultures and additional investigations into causes for poor cell growth of virally-infected primary cells. The HPV-positive HNSCC cell lines currently available commercially have been fully characterised to allow for continued use as an *in vitro* resource. Although all still actively express HPV16 oncogenes, caution should be applied when translating to the clinical environment due to the irregularities in patient demographics and clinicopathological features to the usual HPV cohort. In addition to testing a larger number of OPSCC tumours, CaSki and UMSCC-104 are good representatives of the EMT landscape observed in HPV-positive OPSCC, and due to the EMT-associated phenotype (low E-cadherin, high vimentin) observed in UMSCC-74A, this cell line would be a good model for HPV-negative disease. Functional analysis of the migratory behaviour of HNSCC cell lines determined unique cell movement patterns which could have an impact on disease dissemination and subsequent protein analysis determined podoplanin as a potential marker of collective cell migration in head and neck SCC. IHC analysis on FFPE oropharyngeal cancer tissue highlighted the observation that

HPV-positive tumours do not have an EMT-associated phenotype because they maintain E-cadherin expression, a result which is not mirror in the current OPSCC literature. Podoplanin was significantly upregulated in HPV-positive tumours and although this protein is a marker for invasiveness there was no statistical significance associated between its expression and nodal progression or survival. The capabilities of podoplanin as a potential biomarker to stratify HPV-positive patients requires further validation by a larger cohort of HPV-positive patients with poor outcome, but may provide an alternative prognostic indicator to nodal status in a cohort where nodal invasion does not predict survival. This thesis has shown low E-cadherin expression significantly predicts worse overall and disease-free survival in HPV-negative OPSCC patients. Although other studies have shown a correlation to low E-cadherin and prognosis, these have only been confirmed in overall HNSCC or oral cavity. This result strengthens the evidence further the disparate biology of HPV-negative and HPV-positive OPSCC.

Chapter 8: Publications supporting this thesis

Frances S.T. Greaney-Davies, Janet M. Risk, Max Robinson,
Triantafilos Liloglou, Richard J. Shaw, Andrew G. Schache,
Essential characterisation of human papillomavirus positive head
and neck cancer cell lines,
Oral Oncology, Volume 103, 2020, 104613,
ISSN 1368-8375,
<https://doi.org/10.1016/j.oraloncology.2020.104613>.

Chapter 9: References

1. Pai SI, Westra WH. Molecular pathology of head and neck cancer: Implications for diagnosis, prognosis, and treatment. *Annu Rev Pathol.* 2009;4:49-70.
2. The web site of the national cancer institute.
<https://www.cancer.gov>. Updated 2012. Accessed 01/20, 2020.
3. Winn DM, Lee YC, Hashibe M, Boffetta P, INHANCE consortium. The INHANCE consortium: Toward a better understanding of the causes and mechanisms of head and neck cancer. *Oral Dis.* 2015;21(6):685-693.
4. Marron M, Boffetta P, Zhang ZF, et al. Cessation of alcohol drinking, tobacco smoking and the reversal of head and neck cancer risk. *Int J Epidemiol.* 2010;39(1):182-196.
5. Pereira IF, Firmino RT, Meira HC, Vasconcelos BC, Noronha VR, Santos VR. Osteoradionecrosis prevalence and associated factors: A ten years retrospective study. *Med Oral Patol Oral Cir Bucal.* 2018;23(6):e633-e638.

6. Goldenberg D, Lee J, Koch WM, et al. Habitual risk factors for head and neck cancer. *Otolaryngol Head Neck Surg.* 2004;131(6):986-993.
7. Purdue MP, Hashibe M, Berthiller J, et al. Type of alcoholic beverage and risk of head and neck cancer--a pooled analysis within the INHANCE consortium. *Am J Epidemiol.* 2009;169(2):132-142.
8. Jefferies S, Eeles R, Goldgar D, A'Hern R, Henk JM, Gore M. The role of genetic factors in predisposition to squamous cell cancer of the head and neck. *Br J Cancer.* 1999;79(5-6):865-867.
9. Conway DI, Hashibe M, Boffetta P, et al. Enhancing epidemiologic research on head and neck cancer: INHANCE - the international head and neck cancer epidemiology consortium. *Oral Oncol.* 2009;45(9):743-746.
10. Auerbach AD. Fanconi anemia and its diagnosis. *Mutat Res.* 2009;668(1-2):4-10.
11. Kutler DI, Auerbach AD, Satagopan J, et al. High incidence of head and neck squamous cell carcinoma in patients with fanconi anemia. *Arch Otolaryngol Head Neck Surg.* 2003;129(1):106-112.

12. Xu S, Zhao F, Liang Z, et al. Expression of FANCD2 is associated with prognosis in patients with nasopharyngeal carcinoma. *Int J Clin Exp Pathol.* 2019;12(9):3465-3473.
13. Marur S, D'Souza G, Westra WH, Forastiere AA. HPV-associated head and neck cancer: A virus-related cancer epidemic. *Lancet Oncol.* 2010;11(8):781-789.
14. Pytynia KB, Dahlstrom KR, Sturgis EM. Epidemiology of HPV-associated oropharyngeal cancer. *Oral Oncol.* 2014;50(5):380-386.
15. Upile NS, Shaw RJ, Jones TM, et al. Squamous cell carcinoma of the head and neck outside the oropharynx is rarely human papillomavirus related. *Laryngoscope.* 2014;124(12):2739-2744.
16. Kobayashi K, Hisamatsu K, Suzui N, Hara A, Tomita H, Miyazaki T. A review of HPV-related head and neck cancer. *J Clin Med.* 2018;7(9):10.3390/jcm7090241.
17. Sobin LH, Compton CC. TNM seventh edition: What's new, what's changed: Communication from the international union against cancer and the american joint committee on cancer. *Cancer.* 2010;116(22):5336-5339.

18. Bray F, Ferlay J, Soerjomataram I, Siegel RL, Torre LA, Jemal A. Global cancer statistics 2018: GLOBOCAN estimates of incidence and mortality worldwide for 36 cancers in 185 countries. *CA Cancer J Clin.* 2018;68(6):394-424.
19. Cancer research UK - head and neck cancers statistics. <https://www.cancerresearchuk.org/health-professional/cancer-statistics/statistics-by-cancer-type/head-and-neck-cancers#heading-Zero>. Updated 2017. Accessed 01/21, 2020.
20. Elrefaey S, Massaro MA, Chiocca S, Chiesa F, Ansarin M. HPV in oropharyngeal cancer: The basics to know in clinical practice. *Acta Otorhinolaryngol Ital.* 2014;34(5):299-309.
21. The global cancer observatory, owned by international agency for research on cancer (IARC). gco.iarc.fr/today/online-analysis-map. Updated 2018. Accessed 01/20, 2020.
22. Chaturvedi AK, Anderson WF, Lortet-Tieulent J, et al. Worldwide trends in incidence rates for oral cavity and oropharyngeal cancers. *J Clin Oncol.* 2013;31(36):4550-4559.
23. Schmidt Jensen J, Jakobsen KK, Mirian C, et al. The copenhagen oral cavity squamous cell carcinoma database:

- Protocol and report on establishing a comprehensive oral cavity cancer database. *Clin Epidemiol*. 2019;11:733-741.
24. D'Souza G, Kreimer AR, Viscidi R, et al. Case-control study of human papillomavirus and oropharyngeal cancer. *N Engl J Med*. 2007;356(19):1944-1956.
25. Chesson HW, Dunne EF, Hariri S, Markowitz LE. The estimated lifetime probability of acquiring human papillomavirus in the united states. *Sex Transm Dis*. 2014;41(11):660-664.
26. Chaturvedi AK, Engels EA, Pfeiffer RM, et al. Human papillomavirus and rising oropharyngeal cancer incidence in the united states. *J Clin Oncol*. 2011;29(32):4294-4301.
27. England PH. HPV universal vaccine programme. <https://www.gov.uk/government/collections/hpv-vaccination-programme>. Updated 2019. Accessed 01/28, 2020.
28. Goldenberg D, Begum S, Westra WH, et al. Cystic lymph node metastasis in patients with head and neck cancer: An HPV-associated phenomenon. *Head Neck*. 2008;30(7):898-903.

29. Mehanna H, Paleri V, West CM, Nutting C. Head and neck cancer--part 1: Epidemiology, presentation, and prevention. *BMJ*. 2010;341:c4684.
30. NICE Guideline Updates Team (UK). . 2018.
31. Singhi AD, Westra WH. Comparison of human papillomavirus in situ hybridization and p16 immunohistochemistry in the detection of human papillomavirus-associated head and neck cancer based on a prospective clinical experience. *Cancer*. 2010;116(9):2166-2173.
32. Schache AG, Liloglou T, Risk JM, et al. Evaluation of human papilloma virus diagnostic testing in oropharyngeal squamous cell carcinoma: Sensitivity, specificity, and prognostic discrimination. *Clin Cancer Res*. 2011;17(19):6262-6271.
33. Schache AG, Liloglou T, Risk JM, et al. Validation of a novel diagnostic standard in HPV-positive oropharyngeal squamous cell carcinoma. *Br J Cancer*. 2013;108(6):1332-1339.
34. Gould EA, Winship T, Philbin PH, Kerr HH. Observations on a "sentinel node" in cancer of the parotid. *Cancer*. 1960;13(1):77-78.

35. van Gysen K, Stevens M, Guo L, et al. Validation of the 8(th) edition UICC/AJCC TNM staging system for HPV associated oropharyngeal cancer patients managed with contemporary chemo-radiotherapy. *BMC Cancer*. 2019;19(1):674-019-5894-8.
36. Lydiatt WM, Patel SG, O'Sullivan B, et al. Head and neck cancers-major changes in the american joint committee on cancer eighth edition cancer staging manual. *CA Cancer J Clin*. 2017;67(2):122-137.
37. Duprez F, Berwouts D, De Neve W, et al. Distant metastases in head and neck cancer. *Head Neck*. 2017;39(9):1733-1743.
38. Wiegand S, Zimmermann A, Wilhelm T, Werner JA. Survival after distant metastasis in head and neck cancer. *Anticancer Res*. 2015;35(10):5499-5502.
39. Schuller DE, McGuirt WF, McCabe BF, Young D. The prognostic significance of metastatic cervical lymph nodes. *Laryngoscope*. 1980;90(4):557-570.
40. Shimizu K, Inoue H, Saitoh M, et al. Distribution and impact of lymph node metastases in oropharyngeal cancer. *Acta Otolaryngol*. 2006;126(8):872-877.

41. El Asmar M, Tsai HL, Fakhry C, et al. The prognostic impact of pathologic lymph nodes in HPV-positive oropharyngeal cancers. *Oral Oncol.* 2019;89:23-29.
42. Meyer MF, Meinrath J, Seehawer J, et al. The relevance of the lymph node ratio as predictor of prognosis is higher in HPV-negative than in HPV-positive oropharyngeal squamous cell carcinoma. *Clin Otolaryngol.* 2018;43(1):192-198.
43. Lewis A, Kang R, Levine A, Maghami E. The new face of head and neck cancer: The HPV epidemic. *Oncology (Williston Park).* 2015;29(9):616-626.
44. Mehanna H, West CM, Nutting C, Paleri V. Head and neck cancer--part 2: Treatment and prognostic factors. *BMJ.* 2010;341:c4690.
45. Bhalavat RL, Fakhri AR, Mistry RC, Mahantshetty U. Radical radiation vs surgery plus post-operative radiation in advanced (resectable) supraglottic larynx and pyriform sinus cancers: A prospective randomized study. *European Journal of Surgical Oncology (EJSO).* 2003;29(9):750-756. doi: [https://doi-org.liverpool.idm.oclc.org/10.1016/S0748-7983\(03\)00072-6](https://doi.org.liverpool.idm.oclc.org/10.1016/S0748-7983(03)00072-6).

46. Cancer Research UK C. **Head and neck cancers statistics**. <https://www.cancerresearchuk.org/health-professional/cancer-statistics/statistics-by-cancer-type/head-and-neck-cancers#heading-Two>. Updated 2017. Accessed 30/01, 2020.
47. Ang KK, Harris J, Wheeler R, et al. Human papillomavirus and survival of patients with oropharyngeal cancer. *N Engl J Med*. 2010;363(1):24-35.
48. D'Souza G, Zhang HH, D'Souza WD, Meyer RR, Gillison ML. Moderate predictive value of demographic and behavioral characteristics for a diagnosis of HPV16-positive and HPV16-negative head and neck cancer. *Oral Oncol*. 2010;46(2):100-104.
49. Marzouki HZ, Biron VL, Dziegielewski PT, et al. The impact of human papillomavirus (HPV) status on functional outcomes and quality of life (QOL) after surgical treatment of oropharyngeal carcinoma with free-flap reconstruction. *J Otolaryngol Head Neck Surg*. 2018;47(1):58.
50. Shaw RJ, Lowe D, Woolgar JA, et al. Extracapsular spread in oral squamous cell carcinoma. *Head Neck*. 2010;32(6):714-722.
51. Eldeeb H, Macmillan C, Elwell C, Hammod A. The effect of the surgical margins on the outcome of patients with head and

neck squamous cell carcinoma: Single institution experience.

Cancer Biol Med. 2012;9(1):29-33.

52. Hendry S, Salgado R, Gevaert T, et al. Assessing tumor-infiltrating lymphocytes in solid tumors: A practical review for pathologists and proposal for a standardized method from the international immuno-oncology biomarkers working group: Part 2: TILs in melanoma, gastrointestinal tract carcinomas, non-small cell lung carcinoma and mesothelioma, endometrial and ovarian carcinomas, squamous cell carcinoma of the head and neck, genitourinary carcinomas, and primary brain tumors. *Adv Anat Pathol.* 2017;24(6):311-335.

53. Albers A, Abe K, Hunt J, et al. Antitumor activity of human papillomavirus type 16 E7-specific T cells against virally infected squamous cell carcinoma of the head and neck. *Cancer Res.* 2005;65(23):11146-11155.

54. Tashiro H, Brenner MK. Immunotherapy against cancer-related viruses. *Cell Res.* 2017;27(1):59-73.

55. Ward MJ, Thirdborough SM, Mellows T, et al. Tumour-infiltrating lymphocytes predict for outcome in HPV-positive oropharyngeal cancer. *Br J Cancer.* 2014;110(2):489-500.

56. Doorbar J, Egawa N, Griffin H, Kranjec C, Murakami I. Human papillomavirus molecular biology and disease association. *Rev Med Virol.* 2015;25 Suppl 1:2-23.
57. Van Doorslaer K, Li Z, Xirasagar S, et al. The papillomavirus episteme: A major update to the papillomavirus sequence database. *Nucleic Acids Res.* 2017;45(D1):D499-D506.
58. de Villiers EM, Fauquet C, Broker TR, Bernard HU, zur Hausen H. Classification of papillomaviruses. *Virology.* 2004;324(1):17-27.
59. Chow VT, Leong PW. Complete nucleotide sequence, genomic organization and phylogenetic analysis of a novel genital human papillomavirus type, HLT7474-S. *J Gen Virol.* 1999;80 (Pt 11)(Pt 11):2923-2929.
60. Doorbar J. Molecular biology of human papillomavirus infection and cervical cancer. *Clin Sci (Lond).* 2006;110(5):525-541.
61. Berman TA, Schiller JT. Human papillomavirus in cervical cancer and oropharyngeal cancer: One cause, two diseases. *Cancer.* 2017;123(12):2219-2229.

62. Garland SM, Kjaer SK, Munoz N, et al. Impact and effectiveness of the quadrivalent human papillomavirus vaccine: A systematic review of 10 years of real-world experience. *Clin Infect Dis*. 2016;63(4):519-527.

63. Kirnbauer R, Booy F, Cheng N, Lowy DR, Schiller JT. Papillomavirus L1 major capsid protein self-assembles into virus-like particles that are highly immunogenic. *Proc Natl Acad Sci U S A*. 1992;89(24):12180-12184.

64. Fehrmann F, Laimins LA. Human papillomaviruses: Targeting differentiating epithelial cells for malignant transformation. *Oncogene*. 2003;22(33):5201-5207.

65. D'Abramo CM, Archambault J. Small molecule inhibitors of human papillomavirus protein - protein interactions. *Open Virol J*. 2011;5:80-95.

66. Gravitt PE. Evidence and impact of human papillomavirus latency. *Open Virol J*. 2012;6:198-203.

67. Immunopedia o. Human papillomavirus.

<https://www.immunopaedia.org.za/wp-content/uploads/2014/12/human-papillomavirus-11-jul-11.pdf>.

Updated 2011. Accessed 01/30, 2020.

68. Woodman CB, Collins SI, Young LS. The natural history of cervical HPV infection: Unresolved issues. *Nat Rev Cancer*. 2007;7(1):11-22.
69. McBride AA, Warburton A. The role of integration in oncogenic progression of HPV-associated cancers. *PLoS Pathog*. 2017;13(4):e1006211.
70. Cancer Genome Atlas Research Network, Albert Einstein College of Medicine, Analytical Biological Services, et al. Integrated genomic and molecular characterization of cervical cancer. *Nature*. 2017;543(7645):378-384.
71. Olthof NC, Speel EJ, Kolligs J, et al. Comprehensive analysis of HPV16 integration in OSCC reveals no significant impact of physical status on viral oncogene and virally disrupted human gene expression. *PLoS One*. 2014;9(2):e88718.
72. Parfenov M, Pedamallu CS, Gehlenborg N, et al. Characterization of HPV and host genome interactions in primary head and neck cancers. *Proc Natl Acad Sci U S A*. 2014;111(43):15544-15549.
73. Scarpini CG, Groves IJ, Pett MR, Ward D, Coleman N. Virus transcript levels and cell growth rates after naturally occurring

HPV16 integration events in basal cervical keratinocytes. *J*

Pathol. 2014;233(3):281-293.

74. Huibregtse JM, Scheffner M, Howley PM. A cellular protein

mediates association of p53 with the E6 oncoprotein of human

papillomavirus types 16 or 18. *EMBO J.* 1991;10(13):4129-4135.

75. Hwang SG, Lee D, Kim J, Seo T, Choe J. Human

papillomavirus type 16 E7 binds to E2F1 and activates E2F1-

driven transcription in a retinoblastoma protein-independent

manner. *J Biol Chem.* 2002;277(4):2923-2930.

76. Nevins JR. E2F: A link between the rb tumor suppressor

protein and viral oncoproteins. *Science.* 1992;258(5081):424-429.

77. Ruttkay-Nedecky B, Jimenez Jimenez AM, Nejdil L, et al.

Relevance of infection with human papillomavirus: The role of the

p53 tumor suppressor protein and E6/E7 zinc finger proteins

(review). *Int J Oncol.* 2013;43(6):1754-1762.

78. Vanchieri C. National cancer act: A look back and forward. *J*

Natl Cancer Inst. 2007;99(5):342-345.

79. Dzobo K, Rowe A, Senthebane DA, AlMazyadi MAM, Patten

V, Parker MI. Three-dimensional organoids in cancer research:

The search for the holy grail of preclinical cancer modeling.

OMICS. 2018;22(12):733-748.

80. Courau T, Bonnereau J, Chicoteau J, et al. Cocultures of human colorectal tumor spheroids with immune cells reveal the therapeutic potential of MICA/B and NKG2A targeting for cancer treatment. *J Immunother Cancer*. 2019;7(1):74-019-0553-9.

81. Derda R, Laromaine A, Mammoto A, et al. Paper-supported 3D cell culture for tissue-based bioassays. *Proc Natl Acad Sci U S A*. 2009;106(44):18457-18462.

82. Sodek KL, Ringuette MJ, Brown TJ. Compact spheroid formation by ovarian cancer cells is associated with contractile behavior and an invasive phenotype. *Int J Cancer*. 2009;124(9):2060-2070.

83. Burgstaller G, Oehrle B, Koch I, Lindner M, Eickelberg O. Multiplex profiling of cellular invasion in 3D cell culture models. *PLoS One*. 2013;8(5):e63121.

84. Marur S, D'Souza G, Westra WH, Forastiere AA. HPV-associated head and neck cancer: A virus-related cancer epidemic. *Lancet Oncol*. 2010;11(8):781-789.

85. Hong A, Zhang X, Jones D, et al. Relationships between p53 mutation, HPV status and outcome in oropharyngeal squamous cell carcinoma. *Radiother Oncol*. 2016;118(2):342-349.
86. Ziemann F, Arenz A, Preising S, et al. Increased sensitivity of HPV-positive head and neck cancer cell lines to x-irradiation +/- cisplatin due to decreased expression of E6 and E7 oncoproteins and enhanced apoptosis. *Am J Cancer Res*. 2015;5(3):1017-1031.
87. Gupta AK, Lee JH, Wilke WW, et al. Radiation response in two HPV-infected head-and-neck cancer cell lines in comparison to a non-HPV-infected cell line and relationship to signaling through AKT. *Int J Radiat Oncol Biol Phys*. 2009;74(3):928-933.
88. GEY G. Tissue culture studies of the proliferative capacity of cervical carcinoma and normal epithelium. *Cancer Res*. 1952;12:264-265.
89. Dall KL, Scarpini CG, Roberts I, et al. Characterization of naturally occurring HPV16 integration sites isolated from cervical keratinocytes under noncompetitive conditions. *Cancer Res*. 2008;68(20):8249-8259.

90. Gray E, Pett MR, Ward D, et al. In vitro progression of human papillomavirus 16 episome-associated cervical neoplasia displays fundamental similarities to integrant-associated carcinogenesis. *Cancer Res.* 2010;70(10):4081-4091.
91. Ben-David U, Siranosian B, Ha G, et al. Genetic and transcriptional evolution alters cancer cell line drug response. *Nature.* 2018;560(7718):325-330.
92. Liu YZ, Wang TT, Zhang YZ. A modified method for the culture of naturally HPV-infected high-grade cervical intraepithelial neoplasia keratinocytes from human neoplastic cervical biopsies. *Oncol Lett.* 2016;11(2):1457-1462.
93. Rader JS, Golub TR, Hudson JB, Patel D, Bedell MA, Laimins LA. In vitro differentiation of epithelial cells from cervical neoplasias resembles in vivo lesions. *Oncogene.* 1990;5(4):571-576.
94. Stanley MA, Browne HM, Appleby M, Minson AC. Properties of a non-tumorigenic human cervical keratinocyte cell line. *Int J Cancer.* 1989;43(4):672-676.

95. Llames S, Garcia-Perez E, Meana A, Larcher F, del Rio M. Feeder layer cell actions and applications. *Tissue Eng Part B Rev.* 2015;21(4):345-353.
96. Stanley MA, Parkinson EK. Growth requirements of human cervical epithelial cells in culture. *Int J Cancer.* 1979;24(4):407-414.
97. Pirotte EF, Holzhauser S, Owens D, et al. Sensitivity to inhibition of DNA repair by olaparib in novel oropharyngeal cancer cell lines infected with human papillomavirus. *PLoS One.* 2018;13(12):e0207934.
98. Eltoun I, Fredenburgh J, Myers RB, Grizzle WE. Introduction to the theory and practice of fixation of tissues. *Journal of Histotechnology.* 2001;24(3):173-190.
99. Fox CH, Johnson FB, Whiting J, Roller PP. Formaldehyde fixation. *J Histochem Cytochem.* 1985;33(8):845-853.
100. Grizzle WE. Special symposium: Fixation and tissue processing models. *Biotech Histochem.* 2009;84(5):185-193.

101. Parsons M, Grabsch H. How to make tissue microarrays. *Diagnostic Histopathology*. 2009;15(3):142-150. doi: <https://doi.org/10.1016/j.mpdhp.2009.01.010>.
102. Kononen J, Bubendorf L, Kallioniemi A, et al. Tissue microarrays for high-throughput molecular profiling of tumor specimens. *Nat Med*. 1998;4(7):844-847.
103. Rimm DL, Camp RL, Charette LA, Olsen DA, Provost E. Amplification of tissue by construction of tissue microarrays. *Experimental and Molecular Pathology*. 2001;70(3):255-264. doi: <https://doi.org/10.1006/exmp.2001.2363>.
104. Lee ATJ, Chew W, Wilding CP, et al. The adequacy of tissue microarrays in the assessment of inter- and intra-tumoural heterogeneity of infiltrating lymphocyte burden in leiomyosarcoma. *Sci Rep*. 2019;9(1):14602-019-50888-5.
105. Henriksen KL, Rasmussen BB, Lykkesfeldt AE, Moller S, Ejlersen B, Mouridsen HT. Semi-quantitative scoring of potentially predictive markers for endocrine treatment of breast cancer: A comparison between whole sections and tissue microarrays. *J Clin Pathol*. 2007;60(4):397-404.

106. Visser NCM, van der Wurff AAM, Pijnenborg JMA, Massuger LFAG, Bulten J, Nagtegaal ID. Tissue microarray is suitable for scientific biomarkers studies in endometrial cancer. *Virchows Arch.* 2018;472(3):407-413.
107. Mroz EA, Tward AD, Hammon RJ, Ren Y, Rocco JW. Intra-tumor genetic heterogeneity and mortality in head and neck cancer: Analysis of data from the cancer genome atlas. *PLoS Med.* 2015;12(2):e1001786.
108. Rasmussen JH, Lelkaitis G, Hakansson K, et al. Intratumor heterogeneity of PD-L1 expression in head and neck squamous cell carcinoma. *Br J Cancer.* 2019;120(10):1003-1006.
109. Chen B, van dB, Buschers W, Balm AJM, van Velthuisen MF. Validation of tissue array technology in head and neck squamous cell carcinoma. *Head Neck.* 2003;25(11):922-930.
110. Kaplan NA, Liu X, Tolwinski NS. Epithelial polarity: Interactions between junctions and apical-basal machinery. *Genetics.* 2009;183(3):897-904.
111. Dongre A, Weinberg RA. New insights into the mechanisms of epithelial-mesenchymal transition and implications for cancer. *Nat Rev Mol Cell Biol.* 2019;20(2):69-84.

112. Thiery JP. Epithelial-mesenchymal transitions in tumour progression. *Nat Rev Cancer*. 2002;2(6):442-454.
113. Aroeira LS, Aguilera A, Sanchez-Tomero JA, et al. Epithelial to mesenchymal transition and peritoneal membrane failure in peritoneal dialysis patients: Pathologic significance and potential therapeutic interventions. *J Am Soc Nephrol*. 2007;18(7):2004-2013.
114. Thiery JP, Sleeman JP. Complex networks orchestrate epithelial-mesenchymal transitions. *Nat Rev Mol Cell Biol*. 2006;7(2):131-142.
115. Ugorski M, Dziegiel P, Suchanski J. Podoplanin - a small glycoprotein with many faces. *Am J Cancer Res*. 2016;6(2):370-386.
116. Mahtab EA, Wijffels MC, Van Den Akker NM, et al. Cardiac malformations and myocardial abnormalities in podoplanin knockout mouse embryos: Correlation with abnormal epicardial development. *Dev Dyn*. 2008;237(3):847-857.
117. Wicki A, Lehembre F, Wick N, Hantusch B, Kerjaschki D, Christofori G. Tumor invasion in the absence of epithelial-

mesenchymal transition: Podoplanin-mediated remodeling of the actin cytoskeleton. *Cancer Cell*. 2006;9(4):261-272.

118. Andrews NA, Jones AS, Helliwell TR, Kinsella AR.

Expression of the E-cadherin-catenin cell adhesion complex in primary squamous cell carcinomas of the head and neck and their nodal metastases. *Br J Cancer*. 1997;75(10):1474-1480.

119. Kurtz KA, Hoffman HT, Zimmerman MB, Robinson RA.

Decreased E-cadherin but not β -catenin expression is associated with vascular invasion and decreased survival in head and neck squamous carcinomas. *Otolaryngology - Head and Neck Surgery*. 2006;134(1):142-146. doi: <https://doi-org.liverpool.idm.oclc.org/10.1016/j.otohns.2005.08.026>.

120. Hashimoto T, Soeno Y, Maeda G, et al. Progression of oral squamous cell carcinoma accompanied with reduced E-cadherin expression but not cadherin switch. *PLoS One*. 2012;7(10):e47899.

121. Garcia-Pedrero JM, Garcia-Cabo P, Angeles Villaronga M, et al. Prognostic significance of E-cadherin and beta-catenin expression in HPV-negative oropharyngeal squamous cell carcinomas. *Head Neck*. 2017;39(11):2293-2300.

122. Zhao Z, Ge J, Sun Y, et al. Is E-cadherin immunoexpression a prognostic factor for head and neck squamous cell carcinoma (HNSCC)? A systematic review and meta-analysis. *Oral Oncol.* 2012;48(9):761-767.
123. Huber GF, Zullig L, Soltermann A, et al. Down regulation of E-cadherin (ECAD) - a predictor for occult metastatic disease in sentinel node biopsy of early squamous cell carcinomas of the oral cavity and oropharynx. *BMC Cancer.* 2011;11:217:1-8.
124. Huber GF, Fritzsche FR, Zullig L, et al. Podoplanin expression correlates with sentinel lymph node metastasis in early squamous cell carcinomas of the oral cavity and oropharynx. *Int J Cancer.* 2011;129(6):1404-1409.
125. Hu D, Zhou J, Wang F, Shi H, Li Y, Li B. HPV-16 E6/E7 promotes cell migration and invasion in cervical cancer via regulating cadherin switch in vitro and in vivo. *Arch Gynecol Obstet.* 2015;292(6):1345-1354.
126. Wakisaka N, Yoshida S, Kondo S, et al. Induction of epithelial-mesenchymal transition and loss of podoplanin expression are associated with progression of lymph node

metastases in human papillomavirus-related oropharyngeal carcinoma. *Histopathology*. 2015;66(6):771-780.

127. Lefevre M, Rousseau A, Rayon T, et al. Epithelial to mesenchymal transition and HPV infection in squamous cell oropharyngeal carcinomas: The papillophar study. *Br J Cancer*. 2017;116(3):362-369.

128. Preuss SF, Anagnostos A, Seuthe IM, et al. Expression of podoplanin and prognosis in oropharyngeal cancer. *Eur Arch Otorhinolaryngol*. 2015;272(7):1749-1754.

129. HPV and cancer. <https://www.cancer.gov/about-cancer/causes-prevention/risk/infectious-agents/hpv-and-cancer>.

Updated 2020. Accessed 01/013, 2020.

130. Kreimer AR, Chaturvedi AK. HPV-associated oropharyngeal cancers--are they preventable? *Cancer Prev Res (Phila)*. 2011;4(9):1346-1349.

131. Forastiere A, Koch W, Trotti A, Sidransky D. Head and neck cancer. *N Engl J Med*. 2001;345(26):1890-1900.

132. Hafkamp HC, Manni JJ, Haesevoets A, et al. Marked differences in survival rate between smokers and nonsmokers

with HPV 16-associated tonsillar carcinomas. *Int J Cancer*.

2008;122(12):2656-2664.

133. Mirghani H, Blanchard P. Treatment de-escalation for HPV-driven oropharyngeal cancer: Where do we stand? *Clin Transl Radiat Oncol*. 2017;8:4-11.

134. Hu G, Zhong K, Chen W, Wang S, Huang L. Podoplanin-positive cancer-associated fibroblasts predict poor prognosis in lung cancer patients. *Onco Targets Ther*. 2018;11:5607-5619.

135. Wicki A, Christofori G. The potential role of podoplanin in tumour invasion. *Br J Cancer*. 2007;96(1):1-5.

136. ATCC T. Animal cell culture guide, glossary.

<https://www.lgcstandards->

[atcc.org/Documents/Marketing_Literature/Animal_Cell_Culture_G](https://www.lgcstandards-atcc.org/Documents/Marketing_Literature/Animal_Cell_Culture_Guide/Glossary.aspx?geo_country=gb)

[uide/Glossary.aspx?geo_country=gb](https://www.lgcstandards-atcc.org/Documents/Marketing_Literature/Animal_Cell_Culture_Guide/Glossary.aspx?geo_country=gb). Updated 2014. Accessed

01/21, 2020.

137. Dhanda J. *Molecular indicators and tumour models of extracapsular spread in metastatic oral squamous cell carcinoma*.

[PhD]. University of Liverpool; 2014.

138. Kedjarune U, Pongprerachok S, Arpornmaeklong P, Ungkusonmongkhon K. Culturing primary human gingival epithelial cells: Comparison of two isolation techniques. *J Craniomaxillofac Surg.* 2001;29(4):224-231.
139. Cottler-Fox M, Montgomery M, Theus J. CHAPTER 24 - collection and processing of marrow and blood hematopoietic stem cells. . 2009:249-256. doi: <https://doi.org/10.1016/B978-0-443-10147-2.50028-X> ".
140. Pegg DE. Principles of cryopreservation. *Methods Mol Biol.* 2007;368:39-57.
141. MAZUR P. Kinetics of water loss from cells at subzero temperatures and the likelihood of intracellular freezing. *J Gen Physiol.* 1963;47:347-369.
142. Baboo J, Kilbride P, Delahaye M, et al. The impact of varying cooling and thawing rates on the quality of cryopreserved human peripheral blood T cells. *Sci Rep.* 2019;9(1):3417-019-39957-x.
143. Harris LW, Griffiths JB. Relative effects of cooling and warming rates on mammalian cells during the freeze-thaw cycle. *Cryobiology.* 1977;14(6):662-669.

144. Polak-Vogelzang AA, Angulo AF, Brugman J, Reijgers R. Survival of mycoplasma hyorhinis in trypsin solutions. *Biologicals*. 1990;18(2):97-101.
145. Desjardins P, Conklin D. NanoDrop microvolume quantitation of nucleic acids. *J Vis Exp*. 2010;(45). pii: 2565. doi(45):10.3791/2565.
146. Schache AG, Liloglou T, Risk JM, et al. Evaluation of human papilloma virus diagnostic testing in oropharyngeal squamous cell carcinoma: Sensitivity, specificity, and prognostic discrimination. *Clin Cancer Res*. 2011;17(19):6262-6271.
147. Ukpo OC, Flanagan JJ, Ma XJ, Luo Y, Thorstad WL, Lewis JS, Jr. High-risk human papillomavirus E6/E7 mRNA detection by a novel in situ hybridization assay strongly correlates with p16 expression and patient outcomes in oropharyngeal squamous cell carcinoma. *Am J Surg Pathol*. 2011;35(9):1343-1350.
148. Schneider CA, Rasband WS, Eliceiri KW. NIH image to ImageJ: 25 years of image analysis. *Nat Methods*. 2012;9(7):671-675.
149. Geback T, Schulz MM, Koumoutsakos P, Detmar M. TScratch: A novel and simple software tool for automated

analysis of monolayer wound healing assays. *BioTechniques*.

2009;46(4):265-274.

150. Bremnes RM, Donnem T, Al-Saad S, et al. The role of tumor stroma in cancer progression and prognosis: Emphasis on carcinoma-associated fibroblasts and non-small cell lung cancer.

J Thorac Oncol. 2011;6(1):209-217.

151. Bolt R, Foran B, Murdoch C, Lambert DW, Thomas S, Hunter KD. HPV-negative, but not HPV-positive, oropharyngeal carcinomas induce fibroblasts to support tumour invasion through micro-environmental release of HGF and IL-6. *Carcinogenesis*.

2018;39(2):170-179.

152. Patel C, Brotherton JM, Pillsbury A, et al. The impact of 10 years of human papillomavirus (HPV) vaccination in australia:

What additional disease burden will a nonavalent vaccine

prevent? *Euro Surveill*. 2018;23(41):10.2807/1560-

7917.ES.2018.23.41.1700737.

153. Hanahan D, Weinberg RA. Hallmarks of cancer: The next generation. *Cell*. 2011;144(5):646-674.

154. Trakarnsanga K, Griffiths RE, Wilson MC, et al. An immortalized adult human erythroid line facilitates sustainable and

scalable generation of functional red cells. *Nat Commun.*

2017;8:14750.

155. Hawley-Nelson P, Vousden KH, Hubbert NL, Lowy DR, Schiller JT. HPV16 E6 and E7 proteins cooperate to immortalize human foreskin keratinocytes. *EMBO J.* 1989;8(12):3905-3910.

156. White JS, Weissfeld JL, Ragin CC, et al. The influence of clinical and demographic risk factors on the establishment of head and neck squamous cell carcinoma cell lines. *Oral Oncol.*

2007;43(7):701-712.

157. Rieckmann T, Tribius S, Grob TJ, et al. HNSCC cell lines positive for HPV and p16 possess higher cellular radiosensitivity due to an impaired DSB repair capacity. *Radiother Oncol.*

2013;107(2):242-246.

158. Busch CJ, Kriegs M, Laban S, et al. HPV-positive HNSCC cell lines but not primary human fibroblasts are radiosensitized by the inhibition of Chk1. *Radiother Oncol.* 2013;108(3):495-499.

159. Barr JA, Hayes KE, Brownmiller T, et al. Long non-coding RNA FAM83H-AS1 is regulated by human papillomavirus 16 E6 independently of p53 in cervical cancer cells. *Sci Rep.*

2019;9(1):3662-019-40094-8.

160. Krause CJ, Carey TE, Ott RW, Hurbis C, McClatchey KD, Regezi JA. Human squamous cell carcinoma. establishment and characterization of new permanent cell lines. *Arch Otolaryngol.* 1981;107(11):703-710.

161. Tang AL, Hauff SJ, Owen JH, et al. UM-SCC-104: A new human papillomavirus-16-positive cancer stem cell-containing head and neck squamous cell carcinoma cell line. *Head Neck.* 2012;34(10):1480-1491.

162. Ragin CC, Reshmi SC, Gollin SM. Mapping and analysis of HPV16 integration sites in a head and neck cancer cell line. *Int J Cancer.* 2004;110(5):701-709.

163. Steenbergen RD, Hermsen MA, Walboomers JM, et al. Integrated human papillomavirus type 16 and loss of heterozygosity at 11q22 and 18q21 in an oral carcinoma and its derivative cell line. *Cancer Res.* 1995;55(22):5465-5471.

164. Drexler HG, Uphoff CC. Mycoplasma contamination of cell cultures: Incidence, sources, effects, detection, elimination, prevention. *Cytotechnology.* 2002;39(2):75-90.

165. Wang F, Flanagan J, Su N, et al. RNAscope: A novel in situ RNA analysis platform for formalin-fixed, paraffin-embedded tissues. *J Mol Diagn.* 2012;14(1):22-29.
166. Akagi K, Li J, Broutian TR, et al. Genome-wide analysis of HPV integration in human cancers reveals recurrent, focal genomic instability. *Genome Res.* 2014;24(2):185-199.
167. Friedl F, Kimura I, Osato T, Ito Y. Studies on a new human cell line (SiHa) derived from carcinoma of uterus. I. its establishment and morphology. *Proc Soc Exp Biol Med.* 1970;135(2):543-545.
168. Alvarez-Salas LM, Cullinan AE, Siwkowski A, Hampel A, DiPaolo JA. Inhibition of HPV-16 E6/E7 immortalization of normal keratinocytes by hairpin ribozymes. *Proc Natl Acad Sci U S A.* 1998;95(3):1189-1194.
169. Finegersh A, Kulich S, Guo T, et al. DNA methylation regulates TMEM16A/ANO1 expression through multiple CpG islands in head and neck squamous cell carcinoma. *Sci Rep.* 2017;7(1):15173-017-15634-9.

170. Tomaic V. Functional roles of E6 and E7 oncoproteins in HPV-induced malignancies at diverse anatomical sites. *Cancers (Basel)*. 2016;8(10):10.3390/cancers8100095.
171. Lin CJ, Grandis JR, Carey TE, et al. Head and neck squamous cell carcinoma cell lines: Established models and rationale for selection. *Head Neck*. 2007;29(2):163-188.
172. Forslund O, Sugiyama N, Wu C, et al. A novel human in vitro papillomavirus type 16 positive tonsil cancer cell line with high sensitivity to radiation and cisplatin. *BMC Cancer*. 2019;19(1):265-019-5469-8.
173. Stransky N, Egloff AM, Tward AD, et al. The mutational landscape of head and neck squamous cell carcinoma. *Science*. 2011;333(6046):1157-1160.
174. Nulton TJ, Olex AL, Dozmorov M, Morgan IM, Windle B. Analysis of the cancer genome atlas sequencing data reveals novel properties of the human papillomavirus 16 genome in head and neck squamous cell carcinoma. *Oncotarget*. 2017;8(11):17684-17699.

175. Goldenberg D, Begum S, Westra WH, et al. Cystic lymph node metastasis in patients with head and neck cancer: An HPV-associated phenomenon. *Head Neck*. 2008;30(7):898-903.
176. Faber A, Aderhold C, Goessler UR, et al. Interaction of a CD44+ head and neck squamous cell carcinoma cell line with a stromal cell-derived factor-1-expressing supportive niche: An in vitro model. *Oncol Lett*. 2014;7(1):82-86.
177. Friedl P, Gilmour D. Collective cell migration in morphogenesis, regeneration and cancer. *Nat Rev Mol Cell Biol*. 2009;10(7):445-457.
178. Battaglia RA, Delic S, Herrmann H, Snider NT. Vimentin on the move: New developments in cell migration. *F1000Res*. 2018;7:10.12688/f1000research.15967.1. eCollection 2018.
179. Geraghty RJ, Capes-Davis A, Davis JM, et al. Guidelines for the use of cell lines in biomedical research. *Br J Cancer*. 2014;111(6):1021-1046.
180. Kokkat TJ, Patel MS, McGarvey D, LiVolsi VA, Baloch ZW. Archived formalin-fixed paraffin-embedded (FFPE) blocks: A valuable underexploited resource for extraction of DNA, RNA, and protein. *Biopreserv Biobank*. 2013;11(2):101-106.

181. Stacker SA, Baldwin ME, Achen MG. The role of tumor lymphangiogenesis in metastatic spread. *FASEB J*. 2002;16(9):922-934.
182. Cueni LN, Hegyi I, Shin JW, et al. Tumor lymphangiogenesis and metastasis to lymph nodes induced by cancer cell expression of podoplanin. *Am J Pathol*. 2010;177(2):1004-1016.
183. Chen WS, Cao Z, Sugaya S, et al. Pathological lymphangiogenesis is modulated by galectin-8-dependent crosstalk between podoplanin and integrin-associated VEGFR-3. *Nat Commun*. 2016;7:11302.
184. Hatakeyama H, Mizumachi T, Sakashita T, Kano S, Homma A, Fukuda S. Epithelial-mesenchymal transition in human papillomavirus-positive and -negative oropharyngeal squamous cell carcinoma. *Oncol Rep*. 2014;32(6):2673-2679.
185. Zeisberg M, Neilson EG. Biomarkers for epithelial-mesenchymal transitions. *J Clin Invest*. 2009;119(6):1429-1437.
186. Gao S, Eiberg H, Kroghdal A, Liu CJ, Sorensen JA. Cytoplasmic expression of E-cadherin and beta-catenin correlated with LOH and hypermethylation of the APC gene in oral

squamous cell carcinomas. *J Oral Pathol Med.* 2005;34(2):116-119.

187. Schache AG, Powell NG, Cuschieri KS, et al. HPV-related oropharynx cancer in the united kingdom: An evolution in the understanding of disease etiology. *Cancer Res.* 2016;76(22):6598-6606.

188. Osazuwa-Peters N, Simpson MC, Massa ST, Adjei Boakye E, Antisdell JL, Varvares MA. 40-year incidence trends for oropharyngeal squamous cell carcinoma in the united states. *Oral Oncol.* 2017;74:90-97.

189. De Flora S, La Maestra S. Epidemiology of cancers of infectious origin and prevention strategies. *J Prev Med Hyg.* 2015;56(1):E15-20.

190. Mehanna H, Robinson M, Hartley A, et al. Radiotherapy plus cisplatin or cetuximab in low-risk human papillomavirus-positive oropharyngeal cancer (de-ESCALaTE HPV): An open-label randomised controlled phase 3 trial. *Lancet.* 2019;393(10166):51-60.

191. Gillison ML, Trotti AM, Harris J, et al. Radiotherapy plus cetuximab or cisplatin in human papillomavirus-positive

- oropharyngeal cancer (NRG oncology RTOG 1016): A randomised, multicentre, non-inferiority trial. *Lancet*. 2019;393(10166):40-50.
192. Cancer Research UK. **Cervical cancer statistics**. <https://www.cancerresearchuk.org/health-professional/cancer-statistics/statistics-by-cancer-type/cervical-cancer>. Accessed Aug/27, 2018.
193. Crosbie EJ, Einstein MH, Franceschi S, Kitchener HC. Human papillomavirus and cervical cancer. *Lancet*. 2013;382(9895):889-899.
194. Schache AG. *The molecular and clinical implications of human papillomavirus-16 mediated oropharyngeal squamous cell carcinoma*. [PhD]. University of Liverpool; 2013.
195. Kabsch K, Alonso A. The human papillomavirus type 16 E5 protein impairs TRAIL- and FasL-mediated apoptosis in HaCaT cells by different mechanisms. *J Virol*. 2002;76(23):12162-12172.
196. Yuan CH, Filippova M, Duerksen-Hughes P. Modulation of apoptotic pathways by human papillomaviruses (HPV): Mechanisms and implications for therapy. *Viruses*. 2012;4(12):3831-3850.

197. Filippova M, Filippov VA, Kagoda M, Garnett T, Fodor N, Duerksen-Hughes PJ. Complexes of human papillomavirus type 16 E6 proteins form pseudo-death-inducing signaling complex structures during tumor necrosis factor-mediated apoptosis. *J Virol.* 2009;83(1):210-227.
198. Meyers C. Organotypic (raft) epithelial tissue culture system for the differentiation-dependent replication of papillomavirus. *Methods Cell Sci.* 1996;18:201-210.
199. Anacker D, Moody C. Generation of organotypic raft cultures from primary human keratinocytes. *J Vis Exp.* 2012;(60). pii: 3668. doi(60):10.3791/3668.
200. Fatimah SS, Tan GC, Chua KH, Tan AE, Hayati AR. Effects of epidermal growth factor on the proliferation and cell cycle regulation of cultured human amnion epithelial cells. *J Biosci Bioeng.* 2012;114(2):220-227.
201. Carter RJ, Milani M, Butterworth M, et al. Exploring the potential of BH3 mimetic therapy in squamous cell carcinoma of the head and neck. *Cell Death Dis.* 2019;10(12):912-019-2150-8.
202. Institute NC. **The cancer genome atlas program (TCGA).** <https://www.cancer.gov/tcga>.

203. Kalatova B, Jesenska R, Hlinka D, Dudas M. Tripolar mitosis in human cells and embryos: Occurrence, pathophysiology and medical implications. *Acta Histochem.* 2015;117(1):111-125.
204. Telentschak S, Soliwoda M, Nohroudi K, Addicks K, Klinz FJ. Cytokinesis failure and successful multipolar mitoses drive aneuploidy in glioblastoma cells. *Oncol Rep.* 2015;33(4):2001-2008.
205. Steinbeck RG. Pathologic mitoses and pathology of mitosis in tumorigenesis. *Eur J Histochem.* 2001;45(4):311-318.
206. Chernov Ivanenko IS, Minin AA, Minin AA. Role of vimentin in cell migration. *Ontogenez.* 2013;44(3):186-202.
207. Gilles C, Polette M, Zahm JM, et al. Vimentin contributes to human mammary epithelial cell migration. *J Cell Sci.* 1999;112 (Pt 24)(Pt 24):4615-4625.
208. Jiang W, Freidlin B, Simon R. Biomarker-adaptive threshold design: A procedure for evaluating treatment with possible biomarker-defined subset effect. *J Natl Cancer Inst.* 2007;99(13):1036-1043.

209. Gosho M, Nagashima K, Sato Y. Study designs and statistical analyses for biomarker research. *Sensors (Basel)*. 2012;12(7):8966-8986.
210. Owadally W, Hurt C, Timmins H, et al. PATHOS: A phase II/III trial of risk-stratified, reduced intensity adjuvant treatment in patients undergoing transoral surgery for human papillomavirus (HPV) positive oropharyngeal cancer. *BMC Cancer*. 2015;15:602-015-1598-x.
211. Nystrom ML, Thomas GJ, Stone M, Mackenzie IC, Hart IR, Marshall JF. Development of a quantitative method to analyse tumour cell invasion in organotypic culture. *J Pathol*. 2005;205(4):468-475.

Chapter 10: Appendices

10.1 List of Reagents

Item	Supplier
Cell culture reagents	
Amphotericin B, penicillin, streptomycin (2.5µg/mL, 10,000U/mL)	Sigma
Cell Freezing media	Sigma
Cholera toxin from <i>Vibrio cholerae</i>	Sigma
Dulbecco's Modified Eagle's Medium - high glucose (With 4500 mg/L glucose, L-glutamine, sodium pyruvate, and sodium bicarbonate)	Sigma
Epidermal Growth Factor (EGF) from murine submaxillary gland	Sigma
Glasgow Modified Eagles Medium (GMEM)	Sigma
Heat-Inactivated Foetal Bovine Serum (FBS)	Sigma
Hydrocortisone	Sigma
Isoton II Diluent	Fisher Scientific
Keratinocyte-SFKM Basal Medium 25 mg Bovine Pituitary Extract (BPE) 2.5µg EGF, Human Recombinant	ThermoFisher
L-glutamine (200mM)	Sigma
Minimum Essential Medium (MEM)	Sigma
Non-Essential Amino Acids 100x (NEAA)	Sigma
Nutrient mixture F-12 HAM	Sigma
Penicillin-streptomycin (10,000U/mL)	Sigma
Phosphate Buffered Saline (PBS)	Sigma
RPMI-1640 with L-glutamine and sodium bicarbonate	Sigma
Trypsin-EDTA solution (0.25%)	Sigma
Nucleic acid extraction and testing kits	
1 Kb Plus DNA Ladder	Invitrogen
DNeasy blood and tissue kit	Qiagen

e-Myco™ Mycoplasma PCR detection kit	Chembio
GenePrint® 10 system STR Analysis for Human Cell Line Authentication	Promega
Hi-Di™ Formamide	Applied Biosystems
miRNeasy blood and tissue kit	Qiagen
QuantiTect Reverse Transcription kit	Qiagen
RNase-Free DNase I Set	Qiagen
RNaseZap™	Invitrogen
Stainless steel beads 5mm	Qiagen
SYBR Safe DNA gel stain	Invitrogen
HPV-typing	
CINtec p16 antibodies for IHC*	Roche
Custom HPV16 E2, E6, E7 and HPV18 E6 FAM-labelled MGB Taqman probes.	Applied Biosystems
Custom HPV16 E2, E6, E7 and HPV18 E6 Primers	MWG, Ebersberg Germany
Inform HPV III Family 16 Probe B kit*	Ventana Medical Systems
ISH Iview ^{BLUE} Plus Detection Kit*	Ventana Medical Systems
RNAscope® 2.5 VS Assay*	Advanced cell diagnostics
Taqman Gene Expression Master Mix	Applied biosystems
Taqman RNase P control reagents	Applied Biosystems
Taqman β-Actin (ACTB) control reagents	Applied Biosystems
Uracil-DNA glycosylase (UNG)	Applied Biosystems
Chemicals and buffers	
10% formalin (4% w/v paraformaldehyde)	Sigma
Agarose BioReagent, for molecular biology	Sigma
Chloroform	Fisher chemicals
Ethanol (100%)	
Hydrochloric acid	Fisher chemicals
Isopropanol	Fisher chemicals
Paraffin pellets	Sigma
TBE buffer	Thermo fisher

Organotypic reagents	
0.1 Sodium hydroxide	Sigma
10x DMEM	Sigma
Matrigel (LOT 4114001)	Corning
Rat-tail type I Collagen	Sigma
Staining reagents	
DPX mountant for histology	Sigma
E-cadherin (G-10): sc-8426	Santa Cruz Biotechnology
Envision-Flex High pH target retrieval solution	Dako
Eosin (Aqueous 1%)	Sigma
Flex Negative control (Mouse IgG and IgM)	Dako
Flex System reagents	Dako
Haematoxylin Gill III	Sigma
Monoclonal mouse Anti-human Podoplanin Clone D2-40	Dako
Monoclonal mouse Anti-Vimentin Clone V9	Dako
N-cadherin (D-4): sc-8424	Santa Cruz Biotechnology
Scott's tap water (x10)	Sigma
Xylene	Fisher chemicals
Specialised plasticware	
CellBind™ 6-well plates	Corning
Culture-inserts 2 well for self-insertion	Ibidi
NUNC 6-well plates	Sigma

10.2 Primary cell culture patient demographics

Table 10.1 shows the patient demographic for tissue collected for primary cell culture attempts. Includes Livsample number, age at

diagnosis and final TNM7 staging. Outcome at time of writing – 2019.

10.3 real-time-qPCR (Primary cell lines)

Table 10.2 rt-qPCR HPV16 E6 DNA and cDNA results for primary cell lines Liv57, Liv58 and Liv62 with reference frozen tissue and CaSki . RQ values in relation to CaSki

Table 10.3 rt-PCR HPV16 E6 and HPV18 E6 DNA for Liv91 and Liv92. HeLa as positive control for HPV18 DNA

Table 10.4 rt-qPCR HPV16 E2, E6 and E7 for Liv91, Liv92 and Liv111. Liv111TS2 established on Liv86N Fibroblast feeder layer. HPV16 Control and reference sample CaSki; HPV18 Control and reference sample HeLa

10.4 real-time qPCR CT results (Secondary cell lines)

Table 10.5 Cervical cell lines CaSki and SiHa rt-qPCR HPV16 E2, E6 and E7 DNA and cDNA results. RQ in relation to CaSki

Table 10.6 rt-qPCR HPV16 E2, E6 and E7 DNA results for the expected HPV-negative cell lines UMSCC-4 and UMSCC-74A

Table 10.7 rt-qPCR HPV16 E2, E6 and E7 cDNA results for the HPV-positive head and neck cell lines 93-VU-147T, UMSCC-47 and UPCI:SCC152. RQ in relation to CaSki (Table10.5)

Table 10.8 rt-qPCR HPV16 E2, E6 and E7 DNA and cDNA results for HPV-positive head and neck cell lines UPCI:SCC090, UPCI:SCC154 and UMSCC-104. RQ in relation to CaSki (Table 10.5)

Cell line	Gender/ Age	TNM	Site	ECS	Smoking/Alcohol history Moderate(<28units/week); heavy(>28units/week); non-drinker	HPV status (clinical)	Outcome
Liv53	M/53	T2N2b	Tonsil	N	Yes/Moderate	Positive	Alive
Liv54	F/65	T2N2b	Tonsil	N	Yes/ex drinker	Negative	Alive
Liv56	M/	T3N2c	BOT	Y	Non-smoker/unknown	Positive	Alive
Liv57	M/61	T1N1	Tonsil	Y	ex-smoker/unknown	Positive	Alive
Liv58	M/54	T2N2b	BOT	Y	non-smoker/heavy	Positive	Alive
Liv60	M/69	T2N1	Tonsil	N	ex-smoker/moderate	Positive	Alive
Liv61	M/63	Dysplasia	Tonsil	unknown	yes >20py/heavy	Positive	unknown
Liv62	M/66	T2N0	Tonsil	N	Stopped 6 years ago/moderate	Positive	Alive
Liv64	M/61	T2N2b	Tonsil	N	Stopped 30 years ago/unknown	Negative	Died (other)
Liv65	F/53	T2N2b	Tongue	N	10/day/heavy	Negative	Died of disease
Liv71	M/63	T2N2a	Tonsil	Y	Non-smoker/moderate	Positive	Died of disease
Liv77	M/54	T3N2b	Tonsil	Y	Non-smoker/moderate	Positive	Alive

Liv78	F/65	T3N2b	Tonsil	unknown	Ex-smoker stopped 8 years/heavy	Positive	Alive
Liv79	M/66	unknown	BOT	unknown	unknown	Negative	Alive
Liv81	M/60	T2N2b	Tonsil	Y	Ex-smoker stopped 6 years ago/moderate	Positive	Alive
Liv83	M/49	T2N0	Tonsil	n.a	Non-smoker/moderate	Negative	Alive
Liv84	M/57	T3N2b	Tonsil	N	Ex-smoker/non-drinker	Positive	Died (other)
Liv85	M/62	T3N2a	Tonsil	Y	Ex-smoker (1970)/moderate	Positive	Alive
Liv86	M/61	T2N2b	BOT	Y	Non-smoker/moderate	Positive	Alive
Liv87		T2N2b	BOT	Y	unknown	Negative	Died of disease
Liv88	unknown	T2N0	Tonsil	n.a	Non-smoker/non-drinker	Negative	Alive
Liv89	F/54	T2N1	Tonsil	N	Ex-smoker/moderate	Positive	Alive
Liv90	M/61	T2N0	Tonsil	n.a	Yes >20py/non-drinker	Negative	Alive
Liv91	M/72	T3N1	Tonsil	N	Yes >20py/heavy	Positive	Alive
Liv92	M/68	No residual tumour	Tonsil	n.a	Non-smoker/moderate	Positive	Alive
Liv93	F/65	T2N2a	Tonsil	N	Non-smoker/no data	Positive	Alive

Liv94	M/54	T1NX	BOT	n.a	Non-smoker/moderate	Positive	Alive
Liv95	M/59	T2N1	Soft Palate	N	Yes >20py/moderate	N/A	Alive
Liv97	F/77	T3N0	Tonsil	n.a	Ex-smoker/moderate	Negative	Alive
Liv99	M	T2N1	Tonsil	N	unknown	P16+ve	Alive
Liv100	M	T4aN0	Alveolus	n.a	unknown	Negative	Alive
Liv104	F	T2N2a	BOT	Y	unknown	Negative	Died (other)
Liv105	F	T3N2b	Tonsil	Y	unknown	Positive	Alive
Liv106	M	T2N2b	BOT	Y	unknown	Positive	Alive
Liv107	F/59	T2N0	Tonsil	n.a	Yes >20py/moderate	Negative	Alive
Liv108	M	T2N2B	BOT	N	unknown	Positive	Alive
Liv110	F	unknown	Tongue	unknown	unknown	Negative	Alive
Liv111	M	T2N2b	Tonsil	N	unknown	Positive	Alive

Table 10. 1 Patient demographics for primary cell culture attempts. Abbreviations: M: Male; F: Female; BOT: Base of Tongue; ECS: Extracapsular spread; n/a: not applicable; p/y: pack years.

HPV16 E6 DNA						HPV16 E6 cDNA					
Sample	Target	CT	Δ CT	mean Δ CT	Result	Sample	Target	CT	Δ CT	mean Δ CT	RQ
Liv57 Frozen	HPV16E6	23.301	-4.167			CASKI	ACTINB	23.065	0.860		
Liv57 Frozen	RNASEP	27.467		-4.219	DNA POSITIVE	CASKI	HPV16E6	23.925		0.874	1.000
Liv57 Frozen	HPV16E6	23.762	-4.271			CASKI	ACTINB	22.994	0.888		
Liv57 Frozen	RNASEP	28.033				CASKI	HPV16E6	23.882			
Liv57p5	RNASEP	26.410	1.542			Liv57 Frozen	HPV16E6	41.579	9.789		
Liv57p5	HPV16E6	27.952		1.537	DNA NEGATIVE	Liv57 Frozen	ACTINB	31.790		8.209	0.006
Liv57p5	RNASEP	27.081	1.533			Liv57 Frozen	HPV16E6	39.866	6.630		
Liv57p5	HPV16E6	28.614				Liv57 Frozen	ACTINB	33.236			
Liv58 Frozen	HPV16E6	23.117	-4.402			Liv58 Frozen	HPV16E6	31.690	0.718		
Liv58 Frozen	RNASEP	27.519		-4.285	DNA POSITIVE	Liv58 Frozen	ACTINB	30.972		0.648	1.170
Liv58 Frozen	HPV16E6	23.638	-4.167			Liv58 Frozen	HPV16E6	31.574	0.578		
Liv58 Frozen	RNASEP	27.805				Liv58 Frozen	ACTINB	30.996			
Liv58p4	RNASEP	27.800	1.540			Liv62 Frozen	B-Actin	Undetermined			
Liv58p4	HPV16E6	29.340		1.509	DNA NEGATIVE	Liv62 Frozen	HPV16E6	34.634			
Liv58p4	RNASEP	28.473	1.478			Liv62 Frozen	B-Actin	Undetermined			
Liv58p4	HPV16E6	29.951				Liv62 Frozen	HPV16E6	35.827			
Liv62 Frozen	HPV16E6	24.546	-0.367			Liv57p3	HPV16E6	Undetermined			
Liv62 Frozen	RNASEP	24.912		-0.384	DNA POSITIVE	Liv57p3	ACTINB	27.787			
Liv62 Frozen	RNASEP	25.756	-0.401			Liv57p3	HPV16E6	Undetermined			
Liv62 Frozen	HPV16E6	25.355				Liv57p3	ACTINB	32.475			
Liv62p7	HPV16E6	31.351	1.541			Liv57p5	ACTINB	25.049			
Liv62p7	RNASEP	29.810		1.519	DNA NEGATIVE	Liv57p5	HPV16E6	Undetermined			
Liv62p7	HPV16E6	31.371	1.497			Liv57p5	ACTINB	Undetermined			
Liv62p7	RNASEP	29.874				Liv57p5	HPV16E6	Undetermined			
CASKI	HPV16E6	13.830	-15.127			Liv58p4	ACTINB	27.673			
CASKI	RNASEP	28.957		-15.125	DNA POSITIVE	Liv58p4	HPV16E6	Undetermined			
CASKI	HPV16E6	13.923	-15.123			Liv58p4	ACTINB	33.288			
CASKI	RNASEP	29.047				Liv58p4	HPV16E6	Undetermined			
						Liv62p9	ACTINB	30.363			
						Liv62p9	HPV16E6	Undetermined			
						Liv62p9	ACTINB	34.894			
						Liv62p9	HPV16E6	Undetermined			

Table10.2 rt-qPCR results for primary cell lines Liv57, Liv58 and Liv62 with control CaSki and frozen reference tissue. Δ CT and RQ calculated as described in section 3.8.2 RQ in relation to CaSki

HPV16 DNA							HPV18 DNA					
Sample	Target	CT	Δ CT	mean Δ CT	Result		Sample	Target	CT	Δ CT	mean Δ CT	Result
Liv91TS8	RNASE P	30.320	1.544				Liv91TS8	RNASE P	31.074	0.498		
Liv91TS8	HPV16 E6	31.864		1.443	DNA NEGATIVE		Liv91TS8	HPV18 E6	31.573		0.539	DNA NEGATIVE
Liv91TS8	RNASE P	30.498	1.343				Liv91TS8	RNASE P	31.920	0.579		
Liv91TS8	HPV16 E6	31.840					Liv91TS8	HPV18 E6	32.499			
Liv91TS8	RNASE P	29.976	0.391				Liv92TS5	RNASE P	30.821	0.675		
Liv91TS8	HPV16 E7	30.367		0.390	DNA NEGATIVE		Liv92TS5	HPV18 E6	31.496		0.700	DNA NEGATIVE
Liv91TS8	RNASE P	29.997	0.390				Liv92TS5	RNASE P	31.243	0.726		
Liv91TS8	HPV16 E7	30.387					Liv92TS5	HPV18 E6	31.969			
Liv91TS8	HPV16 E2	31.786	1.255				HeLa	RNASE P	26.7371	-0.05112		
Liv91TS8	RNASE P	30.532		1.455	DNA NEGATIVE		HeLa	HPV18 E6	26.68598		0.081092	1 SAMPLE POSITIVE
Liv91TS8	HPV16 E2	31.127	1.655				HeLa	RNASE P	26.77438	0.213308		
Liv91TS8	RNASE P	29.473					HeLa	HPV18 E6	26.98769			
Liv92TS5	HPV16 E6	30.850	1.275									
Liv92TS5	RNASE P	29.574		1.345	DNA NEGATIVE							
Liv92TS5	HPV16 E6	31.036	1.414									
Liv92TS5	RNASE P	29.622										
Liv92TS5	HPV16 E7	29.466	0.565									
Liv92TS5	RNASE P	28.901		0.546	DNA NEGATIVE							
Liv92TS5	HPV16 E7	29.520	0.527									
Liv92TS5	RNASE P	28.993										
Liv92TS5	HPV16 E2	30.359	2.087									
Liv92TS5	RNASE P	28.273		2.046	DNA NEGATIVE							
Liv92TS5	HPV16 E2	31.949	2.005									
Liv92TS5	RNASE P	29.945										

Table 10.3 rt-qPCR HPV16 E6 and HPV18 E6DNA and results for primary cell lines Liv91 and Liv92. HeLa as positive control

Sample	Target	CT	Δ CT	mean Δ CT	RQ
Liv91TS8	Actin B	25.140			
Liv91TS8	HPV16 E6	Undetermined			
Liv91TS8	Actin B	24.564			
Liv91TS8	HPV16 E6	Undetermined			
Liv91TS8	Actin B	24.427			
Liv91TS8	HPV16 E7	38.796			
Liv91TS8	Actin B	24.387			
Liv91TS8	HPV16 E7	Undetermined			
Liv91TS8	HPV16 E2	Undetermined			
Liv91TS8	Actin B	23.868			
Liv91TS8	HPV16 E2	Undetermined			
Liv91TS8	Actin B	24.085			
Liv92TS5	HPV16 E6	Undetermined			
Liv92TS5	Actin B	31.746			
Liv92TS5	HPV16 E6	Undetermined			
Liv92TS5	Actin B	32.218			
Liv92TS5	HPV16 E7	Undetermined			
Liv92TS5	Actin B	Undetermined			
Liv92TS5	HPV16 E7	Undetermined			
Liv92TS5	Actin B	Undetermined			
Liv92TS5	HPV16 E2	Undetermined			
Liv92TS5	Actin B	31.957			
Liv92TS5	HPV16 E2	Undetermined			
Liv92TS5	Actin B	35.353			
CASKI	HPV16 E2	23.620	2.635		
CASKI	Actin B	20.986		3.191	1
CASKI	HPV16 E2	25.056	3.747		
CASKI	Actin B	21.309			

Sample	Target	CT	Δ CT	mean Δ CT	RQ
LIV111TS2	HPV16 E6	Undetermined			
LIV111TS2	B Actin	20.00794792			
LIV111TS2	HPV16 E6	Undetermined			
LIV111TS2	B Actin	18.63320923			
LIV111TS2	HPV16 E7	42.20497894			
LIV111TS2	B Actin	Undetermined			
LIV111TS2	HPV16 E7	Undetermined			
LIV111TS2	B Actin	18.64832878			
LIV111ST1	HPV16 E6	Undetermined			
LIV111ST1	B Actin	Undetermined			
LIV111ST1	HPV16 E6	Undetermined			
LIV111ST1	B Actin	2.567833424			
LIV111ST1	HPV16 E7	17.04752922			
LIV111ST1	B Actin	3.284211636			
LIV111ST1	HPV16 E7	38.89336395			
LIV111ST1	B Actin	Undetermined			
LIV111TS2	B Actin	20.88933945	10.401		
LIV111TS2	HPV18 E6	31.29031181		11.348	5E-04
LIV111TS2	B Actin	21.69809532	12.295		
LIV111TS2	HPV18 E6	33.99337769			
LIV111ST1	B Actin	17.89359856			
LIV111ST1	HPV18 E6	Undetermined			
LIV111ST1	B Actin	Undetermined			
LIV111ST1	HPV18 E6	Undetermined			
HeLa	HPV18 E6	18.216	-0.057		
HeLa	B Actin	18.273		0.313	1
HeLa	HPV18 E6	18.403	0.684		
HeLa	B Actin	17.718			

Table 10.4 rt-qPCR cDNA HPV16 E6 E7 and E2; HPV18 E8. HPV16 reference control CaSki; HPV18 reference control HeLa

Cervical cell lines HPV16 DNA						Cervical cell lines HPV16 cDNA					
Sample	Target	CT	ΔCT	mean ΔCT	Result	Sample	Target	CT	ΔCT	mean ΔCT	RQ (compared to CaSki)
CASKI	HPV16 E6	13.368	-23.044			CASKI	HPV16 E6	23.65297	-4.5676		
CASKI	RNASE P	36.412		-25.931	DNA POSITIVE	CASKI	Actin B	28.22056		-3.08166	1
CASKI	HPV16 E6	12.972	-28.818			CASKI	HPV16 E6	23.79485	-1.59572		
CASKI	RNASE P	41.790				CASKI	Actin B	25.39057			
CASKI	HPV16 E7	11.526				CASKI	HPV16 E7	17.30857			
CASKI	RNASE P	Undetermined			UNSUCCESSFUL ASSAY	CASKI	Actin B	Undetermined			
CASKI	HPV16 E7	11.368				CASKI	B Actin	21.60114	-11.1971	-11.1971	1
CASKI	RNASE P	Undetermined				CASKI	HPV16 E7	10.40405			
CASKI	HPV16 E2	14.000	2.141			CASKI	HPV16 E2	23.62023	2.634655		
CASKI	RNASE P	11.859		1.640	DNA NEGATIVE	CASKI	Actin B	20.98557		2.634655	1
CASKI	HPV16 E2	14.487	1.138			CASKI	HPV16 E2	25.05575	3.74712		
CASKI	RNASE P	13.349				CASKI	Actin B	21.30863			
SiHa	HPV16 E6	21.619	-1.465			SiHa	HPV16 E6	25.38152	1.352108		
SiHa	RNASE P	23.084		-1.524	DNA POSITIVE	SiHa	Actin B	24.02942		1.346585	0.046448
SiHa	HPV16 E6	20.979	-1.584			SiHa	HPV16 E6	25.76544	1.341063		
SiHa	RNASE P	22.563				SiHa	Actin B	24.42438			
SiHa	HPV16 E7	20.393	-2.674			SiHa	HPV16 E7	20.31271	-3.93601		
SiHa	RNASE P	23.066		-2.542	DNA POSITIVE	SiHa	Actin B	24.24871		-3.74919	0.005727
SiHa	HPV16 E7	20.117	-2.410			SiHa	HPV16 E7	20.7287	-3.56237		
SiHa	RNASE P	22.527				SiHa	Actin B	24.29107			

Table 10.5 Cervical cell line DNA and cDNA rt-qPCR results for HPV16 E2, E6 and E7. RQ in relation to CaSki

HPV-NEGATIVE Cell lines HPV16 DNA						
Sample	Target	CT	Δ CT	mean Δ CT	Result	
UMSCC-4	HPV16 E6	29.58421707	1.444			
UMSCC-4	RNASE P	28.14040565		1.404	DNA NEGATIVE	
UMSCC-4	HPV16 E6	29.27510071	1.364			
UMSCC-4	RNASE P	27.91119576				
UMSCC-4	HPV16 E7	28.26781273	0.505			
UMSCC-4	RNASE P	27.76302147		0.501	DNA NEGATIVE	
UMSCC-4	HPV16 E7	28.19425583	0.497			
UMSCC-4	RNASE P	27.6969986				
UMSCC-4	HPV16 E2	28.41178322	1.624			
UMSCC-4	RNASE P	26.78730965		1.637	DNA NEGATIVE	
UMSCC-4	HPV16 E2	28.19920921	1.650			
UMSCC-4	RNASE P	26.54880905				
UMSCC-74A	HPV16 E6	31.78856277	1.427			
UMSCC-74A	RNASE P	30.36147499		1.385	DNA NEGATIVE	
UMSCC-74A	HPV16 E6	31.73732758	1.343			
UMSCC-74A	RNASE P	30.39403343				
UMSCC-74A	HPV16 E7	30.6310215	0.425			
UMSCC-74A	RNASE P	30.20578575		0.434	DNA NEGATIVE	
UMSCC-74A	HPV16 E7	30.82175827	0.443			
UMSCC-74A	RNASE P	30.37919617				
UMSCC-74A	HPV16 E2	30.91132545	1.006			
UMSCC-74A	RNASE P	29.90493584		1.243	DNA NEGATIVE	
UMSCC-74A	HPV16 E2	31.0835228	1.479			
UMSCC-74A	RNASE P	29.6043396				

Table 10.6 rt-qPCR DNA results for E2, E6 and E7 on expected HPV-negative head and neck cell lines

Sample	Target	HPV Positive Cell lines cDNA			
		CT	Δ CT	mean Δ CT	RQ
UPCISCC152	HPV16 E6	Undetermined			
UPCISCC152	B Actin	18.217			
UPCISCC152	HPV16 E6	Undetermined			
UPCISCC152	B Actin	19.975			
UPCISCC152	HPV16 E7	21.873	2.761		
UPCISCC152	B Actin	19.112		2.194	9.31E-05
UPCISCC152	HPV16 E7	23.236	1.627		
UPCISCC152	B Actin	21.609			
UPCISCC152*	HPV16 E2				1.28
93-VU-147T	HPV16 E6	25.326	4.983		
93-VU-147T	B Actin	20.343		4.589	4.91E-03
93-VU-147T	HPV16 E6	27.475	4.195		
93-VU-147T	B Actin	23.280			
93VU147T	HPV16 E7	18.520	5.905		
93VU147T	B Actin	12.615		5.602	8.77E-06
93VU147T	HPV16 E7	21.926	5.299		
93VU147T	B Actin	16.627			
93-VU-147T	HPV16 E2	28.092	4.935		
93-VU-147T	B Actin	23.157		4.798	0.33
93-VU-147T	HPV16 E2	28.131	4.661		
93-VU-147T	B Actin	23.469			
UMSCC47	B Actin	17.725			
UMSCC47	HPV16 E6	Undetermined			
UMSCC47	B Actin	18.108			
UMSCC47	HPV16 E6	Undetermined			
UMSCC47	B Actin	18.259	0.390		
UMSCC47	HPV16 E7	18.650		0.934	2.23E-04
UMSCC47	B Actin	18.274	1.478		
UMSCC47	HPV16 E7	19.752			
UMSCC-47	HPV16 E2	Undetermined			
UMSCC-47	Actin B	24.38337135			
UMSCC-47	HPV16 E2	Undetermined			
UMSCC-47	Actin B	24.27910995			

Table 10.7 cDNA rt-qPCR results for UPCI:SCC152. *Result taken from [174], 93-VU-14T and UMSCC-47 for HPV16 E2, E6 and E7. RQ in relation to CaSki (Table 10.5)

HPV-POSITIVE Cell lines HPV16 DNA						HPV-POSITIVE Cell lines HPV16 cDNA					
Sample	Target	CT	ΔCT	mean ΔCT	Result	Sample	Target	CT	ΔCT	mean ΔCT	RQ
UMSCC-104	HPV16 E6	28.535	-0.916			UMSCC-104	HPV16 E6	26.170	-0.327		
UMSCC-104	RNASE P	29.451		-0.878	DNA POSITIVE	UMSCC-104	Actin B	26.497		-0.486	0.17
UMSCC-104	HPV16 E6	28.574	-0.841			UMSCC-104	HPV16 E6	26.440	-0.644		
UMSCC-104	RNASE P	29.414				UMSCC-104	Actin B	27.085			
UMSCC-104	HPV16 E7	27.659	-1.450			UMSCC104	B Actin	19.360			
UMSCC-104	RNASE P	29.108		-1.463	DNA POSITIVE	UMSCC104	HPV16 E7	17.409	-1.951	-1.003	8.54E-04
UMSCC-104	HPV16 E7	27.647	-1.477			UMSCC104	B Actin	20.883			
UMSCC-104	RNASE P	29.124				UMSCC104	HPV16 E7	20.828	-0.055		
UMSCC-104	HPV16 E2	28.853	2.157			UMSCC-104	HPV16 E2	26.508	2.879		
UMSCC-104	RNASE P	26.696		1.648	DNA NEGATIVE	UMSCC-104	Actin B	23.630		2.772	1.34
UMSCC-104	HPV16 E2	29.428	1.139			UMSCC-104	HPV16 E2	27.232	2.665		
UMSCC-104	RNASE P	28.290				UMSCC-104	Actin B	24.567			
UPCI:SCC090	HPV16 E6	14.209	-11.425			UPCI:SCC090	HPV16 E6	23.405	-13.675		
UPCI:SCC090	RNASE P	25.634		-15.626	DNA POSITIVE	UPCI:SCC090	Actin B	37.080		-13.890	1.79E+03
UPCI:SCC090	HPV16 E6	14.166	-19.827			UPCI:SCC090	HPV16 E6	23.720	-14.104		
UPCI:SCC090	RNASE P	33.993				UPCI:SCC090	Actin B	37.824			
UPCI:SCC090	RNASE P	18.645	4.999			UPCISCC090	HPV16 E7	18.765	8.485	3.497	3.77E-05
UPCI:SCC090	HPV16 E7	13.646		4.999	DNA NEGATIVE	UPCISCC090	B Actin	10.279			
UPCI:SCC090	RNASE P	Undetermined				UPCISCC090	HPV16 E7	19.32439	-1.492		
UPCI:SCC090	HPV16 E7	13.787				UPCISCC090	B Actin	20.81632			
UPCI:SCC090	HPV16 E2	16.494	1.022			UPCI:SCC090	HPV16 E2	28.328	2.721		
UPCI:SCC090	RNASE P	15.472		1.022	DNA NEGATIVE	UPCI:SCC090	Actin B	25.607		2.738	1.37
UPCI:SCC090	HPV16 E2	Undetermined				UPCI:SCC090	HPV16 E2	29.427	2.756		
UPCI:SCC090	RNASE P	Undetermined				UPCI:SCC090	Actin B	26.672			
UPCI:SCC154	RNASE P	26.827	-0.078			UPCI:SCC154	Actin B	23.951	7.080		
UPCI:SCC154	HPV16 E6	26.905		0.004	DNA NEGATIVE	UPCI:SCC154	HPV16 E6	31.032		6.848	1.03E-03
UPCI:SCC154	HPV16 E6	26.849	0.086			UPCI:SCC154	Actin B	24.424	6.616		
UPCI:SCC154	RNASE P	26.763				UPCI:SCC154	HPV16 E6	31.040			
UPCI:SCC154	RNASE P	26.654	-0.199			UPCI:SCC154	Actin B	23.370	1.577		
UPCI:SCC154	HPV16 E7	26.852		-0.148	DNA POSITIVE	UPCI:SCC154	HPV16 E7	24.947		1.464	1.54E-04
UPCI:SCC154	RNASE P	26.800	-0.098			UPCI:SCC154	Actin B	23.775	1.351		
UPCI:SCC154	HPV16 E7	26.897				UPCI:SCC154	HPV16 E7	25.126			
UPCI:SCC154	HPV16 E2	Undetermined				UPCI:SCC154	HPV16 E2	Undetermined			
UPCI:SCC154	RNASE P	Undetermined				UPCI:SCC154	Actin B	23.263			
UPCI:SCC154	HPV16 E2	27.168	1.986			UPCI:SCC154	HPV16 E2	Undetermined			
UPCI:SCC154	RNASE P	25.183		1.986	DNA NEGATIVE	UPCI:SCC154	Actin B	22.856			

Table 10.8 DNA and cDNA rt-qPCR results for HPV16 E2, E6 and E7 for UMSCC-104, UPCI:SCC090 and UPCI:SCC154. RQ calculated in relation to CaSki (Table 10.5)

10.5 Organotypics

10.5.1 Materials and Methods

Gel formation

Various alternative methods to produce successful organotypic three-dimensional (3D) cell culturing were attempted with the aim of embedding fibroblasts within Matrigel™:collagen discs, seeding keratinocytes/tumour cells on to and imaging their invasion through the gel. The protocol has been previously described by Jagtar Dhanda and Nystrom et al^{137,211}.

Due to their fast proliferation and higher passage capabilities, fibroblasts derived from Liv86 normal tissue and Human Foreskin Fibroblasts (HFF1) were cultured to high cell numbers. Initially, gels were made by mixing 1 volume FBS; 1 volume 10X DMEM; 3.5 volumes rat-tail type I collagen and 3.5 volumes Matrigel on ice in a 15ml falcon. For each gel required, 1 volume = 100µL. To enable collagen setting, pH was altered to give an alkaline environment by adding 0.1M NaOH dropwise until the solution turned from a yellow to a pale pink colour. 1 volume of fibroblasts (1×10^6 cells counted as per 3.4.5) was mixed into the gel by

gentle pipetting. 1ml of gel/fibroblast solution was pipetted into wells of a 24-well plate and left to solidify at 37°C for 1hour.

250,000 of the desired invasive cells were seeded in 1ml on top of the solid gels and returned to the incubator (37°C/5% CO₂) for 24 hours.

To mimic the oropharyngeal environment, gels were lifted to an air-liquid interface with the Matrigel disc slightly submerged in media and the keratinocytes/cancer cells exposed to the air. This was achieved by constructing steel grids to fit within 12-well plates and membranes for the gels to sit upon. To prepare the membrane nylon sheets were cut into 2x2cm squares and coated with a solution of 7 volumes collagen, 1 volume 10X DMEM, 1 volume sterile water and 1 volume FBS, neutralised with 0.1M NaOH. 250µL was added to each sheet and incubated for 15mins at 37°C before being stored in PBS overnight at 4°C before use. Forceps and spatulas were used to lift the gels out of the 24-well plate and place on top of the nylon sheet on top of the steel grid (Figure 10.1). Supplemented DMEM:F12 (Table 3.1) was added

until the nylon sheet was submerged. Gels were cultured for 14 days with media changes every 2 days before embedding.

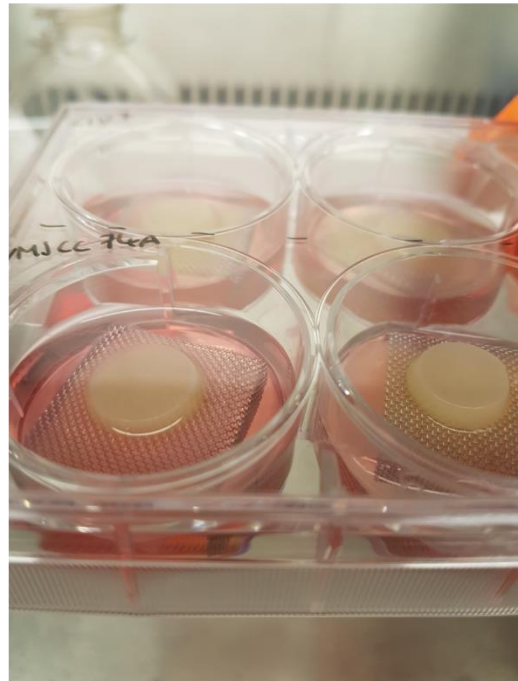
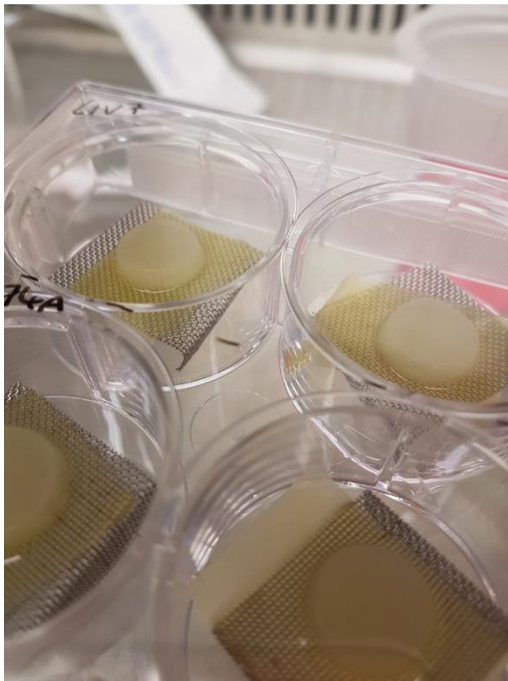
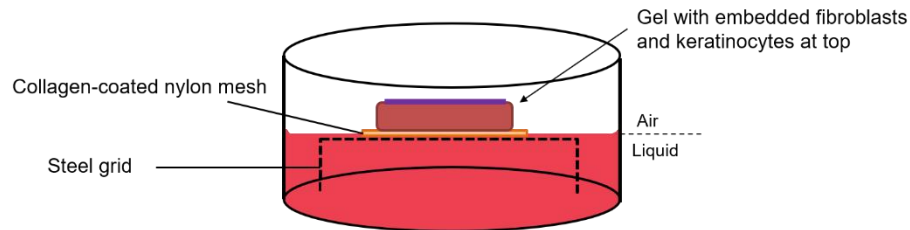


Figure 10.1 Diagram and photographs of organotypics with air-liquid interface configuration

Embedding and sectioning

After culturing, gels were carefully removed and cut in half vertically with a Swann no.11 scalpel. Each half was fixed in 4% paraformaldehyde for 24hours before processing. Gels were wrapped in 'rizla' paper and secured in a cassette for standard tissue processing utilising fixation in alcoholic formalin,

dehydration in 95% and 100% ethanol, xylene as a clearing agent and finally paraffin infiltration. The dissected gels were embedded with cut ends at the superficial aspect of paraffin blocks and sectioned at 4 μ M for mounting on SuperFrost Plus Adhesion slides. Sections were dried and stained with the H&E protocol described in 3.11.1

10.5.2 Results

There were multiple attempts to establish a robust gel that could withstand transfer to the air:liquid interface and required a basic gel to solidify. However, although keratinocytes were seeded in high numbers (250,000) per well, H&E staining revealed no adherence or formation of proliferating cells. Multiple keratinocytes were attempted including Liv7 (which had produced successful organotypics previously), and all the characterised secondary cell lines. Figure 10.2 demonstrates the highest achieved keratinocyte layer (SiHa), however this was not covered across whole of gel.

10.6 Migration videos

USB attached to back cover contains the gif. video files of wound gap live imaging described in section 3.9 and 5.2.2: 93-VU-147T; CaSki; SiHa; UMSCC-4; UMSCC-74A; UMSCC-104 and UPCI:SCC154. All videos are 15fps and each time point was captured at 10min intervals to a maximum of 48hours (UPCI:SCC154). In addition, there is a video .gif file demonstrating a tripolar mitosis event that was observed in SiHa.

10.7 TMA Overall scoring sheets

Table 10.9 gives the demographics and overall scores for the HPV-negative cohort that was studied in Chapter 7. Nodal status 0=node negative; 1=node positive; Outcome 0=alive; 1=Died of disease, 2=Died of other; DFS: Disease-free survival, includes death and recurrence;

PT Number	HPV (p16/DNA- ISH) (0/1)	Gender	Site of lesion	Pt	pN	OUTCOME 1=DOD; 2=died; other	DFS	E-cad	Vim	PDPN	EMT-Pos	Invasion	
												LowECAD/HighPDPN	HighVIM/HighPDPN
20	0	M	tonsil	4	0	0	0	0	0	0	0	0	0
5	0	M	BOT	3	0	0	0	0	0	1	0	1	0
9	0	F	soft palate	1	0	1	0	0	0	0	0	0	0
1	0	F	oropharynx	4	0	0	0	0	0	0	0	0	0
14	0	F	BOT	2	0	0	0	0	0	0	0	0	0
47	0		soft palate	2	0	1	0	1	0	1	0	0	0
19	0	F	oropharynx	2	0	1	0	1	0	1	0	0	0
42	0	F	soft palate	2	0	0	0	1	1	1	0	0	1
15	0	F	oropharynx	3	1	2	1	0	0	0	0	0	0
27	0	M	tonsil	4	1	1	1	0	0	1	0	1	0
2	0	M	tonsil	4	1	0	0	0	0	1	0	1	0
10	0	M	soft palate	3	1	0	0	0	1	1	1	1	1
13	0	F	soft palate	2	1	2	0	1	0	1	0	0	0
7	0	M	tonsil	3	1	0	0	1	0	1	0	0	0
54	0		BOT	1	1	0	0	1	0	0	0	0	0
3	0	M	soft palate	4	1	1	1	0	0	0	0	0	0
4	0	M	tonsil	2	1	0	0	0	0	0	0	0	0
6	0	M	tonsil	2	1	0	0	0	0	1	0	1	0
43	0	M	tonsil	4	1	1	1	0	0	0	0	0	0
30	0	F	tonsil	3	1	1	1	0	0	0	0	0	0
74	0	M	Tonsil	2	1	0	0	0	1	0	1	0	0
16	0	M	tonsil	2	1	1	1	0	1	1	1	1	1
17	0	M	BOT	3	1	1	1	0	1	0	1	0	0
26	0	M	tonsil	3	1	1	1	0	1	1	1	1	1
21	0	M	tonsil	2	1	1	1	0	1	1	1	1	1
97	0	m	tonsil	2	1	0	0	1	0	0	0	0	0
73	0	M	Soft Palate	3	1	0	0	1	0	0	0	0	0
12	0	M	BOT	2	1	2	0	1	0	1	0	0	0
8	0	M	BOT	2	1	2	0	1	0	1	0	0	0
22	0	M	oropharynx	2	1	0	0	1	0	0	0	0	0
11	0	M	tonsil	4a	1	1	0	1	0	1	0	0	0
34	0	M	tonsil	3	1	1	1	1	1	1	0	0	1
56	0		BOT	1	1	0	0	1	1	1	0	0	1
18	0	F	oropharynx	3	1	1	1						
24	0	M	tonsil			1	0	0	0	0	0	0	0
25	0	M	tonsil			1	1	0	0	0	0	0	0
29	0	M	oropharynx			2	1	0	0	0	0	0	0
32	0	M	tonsil					0	1	0	1	0	0
23	0	F	BOT			2	0	0	1	1	1	1	1
28	0	M	tonsil					0	1	1	1	1	1
31	0	F	oropharynx			0	1	0	1	1	1	1	1
58	0	M	BOT					0	0	0	0	0	0
33	0		tonsil			0	1	0	0	0	0	0	0
55	0		BOT	2		1	1	0	1	1	1	1	1
59	0	M	BOT			2	0						

Table 10.9 IHC results for HPV-negative tumours. IHC scores(green) categorised as 0=low/1=high.

PT Number	HPV (p16/DNA- ISH) (0/1)	Gender	Site of lesion	Pt	pN	OUTCOME 1=DOD; 2=died other	DFS	E-cad	Vim	PDPN	EMT-Pos	Invasion	
												LowECAD/HighPDPN	HighVIM/HighPDPN
91	1	M	BOT	2	0	2	0	0	0	1	0	1	0
53	1		tonsil	Cis	0	0	0	0	1	1	1	1	0
77	1	M	Oropharynx	2	0	1	0	1	0	1	0	0	1
49	1		tonsil	2	0	0	0	1	0	0	0	0	0
72	1	M	Tonsil	3	0	0	1	1	0	1	0	0	0
87	1	M	Tonsil	3	0	1	1	1	0	1	0	0	0
89	1	M	Tonsil	3	0	0	0	1	1	1	0	0	1
41	1		oropharynx	3	0	0	0	1	1	1	0	0	1
93	1	M	Tonsil	2	0	0	0						
67	1	M	Soft Palate	4b	1	2	0	0	1	1	1	1	1
69	1	M	Soft Palate	4	1	0	0	1	0	0	0	0	0
76	1	F	Tonsil	2	1	0	0	1	0	1	0	0	0
99	1	m	tonsil	1	1	0	0	1	0	1	0	0	0
85	1	M	Tonsil	2	1	0	0	1	0	1	0	0	0
78	1	M	BOT	1	1	2	0	1	1	1	0	0	1
101	1	m	tonsil	2	1	0	0	1	1	1	0	0	1
88	1	F	Tonsil	2	1	0	0				0		
65	1	M	Tonsil	3	1	0	0	0	0	1	0	1	0
105	1	f	tonsil	3	1	0	0	0	0	1	0	1	0
52	1		tonsil	3c	1	0	0	0	1	1	1	1	1
100	1	m	BOT	3	1	0	0	0	1	0	1	0	0
45	1		BOT	2	1	0	0	0	1	0	1	0	0
38	1		tonsil	2	1	0	0	0	1	1	1	1	1
68	1	F	BOT	2	1	0	0	1	0	0	0	0	0
80	1	M	Oropharynx	3	1	0	0	1	0	0	0	0	0
90	1	M	Tonsil	3	1	0	0	1	0	0	0	0	0
63	1	M	BOT	3	1	0	0	1	0	1	0	0	0
86	1	M	Tonsil	2	1	0	0	1	0	1	0	0	0
92	1	F	Tonsil	2	1	0	0	1	0	1	0	0	0
71	1	M	Tonsil	3	1	0	0	1	0	1	0	0	0
51	1		oropharynx	3	1	1	1	1	0	1	0	0	0
84	1	M	BOT	3	1	0	0	1	0	1	0	0	0
36	1		BOT	2	1	0	0	1	0	1	0	0	0
81	1	M	Tonsil	3	1	0	0	1	1	1	0	0	1
98	1	m	BOT	3	1	0	0	1	1	0	0	0	0
75	1	M	Tonsil	4	1	2	1	1	1	1	0	0	1
94	1	M	BOT	2	1	0	0	1	1	1	0	0	1
83	1	F	Tonsil	3	1	0	0	1	1	1	0	0	1
66	1	M	Tonsil	2	1	0	0	1	1	1	0	0	1
39	1		tonsil	2	1	0	0	1	1	1	0	0	1
79	1	F	Tonsil	3	1	0	0	1	1	1	0	0	0
70	1	M	Tonsil	2	1	2	0	1	1	1	0	0	0
60	1	M	Tonsil	3	1	0	0	1	1	1	0	0	1
95	1	M	Tonsil	2	1	0	0	1	1	1	0	0	1
103	1	m	tonsil	2	1	0	0	1	1	0	0	0	1
106	1	m	tonsil	2	1	0	0	1	1	1	0	0	1
37	1		tonsil	2	1	0	0	1	1	1	0	0	0
35	1		tonsil	2	1	0	0	1	1	0	0	0	0
104	1	m	tonsil	3	1	0	0	1	1	0	0	0	0
96	1	m	BOT	3	1	0	0						
64	1	M	Tonsil	X	1								
102	1	m	tonsil	2	1	0	0						
61	1	F	Tonsil		1	0	0						
62	1	M	Soft Palate			1	1	1	0	1	0	0	0

Table 10.10 IHC overall scores for HPV-positive tumours. IHC scores(green) as 0=low/1=high

